Trypanosoma brucei editosomes have a single, bifunctional reaction center – Evidence for a non–collisional reaction mechanism

Vom Fachbereich Biologie der Technischen Universität Darmstadt

zur

Erlangung des akademischen Grades
eines *Doctor rerum naturalium*
genehmigte Dissertation von

M.Sc.
Venkata Subbaraju Katari
aus Siddhapuram, Andhra Pradesh, Indien

1. Referent: Prof. Dr. H. Ulrich Göringer
2. Referent: Prof. Dr. Christian Hammann

Tag der Einreichung: 05.09.2013
Tag der mündlichen Prüfung: 06.12.2013

Darmstadt 2014
D17

Die vorliegende Arbeit wurde am Fachbereich Biologie der Technischen Universität Darmstadt im Arbeitskreis Molekulare Genetik (Prof. Dr. H. Ulrich Göringer) angefertigt. Die Arbeit wurde in Teilen durch das Howard Hughes Medical Institute (HHMI), USA und die Deutsche Forschungsgemeinschaft (DFG-SFB902) finanziert.

Teile der Arbeit gingen in folgende Veröffentlichungen ein:

Göringer HU, Katari VS, Böhm C. (2011) **The structural landscape of native editosomes in African trypanosomes**. *Wiley Interdiscip. Rev. RNA* 2:395–407.

Böhm C, Katari VS, Brecht M, Göringer HU. (2012) ***Trypanosoma brucei* 20S editosomes have one RNA substrate-binding site and execute RNA unwinding activity**. *J. Biol. Chem.* 287:26268-26277.

Katari VS, van Esdonk L, Göringer HU. (2013) **Molecular crowding inhibits U-insertion/deletion RNA editing *in vitro* – consequences for the *in vivo* reaction.** doi: 10.1371/journal.pone.0083796.

Kruse E, Katari VS, Göringer HU. (2013) **U-insertion/deletion-type RNA editing is not regulated throught the cell cycle of African trypanosomes.** submitted.

CONTENTS

“Everyone needs an editor.”
– Tim Foote

General Introduction

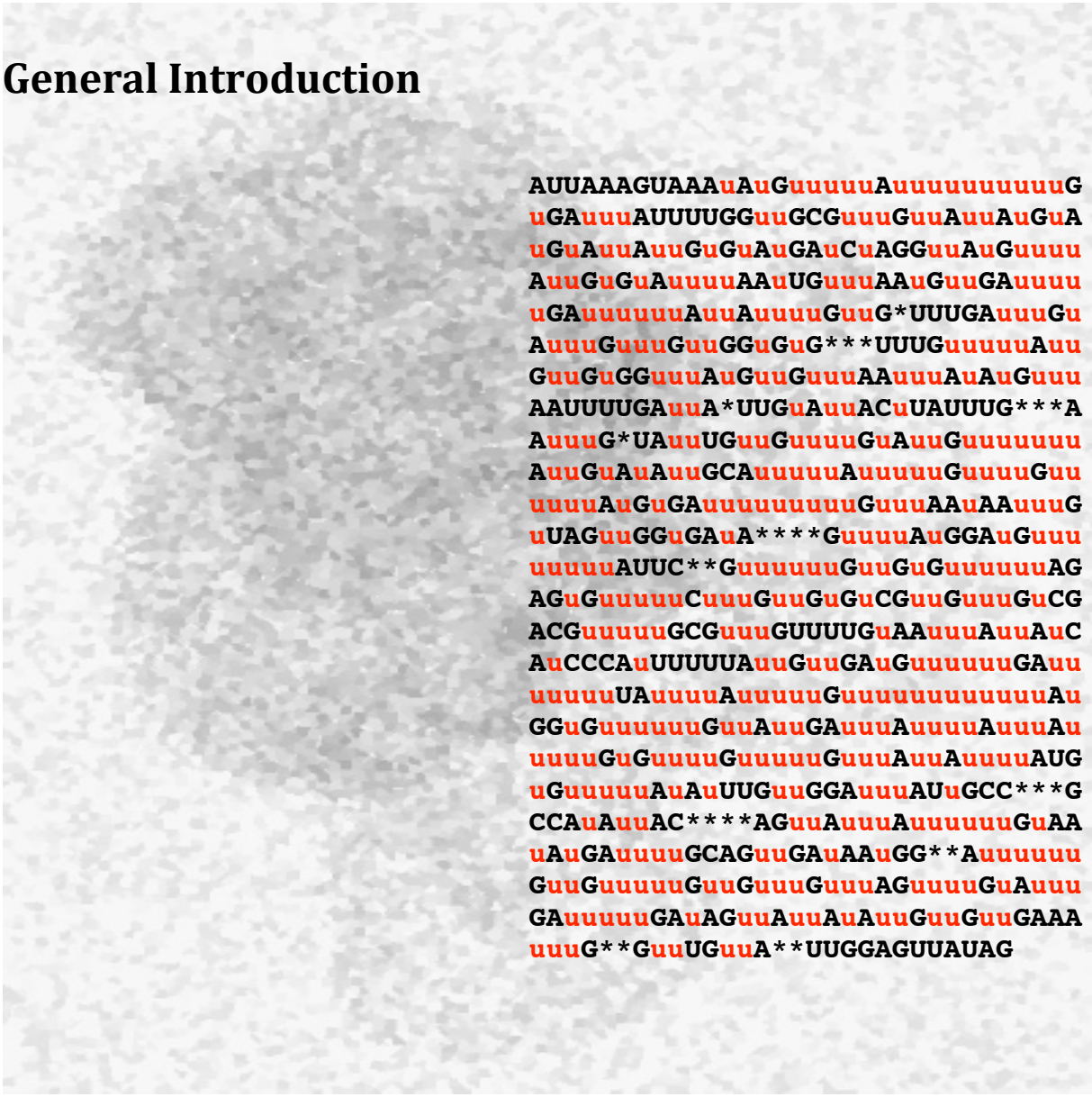

Sequence of the edited transcript of the subunit 6 of the mitochondrial ATPase (A6). U's inserted: red, U's deleted: *.

GENERAL INTRODUCTION

The RNA editing reaction in kinetoplastid protozoa such as African trypanosomes is a unique and probably the most bizarre posttranscriptional modification reaction in any living system (Benne, 1986). The reaction is required for the expression of mitochondrial genes and thus is essential for the survival of the organism. RNA editing is characterized by the insertion and/or deletion of exclusively U-nucleotides thereby converting otherwise cryptic pre-edited (pre-) mRNAs into translatable transcripts. In African trypanosomes, more than 3000 U-residues are inserted and about 300 Us deleted at hundreds of editing sites in 12 different pre-mRNAs (for a recent review see Hajduk and Ochsenreiter, 2010). The process is site specific and requires small, noncoding RNAs, known as guide RNAs (gRNAs) (Blum et al., 1990; Blum and Simpson, 1990; Schmid et al., 1995; Hermann et al., 1997). gRNAs act as quasi templates in the process. They initiate the editing reaction by the formation of a hybrid gRNA/pre-mRNA molecule, which adopts a three-way helix junction topology (Leung and Koslowskz, 2001; Yu and Koslowsky, 2006; Reifur and Koslowsky, 2008). The structure includes a short 'anchoring' duplex element that borders the sequence to be edited. Unpaired gRNA nucleotides next to the anchor region specify U-insertion events with free UTP as a substrate; nonbase-paired uridylates in the pre-mRNA become deleted (Seiwert and Stuart, 1994; Frech and Simpson, 1996; Kable et al., 1996; Seiwert et al., 1996). By utilizing different gRNAs, alternative editing events can occur, which contribute to generate protein diversity within the mitochondria of the parasites (Ochsenreiter and Hajduk, 2006; Ochsenreiter et al., 2008; Ochsenreiter, 2008a).

RNA editing: An enzyme-driven multistep reaction cycle

Early experimental evidence already suggested that RNA editing involves mitochondrial protein components and that the reaction is likely catalyzed by high molecular mass protein complexes (Pollard et al., 1992; Göringer et al., 1994; Köller et al., 1994; Corell et al., 1996; Rusché et al., 1997; Peris et al., 1997). In analogy to ribosomes and spliceosomes, the complexes have been termed editosomes and they function as a reaction platform for the catalysis of the processing reaction in a series of enzyme-driven steps (Blum et al., 1990; Frech and Simpson, 1996; Sabatini and Hajduk, 1995) (Fig. 1). In recent years, the protein inventory of the editosome has been studied in detail and polypeptide candidates for every step of a minimal reaction cycle have been identified (Table 1) (reviewed in Hajduk and Ochsenreiter, 2010; Carnes and Stuart, 2008). The first enzyme-driven step of the reaction cycle is the endonucleolytic cleavage of the pre-mRNA at the first unpaired nucleotide upstream of the pre-mRNA/gRNA duplex. Three related proteins TbMP90, TbMP63, and TbMP67, which all contain U1-like Zn-finger motifs, an RNaseIII domain and a dsRBM sequence possess endonuclease activity. TbMP90 is specific for the cleavage at deletion sites, whereas TbMP63 cleaves at insertion sites (Carnes et al., 2005; Trotter et al., 2005). The function of TbMP67 is not yet fully understood. At a deletion site the endonucleolytic cleavage is followed by the removal of unpaired Us. U-nucleotide-specific ribonuclease (exoUase) activity was identified for TbMP99 and TbMP100, two related proteins with

N-terminal 5'/3' exonuclease and *C*-terminal endo/exo/phosphatase motifs (Kang et al., 2005; Rogers et al., 2007). In addition, these proteins possess nucleotidyl phosphatase activity (Niemann et al., 2009). TbMP42, a protein with two C_2H_2-Zn-finger domains and a putative oligonucleotide/oligosaccharide binding (OB)-fold executes endo- and exoribonuclease activity *in vitro*, likely following a two-metal ion reaction mechanism (Brecht et al., 2005; Niemann et al., 2008). Following endo-nucleolytical cleavage at an insertion site, Us are added to the 3'-end of the 5'-cleavage product of the mRNA in a gRNA-dependent fashion. This step of the reaction is catalyzed by TbMP57, a protein with a catalytic poly(A) polymerase (PAP) domain that executes terminal uridylyltransferase (TUTase) activity (Ernst et al., 2003). At the end of the processing cycle the two editing-specific RNA ligases TbMP48 and TbMP52 rejoin the two processed mRNA fragments (McManus et al., 2001; Rusché et al., 2001; Gao and Simpson, 2003; Deng et al., 2004).

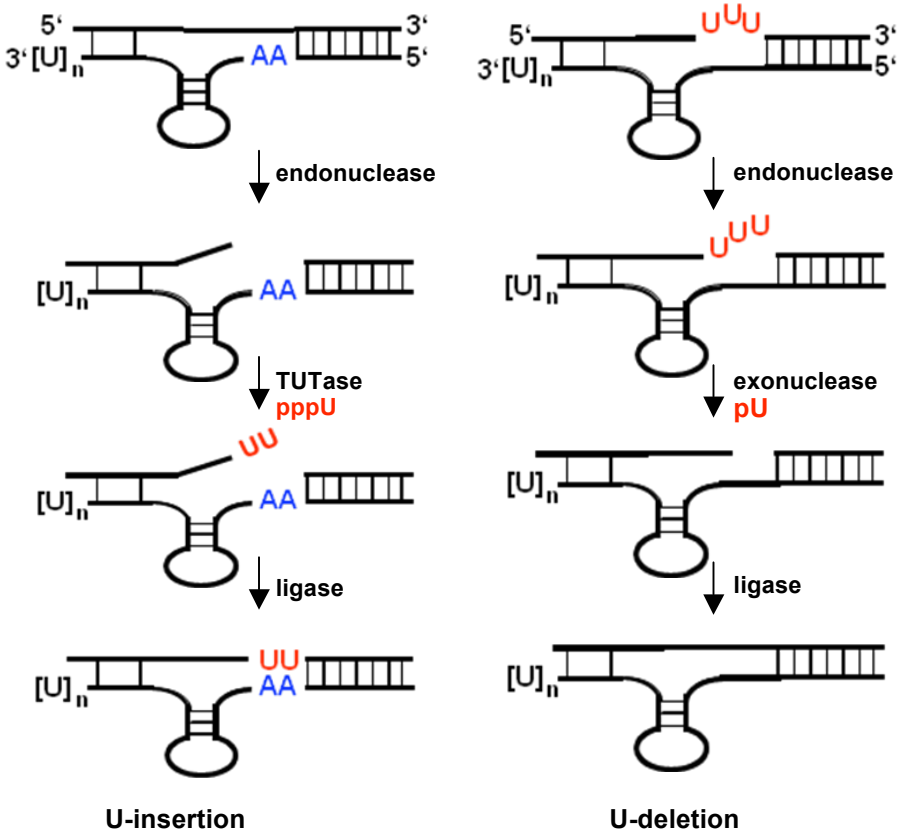

Figure 1. Mechanistic outline of the basal reaction steps of U-insertion (left) and U-deletion (right) RNA editing in *Trypanosoma brucei*. Guide RNA molecules interact with cognate pre-edited mRNAs via anti-parallel base pairing thereby forming a three-helix junction RNA hybrid. The interaction relies on Watson/Crick-type base-pairing as well as non-canonical G:U bp. Endonucleolytic cleavage of the pre-mRNA occurs at the first non-base-paired nucleotide (nt) upstream of the so-called anchor duplex. U-insertion editing continues by adding U nt (from UTP) to the 3'-end of the 5' pre-mRNA cleavage fragment. The reaction is catalyzed by a terminal uridylyltransferase (TUTase). During deletion editing, U nts are removed from the 3'-end of the 5' cleavage fragment, using the activity of a 3' exonuclease (exoUase). In both cases, the number of U's (inserted or deleted) is specified by the "guiding" sequence of the gRNA. Resultant pre-mRNA cleavage fragments are finally ligated by an RNA ligase. Several editing cycles must occur until all editing sites specified by one gRNA are processed. Complete editing of a pre-mRNA requires in most cases multiple gRNAs. The reaction proceeds with a 3' to 5' directionality on the pre-mRNA. Figure adapted from Göringer, 2012.

Aside from these core activities that catalyze the main steps of the reaction

cycle several accessory factors are required (for reviews see Carnes and Stuart, 2008; Göringer et al., 2008). These proteins presumably bind only temporarily to the editosome to contribute additional functionality (Table 1). This includes the matchmaking-type RNA/RNA annealing factors gBP21 and gBP25 (Köller et al., 1997; Allen et al., 1998; Müller et al., 2001; Blom et al., 2001; Müller and Göringer, 2002; Aphasizhev et al., 2003; Schumacher et al., 2006), the proteins RBP16 (Hayman and Read, 1999; Pelletier et al., 2000; Miller and Read, 2003; Pelletier and Read, 2003), TbRGG1 (Vanhamme et al., 1998; Hashimi et al., 2008), REAP1 (Madison-Antenucci et al., 1998; Madison-Antenucci and Hajduk, 2001; Hans et al., 2007), and RBP38 (Sbicego et al., 2003). It also includes the 3'-end-specific TUTase KRET1 (Aphasizhev et al., 2002; Aphasizhev et al., 2003; Aphasizheva and Aphasizhev, 2010) and the mitochondrial DExH/D protein mHel61p (Göringer et al., 2008; Missel and Göringer, 1994; Missel et al., 1997). Although the presence of accessory editing factors is unquestioned, no knowledge concerning the dynamic interplay of these proteins with the editosome exist. Unfortunately, this also holds true for the internal dynamic of the catalytic machinery itself.

Editosome	Motif	Identified/Proposed function
MP18	OB fold	gRNA binding
MP19	OB fold	Interaction
MP24	OB fold	gRNA binding
MP41	U1-like	Interaction
MP42*	Zn-finger, OB fold	Endo/exonuclease; organization
MP44	RNaseIII, Pumilio, U1-like	Editosome integrity
MP46	RNaseIII, Pumilio, U1-like	Editosome integrity
MP47	U1-like	Interaction
MP48/REL2	Ligase, tau, K	RNA ligase
MP49	U1-like	Interaction
MP52/REL1	Ligase, tau, K	RNA ligase
MP57/RET2	NZ, PAP-core, PAP-assoc	TUTase
MP61/REN2	RNaseIII, dsRBM, U1-like	Interaction-specific endonuclease
mHel61p	DExH/D-box Helicase	RNA helicase, RNPase
MP63	Zn-finger, OB-fold	Interaction
MP67/REN3	RNaseIII, dsRBM, U1-like	COXII-specific endonuclease
MP81	Zn-finger, OB-fold	Interaction
MP90/REN1	RNaseIII, dsRBM, U1-like	Deletion-specific endonuclease
MP99/REX2	5'/3' exonuclease, EEP-domain	Nuclease/nucleotidyl phosphatase
MP100/REX1	5'/3' exonuclease, EEP-domain	Nuclease/nucleotidyl phosphatase
Accessory Proteins		
gBP21	R-rich	RNA matchmaking
gBP25	R-rich	RNA matchmaking
RBP16	Cold shock domain, RGG	Interaction
TbRGG1	RGG	mRNA stabilization
KRET1	NT, PAP-core, PAP-assoc, Zn-finger	TUTase

Table 1. List of the editosomal protein inventory. Most peptides are annotated according to the nomenclature: TbMPxx: *Trypanosoma brucei* mitochondrial protein, kDa. Sequence motifs are annotated in the middle column. The suggested function is derived from experiments or sequence predictions. "Interaction" means binding RNA/protein, no catalytic activity has been discovered. EEP: endo-exo-phosphatase; RNaseIII: endoribonuclease motif from RNaseIII; dsRBM: double-stranded RNA binding motif; U1-like: U1-like Zn-finger motif; Pumilio: Pumilio domain RNA binding motifs; ligase: signatur ligase motif; tau and K: putative microtubule associated tau and kinase light chain domains; RGG: arginine-glycine-glycine motif; R-rich: arginine-rich domain; DExH/D-box: aspartate-glutamate-x-histidine/aspartate helicase consensus sequence.

Endogenous RNA editing complexes

Native editosomes of African trypanosomes have been enriched from the endogenous steady state pool of mitochondrial editing complexes by a variety of biochemical protocols (for a review see Panigrahi et al., 2007). Starting material are usually insect-stage trypanosomes, which rely on fully developed mitochondria for their energy consumption and thus are expected to have maximal RNA editing activity. Nonsynchronized cells are harvested at mid-log growth conditions and are used to isolate mitochondrial vesicles by various cell disruption and subcellular fractionation methods (Hermann et al., 1997; Göringer et al., 1994; Rusché et al., 1997; Hauser et al., 1996). Mitochondrial vesicle preparations are converted into low-salt detergent lysates using low concentrations of non-ionic detergents followed by isokinetic density gradient centrifugation techniques or column purification schemes. Following these protocols, active editing complexes harboring as little as 7 (Rusché et al., 1997), 13 (Golas et al., 2009; Aphasizhev et al., 2003) or up to 20 polypeptides (Panigrahi et al., 2001) have been described. However, all enrichment protocols generate low yields of complexes, either suggesting low steady state concentrations or low kinetic/thermodynamic and/or chemical (i.e., redox) stabilities of the complexes. Therefore, more recent purification schemes have applied near native enrichment conditions mainly following the tandem affinity purification (TAP) protocol as developed by Rigaut et al., 1999. The procedure relies on transgenic trypanosomes that conditionally express TAP-tagged versions of different editosomal proteins (reviewed in Panigrahi et al., 2007). The TAP-tag contains protein A and calmodulin binding domains separated by a tobacco etch virus (TEV) protease cleavage site, which allows for chemically moderate, i.e., 'native-like' chromatographic separation and elution conditions.

TAP-tagged editosome preparations have been visualized by transmission electronmicroscopy (TEM) and by cryo-EM (Golas et al., 2009; Kastner et al., 2008). Raw EM images display monodisperse populations of two classes of high molecular mass assemblies in addition to some high molecular mass aggregates. The two classes consist of 'large', asymmetric complexes of up to 26 nm in diameter as well as 'smaller', elongated complexes with dimension of 21 x 26 nm. Both types of complexes are characterized by well-defined, compact shapes with distinct structural features including surface areas of different electron density. In line with previous experimental data (Pollard et al., 1992; Corell et al., 1996), sedimentation analysis characterized the two particle classes as high molecular mass assemblies with apparent S-values of 20S and 35–40S (Golas et al., 2009). Unfortunately no 'real' S-value determination has been attempted to date. Importantly, 35–40S complexes have been shown to be associated with endogenous RNA including pre-mRNA and gRNA (Pollard et al., 1992; Corell et al., 1996; Golas et al., 2009) and thus likely embody the steady state population of editing complexes actively engaged in the processing reaction. 20S complexes are 'protein-only' assemblies (Rusché et al., 1997; Golas et al., 2009) that consist of 13 polypeptides: TbMP100, TbMP99, TbMP90, TbMP67, TbMP63, TbMP61, TbMP57, TbMP52, TbMP48, TbMP46, TbMP44, TbMP42, and TbMP24. This includes all of the aforementioned core activities of the editing reaction cycle

and thus, 20S complexes are competent to faithfully edit synthetic pre-edited insertion and deletion substrate mRNAs in a gRNA-dependent fashion (Igo et al., 2000; Igo et al., 2002; Carnes and Stuart, 2007). By contrast, isolated 35–40S complexes are inactive to bind and process synthetic pre-mRNA molecules likely because their RNA binding site/sites is/are occupied with endogenous RNA (Golas et al., 2009).

Landmarks of the consensus structure of the 35-40S editosome

Two-dimensional (2D) class averaging methods in combination with 3D averaging algorithms combining random conical tilt (RCT) (Rademacher et al., 1987) and weighted averaging methods (Sigworth, 1998) have been used to derive a consensus 3D structure of the 35–40S complex (Fig. 2). The structure is characterized by defined landmarks: an elongated, straight to slightly convex platform is packed against a semispherical element. The platform extends on two sides into small head-like protrusions: one oriented to the top, the other to the bottom forming a larger foot-like extension. The semispherical back is packed against the platform as a tight network and the interface between both elements is marked by incisions in the upper and lower part. The semispherical back element is asymmetric in its appearance displaying on one side a protruding shoulder-type element and on the other side an inclination or proclivity. A structure refinement of the 35–40S complex by cryonegative staining EM resulted in a resolution of 13–19 nm and the surface of the complex was calculated to enclose a molecular mass of 1.45 ± 0.15 MDa (Golas et al., 2009). The data have been further used to calculate a theoretical sedimentation coefficient of 35–41S (Garcia de la Torre et al., 2001), which is in agreement with the experimentally derived apparent sedimentation behavior observed in isokinetic glycerol gradients (Pollard et al., 1992; Peris et al., 1997).

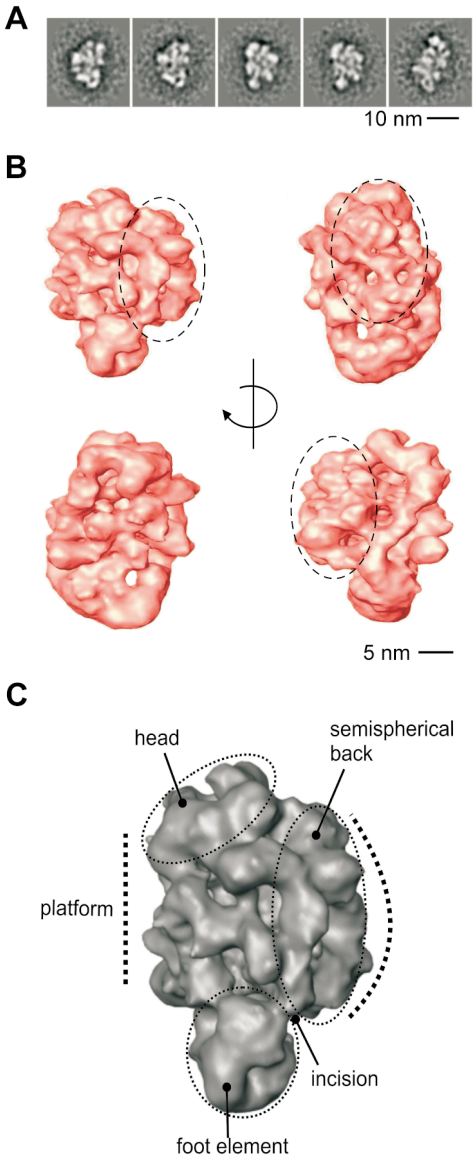

Figure 2. Consensus structure of the *Trypanosoma brucei* 35–40S RNA editing complex (Golas et al., 2009). (A) Raw electron microscopy images of five individual complexes in different orientations. (B) Model of the consensus structure of the 35–40S complex. Four shaded surface views are shown rotated clockwise in 90° increments along the vertical axis. Prominent structural landmarks are labeled in (C).

Structural landscape of the 35-40S editosome

EM analysis of several thousands of individual 35–40S particles revealed a

diverse structural landscape of the 35–40S complexes. This is not unexpected as the purified particles represent the endogenous steady state pool of stable editing complexes, which likely differ in their functional and/or assembly state as well as the type of substrate RNA that is bound to it. Although most of the complexes show a density profile in line with the described consensus structure, variable regions are apparent in the periphery of the semispherical back element and in the size and position of the foot-like domain. A 3D multivariate statistical analysis (MSA) (Liu et al., 2004) using aligned 3D RCTs as an input (Sander et al., 2006) revealed a minimum of six morphologically different 3D subtypes (Fig. 3). Four of the 3D struc-tures display all the structural characteristics of the consensus structure and differ only in the proportions of the semispherical back ranging from 'small' to 'extensive'. The different subpopulations were quantified by various independent methods including competitive multireference alignment (cMRA) demonstrating that about 40% of the particles adopt the consensus structure conformation, whereas all other subpopulations occurred at a frequency of roughly 10–20%. The data are in accord with biochemical experiments that have shown that the hydrodynamic size of the 35–40S complexes is to a certain degree variable. The apparent S-value varies depending on the extent of editing in substrate mRNAs in the complex (Poll-ard et al., 1992; Madison-Antenucci et al., 2002), which could be a consequence of the increased molecular mass of the mRNA itself, or due to other factors that associate with the complex at this stage of the reaction cycle.

Landmarks of the consensus structure of the 20S editosome

As mentioned above, raw EM images of purified 20S editosomes show a monodisperse population of elongated, slightly bent particles with dimensions of up to 21–26 nm. The 2D class averages show a variety of different projections: triangular, bent, semicircular, and elongated–indicating a heterogeneous sample composition.

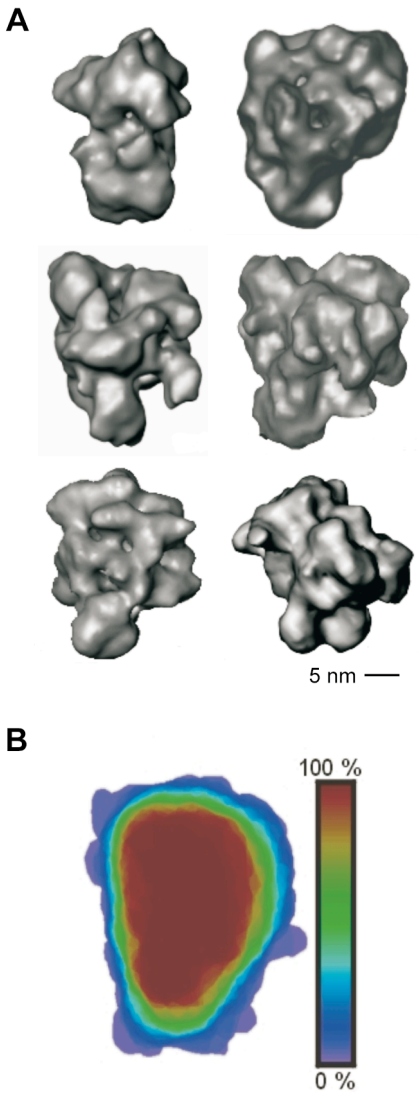

Figure 3. Structural landscape of the *Trypanosoma brucei* 35–40S editosome (Golas et al., 2009). (A) Refined models of six representative 3D class averages. (B) Shape profiling of the 35–40S complex by color-scale encoded overlays. The data demonstrate that the majority of complexes consist of a platform density that converges in a semispherical back element (red).

The derived consensus structure of the 20S complex is characterized by an elongated, slightly bent appearance (Fig. 4), which results in a concave/convex shape, displaying one concave and one convex contour on opposite sides. The particle is composed of two globular domains roughly equal in size. Both subdomains interact extensively in an interface region where a protruding arm extends on one side and a triangular protrusion emerges from the opposite side. The two subdomains differ in their structural details indicating that 20S editosomes are no homodimers. The consensus structure was refined by cMRA to a resolution of 1.97–2.20 nm using cryo-EM data sets. The refined 3D reconstruction is characterized by additional fine structural details especially in the interface region between the two equally sized subdomains. The surface representation of the 20S particle was estimated to enclose a molecular mass of 800 ± 80 kDa. The value is consistent with the sum of all proteins identified in the biochemical analysis (790 kDa), assuming that every protein is present in single copy (Golas et al., 2009). A theoretical sedimentation coefficient was calculated to 21–26S, in line with the experimentally determined apparent value of 20–24S (Pollard et al., 1992; Corell et al., 1996).

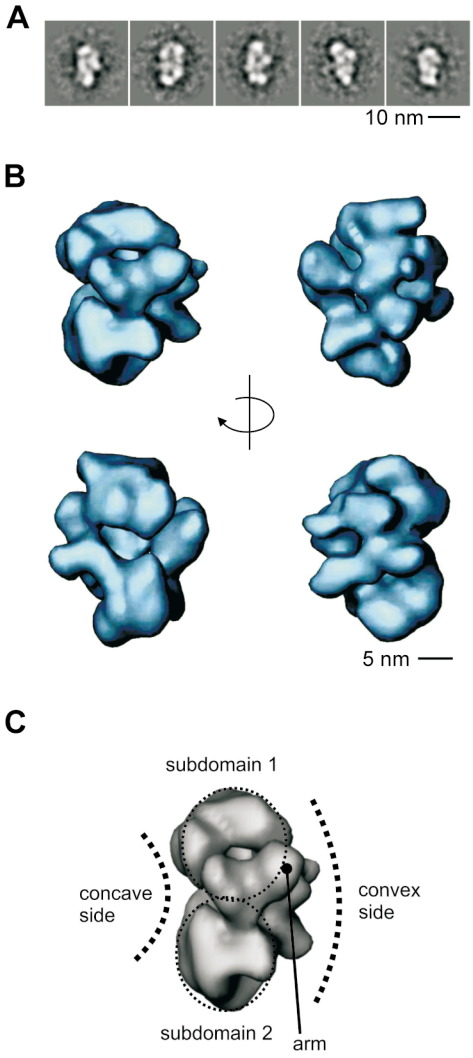

Figure 4. Consensus structure of the *Trypanosoma brucei* 20S RNA editing complex (Golas et al., 2009). (A) Raw electron microscopy images of five individual complexes in different orientations. (B) Model of the consensus structure of the 20S complex. Four shaded surface views are shown rotated clockwise in 90° increments along the vertical axis. Prominent structural landmarks are labeled in (C).

Structural landscape of the 20S editosome

An MSA of the 3D RCTs of the 20S complex revealed a defined structural landscape and identified four morphological 20S subtypes. These subtypes differ in the relative positions of the two subdomains resulting in different curvatures of the particles and most prominently in the presence of a semispherical element that is packed against the interface region (Fig. 5). The first subgroup contains particles that show a clear separation into two subdomains of about equal size connected by an interface. The two subdomains adopt variable relative positions thereby altering the bent appearance of the complexes. The second subgroup also shows a bipartite shape, but in addition displays a small semispherical element similar to the 35–40S complexes. The third and fourth subgroup exhibit more elon-

gated structures but still are characterized by the described bipartite overall shape. Furthermore, subtype number four possesses an extra domain attached to the main body in the upper right region. An overlay of all 3D shapes identified that the majority of complexes has an elongated, slightly curved shape, whereas in some particles additional densities are attached to the upper region. Using cMRA the abundance of the 3D subtypes was calculated and confirmed that about

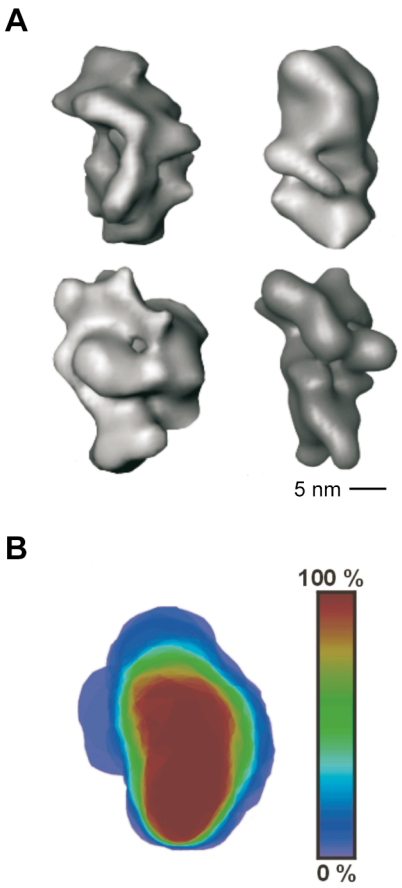

Figure 5. Structural landscape of the *Trypanosoma brucei* 20S editosome (Golas et al., 2009). (A) Refined models of four representative 3D class averages. (B) Shape profiling of the 20S complex by color-scale encoded overlays. The data demonstrate that the majority of complexes are composed of two subdomains connected by a broad interface (red).

25–35% of all complexes were assigned to two 3D subgroups, which exhibit the highest visual similarity to the consensus structure.

Interconversion of 20S and 35-40S complexes

The structural relationship between 20S and 35–40S editosomes has been investigated by applying a multistep fitting approach. 3D class averages of 20S and 35–40S complexes with similar morphological features were used as anchor points to manually dock 20S complexes into 35–40S complexes. The docking process was refined through a 3D alignment procedure, which demonstrated that 20S complexes represent a large part of the platform density of the 35–40S complexes including in some cases small subdomains of the semispherical back. 20S complexes can be integrated in the head domain, the upper part of the platform and part of the back domain of the 35–40S complex (Fig. 6). By contrast, the foot domain, the lower part of the platform density and the majority of the semispherical back appears to be composed of compo-

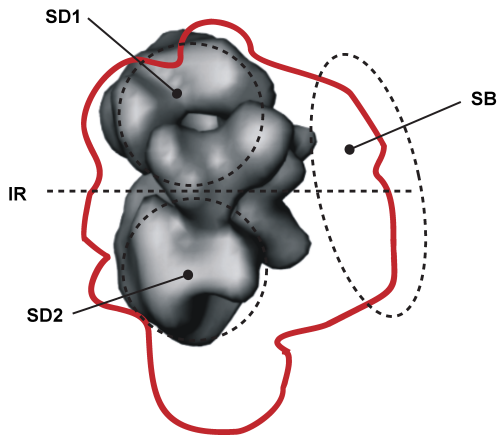

Figure 6. Integration of the consensus 20S structure into an outline (red) of the consensus 35-40S complex. The two nearly globular 20S subdomains are labeled SD1 and SD2. IR marks the interface region that connects subdomain1 with subdomain2. The semispherical back (SB) is in contact with both subdomains and reaches into the interface region. The semispherical element consists of bound substrate RNA.

nents that have no structural correlate in the 20S particles. As the main bio-

chemical difference between 20S and 35–40S complexes is their RNA content it is enticing to speculate that the semispherical back of the 35–40S complexes represents gRNA and/or pre-mRNA molecules only – although the presence of a small number of additional proteins cannot be excluded. Minor differences in the orientation of distinct subdomains are also visible. This involves some positional differences of the head-like and foot-like protuberances, which suggests conformational and/or compositional changes of the complexes, possibly indicating different functional stages within the processing cycle. Together, the data corroborate a structural relation of the two complexes and imply a common structural core of the editing machinery. Experimental confirmation of the described scenario was gained from interconversion RNase digestion experiments. Treatment of 20S and 35–40S complexes with single- and double-strand-specific RNases resulted in a concentration-dependent decrease in the amount of 35–40S editosomes and at the same time in an increase of 20S complexes. Conversely, incubation of isolated 20S editosomes with *Trypanosoma brucei* mitochondrial RNA, which contains pre- and partially edited mRNAs as well as gRNAs, generated 35–40S complexes in a concentration-dependent fashion (Golas et al., 2009). The substrate RNA/20S interaction is of high affinity with equilibrium dissociation constants (K_d) in the nanomolar concentration range (Golas et al., 2009).

Functional subdomains and RNA reaction center

Next to unraveling the protein inventory of the 20S complex, attempts have been published to describe the interconnectivity and general organization of individual proteins within the particle (Schnaufer et al., 2003; Schnaufer et al., 2010). Although the precise architecture is far from being understood, it is undisputed that functional 20S particles can be assembled in the absence of pre-edited mRNA and gRNA (Domingo et al., 2003). Furthermore, biochemical data suggest that insertion and deletion RNA editing may be catalyzed by separate editing subcomplexes or subdomains (for a review see Carnes and Stuart, 2008). This is ostensibly supported by the fact that the editing core activities are present in protein pairs or even higher numbers (Hajduk and Ochsenreiter, 2010; Stuart et al., 2005). Yeast two-hybrid (Y2H) and co-immunoprecipitation experiments identified possible protein/protein interaction partners among different editosomal proteins, which together suggest that 20S complexes consist of structurally separated insertion and deletion subdomains (Schnaufer et al., 2003). The insertion domain is assembled around a trimeric protein core involving the TUTase TbMP57, the RNA editing ligase TbMP48, and protein TbMP81. The deletion subdomain relies on the heterotrimeric interaction of the exoUase TbMP99, the RNA editing ligase TbMP52, and protein TbMP63. Other polypeptides associate with both subdomains such as TbMP44 and TbMP24 (Wang et al., 2003; Salavati et al., 2006). TbMP18 likely represents a protein that is located at the interface between both subdomains (Law et al., 2007). Some of these results have been confirmed using TAP-tagged editosome preparations (reviewed in Carnes and Stuart, 2008) and have provided insight into the structure/function correlation of various proteins in the 20S complex.

Although no experimental evidence exists, it is tempting to speculate that

the compositionally different deletion and insertion subdomains correspond to the bipartite substructures of the 20S consensus model (Fig. 4). The model obviously displays two non-identical nearly globular subdomains, which are connected through an interface region in line with the above described biochemical data. Whether that implies that both subdomains have independent RNA binding sites is not known to date. However, based on the structural details of the 35–40S complexes, in which the semispherical back of the complex was identified as bound substrate RNA, it is more likely that the 20S complex has only one RNA interaction site. The binding site covers a substantial part on one side of the 20S surface and in part reaches into the interface region in-between the two globular subdomains. Thus, a single catalytic core for both editing reactions might be positioned at the interface between the deletion and insertion subdomains representing a 'dual mode' reaction center that is triggered by the chemical nature of the bound substrate RNA. Deletional editing substrates activate the deletion subdomain and insertion-type substrate RNAs become processed by the insertion subdomain.

Compositionally distinct 20S complexes

Evidence for functionally and compositionally distinct 20S complexes has been derived from the analysis of editing complexes isolated from transgenic trypanosome strains that conditionally express TAP-tagged variants of different editosomal proteins. Tandem affinity-purified editosomes possess in some cases only a subcollection of the 20S protein inventory and these compositional differences are mirrored in functional differences (Panigrahi et al., 2006). For instance, TbMP-90-TAP editosomes execute only deletional RNA editing, whereas TbMP61-TAP complexes only process insertional editing substrate RNAs. Protein TbMP100 is only present in TbMP90-TAP editing complexes, whereas TbMP81, TbMP63, TbMP42, TbMP24, TbMP18, TbMP46, TbMP44, TbMP57, TbMP99, TbMP52, and TbMP48 seem to be ubiquitous. On the contrary, the three proteins TbMP99, TbMP61, and TbMP67 have been shown to be mutually exclusive in certain complexes. Based on these data, Carnes et al., 2008 suggested that at least three compositionally distinct editosomes exist. Whether these partially assembled machineries contribute to the endogenous, steady state ensemble of editosomes in genetically unaltered, i.e., wildtype trypanosomes is not known. However, the data at least demonstrate that multiple assembly pathways exist for the processing machinery and that heterogeneous populations of 20S complexes are tolerated in *in vivo* isolates. Therefore, some partially assembled editosomes may contribute to the structural landscape of 20S complexes identified in the cryo-EM analysis as described above. In addition, it cannot be excluded that the composition of editosomes may be in a dynamic equilibrium. Individual components like the above described accessory factors (Göringer et al., 2008) may at different stages of the assembly pathway shuttle in and out of the complex thereby further expanding the structural landscape of the particle.

'Quasi' 35-40S complexes

Taken together, the described experimental data can be summarized to derive a first picture that correlates some of the prominent structural features of the 20S and 35–40S complexes with functional attributes of the

RNA editing reaction cycle. Steady state editosome preparations in African trypanosomes consist of a mixture of two classes of high molecular mass complexes: 35–40S complexes represent the editing machinery that is actively engaged in the processing reaction, whereas 20S complexes are preassembled precursor complexes that consist of proteins only. The binding of substrate RNAs converts 20S editosomes into 35–40S complexes and depending on the type of RNA differently shaped 35–40S complexes are formed. Altogether 12 pre-edited mRNAs and literally hundreds of gRNA and partially edited mRNA molecules are present in African trypanosomes. gRNAs have molecular masses around 20 kDa, whereas the involved mRNAs vary between 60 kDa (unedited CR3) and 450 kDa (edited ND7). As a consequence, their hydrodynamic radius must vary and at steady state conditions this results in a broad structural landscape of multiple 35–40S complexes with different overall shapes. However, these particles differ predominantly in only one structural feature: the semispherical back element. This part of the complex represents the RNA interaction site of the editosome, which implies that 20S editosomes have only one RNA binding domain that interacts with a large structural ensemble of differently sized and folded substrate RNAs. The RNA binding site covers a large surface area on one side of the 20S particle and contacts the interface between the two nonidentical, globular subdomains of the 20S editosome.

The identified structural landscape of the 20S steady state population can be explained following a similar line of arguments. Clearly, the majority of these complexes are protein-only particles with a defined polypeptide architecture and perhaps multiple assembly routes. However, 20S editosomes that are associated with small substrate RNAs [for instance unedited CR3 (60 kDa) or unedited S12 (80 kDa)] should not significantly differ in their hydrodynamic behavior from the protein-only 20S complexes and thus likely co-purify. This is supported by the observation that the most prominent structural difference in some of the 20S subtypes is a small additional 'back' domain located exactly in an area that coincides with the semispherical back in the 35–40S complexes. In functional terms, these complexes represent RNA loaded 'quasi' 35–40S complexes, despite the fact that their hydrodynamic properties are only around 20S (Fig. 7). Due to their small size and perhaps more importantly due to very low concentrations, the bound RNAs are difficult to identify and it should be noted that

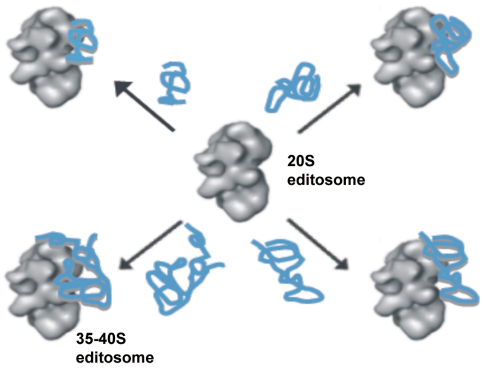

Figure 7. Molecular ensembles of active editosomes. 20S editosomes interact with a large intracellular pool of substrate RNAs (blue ribbons) with different molecular masses and folding characteristics and as a consequence with different hydrodynamic radii. This results in a sizeable structural landscape of RNA-bound editosomes, which differ for the most part in the dimension of the semispherical back element. The binding of 'large' substrate RNAs generates 35–40S editosomes, whereas the binding of 'small' RNA ligands results in RNA-loaded editosomes with S-values only marginally above 20S.

differing results addressing the presence of RNA in 20S preparations have been reported (Pollard et al., 1992;

Corell et al., 1996; Rusché et al., 1997). The protein-only 20S editosome is characterized by a bipartite appearance with two prominent globular subdomains. Both subdomains, however, differ in their structural details indicating that the particle is not a homodimer. In conjunction with the described biochemical data, these substructures likely represent separate insertion and deletion subdomains and they are assembled around different protein core elements in line with the different enzyme requirements that catalyze the two types of editing reactions. The two subdomains connect in an interface region, which is linked to the RNA binding domain of the complex. This suggests a working model in which the editosome reaction center is located at the interface of the insertional and deletional subdomains thereby presenting a catalytic core of bifunctional quality. As a result, editosome-bound substrate RNA can be in physical contact with both catalytic machineries and depending on the RNA editing domain, both, U-insertions and deletions can be executed on the same pre-mRNA. This is further supported by the fact that single gRNAs can mediate insertion as well as deletion editing (Blum et al., 1990; Maslov and Simpson, 1992). Understanding the conformational dynamic and adaptive recognition at the catalytic center of the editosome will be the next experimental and perhaps conceptual challenge.

References

Allen TE, Heidmann S, Reed R, Myler PJ, Göringer HU and Stuart KD. (1998) Association of guide RNA binding protein gBP21 with active RNA editing complexes in *Trypanosoma brucei*. *Mol. Cell Biol.* 18:6014–6022.

Aphasizhev R, Aphasizheva I and Simpson L. (2003) A tale of two TUTases. *Proc. Natl. Acad. Sci. U.S.A.* 100: 10617–10622.

Aphasizhev R, Aphasizheva I, Nelson RE and Simpson L. (2003) A 100-kD complex of two RNA-binding proteins from mitochondria of *Leishmania tarentolae* catalyzes RNA annealing and interacts with several RNA editing components. *RNA* 9:62–76.

Aphasizhev R, Aphasizheva I, Nelson RE, Gao G, Simpson AM, Kang X, Falick AM, Sbicego S and Simpson L. (2003) Isolation of a U-insertion/deletion editing complex from *Leishmania tarentolae* mitochondria. *EMBO J.* 22:913–924.

Aphasizhev R, Sbicego S, Peris M, Jang SH, Aphasizheva I Simpson AM, Rivlin A and Simpson L. (2002) Trypanosme mitochondrial 3' terminal uridylyl transferase (TUTase): the key enzyme in U-insertion/deletion RNA editing. *Cell* 108:637–648.

Aphasizheva I and Aphasizhev R. (2010) RET1-catalyzed uridylylation shapes the mitochondrial transcriptome in *Trypanosoma brucei*. *Mol. Cell Biol.* 30:1555–1567.

Benne R, Van Den Burg J, Brakenhoff JP, Sloof P, Van Boom JH and Tromp MC. (1986) Major transcript of the frame shifted coxII gene from trypanosome mitochondria contains four nucleotides that are not encoded in the DNA. *Cell* 46:819–826.

Blom D, Burg Jv, Breek CK, Speijer D, Muijsers AO and Benne R. (2001) Cloning and characterization of two guide RNA-binding proteins from mitochondria of *Crithidia fasciculata*: gBP27, a novel protein, and gBP29, the orthologue of *Trypanosoma brucei* gBP21. *Nucl. Acids Res.* 29:2950–2962.

Blum B and Simpson L. (1990) Guide RNAs in kinetoplastid mitochondria have a nonencoded 3' oligo(U) tail involved in recognition of the preedited region. *Cell* 62:391–397.

Blum B, Bakalara N and Simpson L. (1990) A model for RNA editing in kinetoplastid mitochondria: ''guide'' RNA molecules transcribed from maxicircle DNA provide the edited information. *Cell* 60:189–198.

Brecht M, Niemann M, Schlüter E, Müller UF, Stuart K and Göringer HU. (2005) TbMP42, a protein component of the RNA editing complex in African trypanosomes has endo-exoribonuclease activity. *Mol. Cell* 17:621–630.

Carnes J and Stuart K. (2007) Uridine insertion/deletion editing activities. *Meth Enzymol.* 424:25–54.

Carnes J and Stuart K. (2008) Working together: the RNA editing machinery in *Trypanosoma brucei*. In: Göringer HU, ed. *RNA Editing, Nucleic Acids and Molecular Biology*, vol. 20. Heidelberg: Springer Publishing, 143–164.

Carnes J, Trotter JR, Ernst NL, Steinberg A and Stuart K. (2005) An essential RNase III insertion editing endonuclease in *Trypanosoma brucei*. *Proc. Natl. Acad. Sci. U.S.A.* 102:16614–16619.

Carnes J, Trotter JR, Peltan A, Fleck M and Stuart K. (2008) RNA editing in *Trypanosoma brucei* requires three different editosomes. *Mol. Cell Biol.* 28:122–130.

Corell RA, Read LK, Riley GR, Nellissery JK, Allen TE, Kable ML, Wachal MD, Seiwert SD, Myler PJ and Stuart KD. (1996) Complexes from *Trypanosoma brucei* that exhibit deletion editing and other editing-associated properties. *Mol. Cell Biol.* 16:1410–1418.

Deng J, Schnaufer A, Salavati R, Stuart KD and Hol WG. (2004) High resolution crystal structure of a key editosome enzyme from *Trypanosoma brucei*: RNA editing ligase 1. *J. Mol. Biol.* 343:601–613.

Domingo GJ, Palazzo SS, Wang B, Pannicucci B, Salavati R and Stuart KD. (2003) Dyskinetoplastic *Trypanosoma brucei* contains functional editing complexes. *Eukaryot. Cell* 2:569–577.

Ernst NL, Panicucci B, Igo RP Jr, Panigrahi AK, Salavati R and Stuart K. (2003) TbMP57 is a 3' terminal uridylyl transferase (TUTase) of the *Trypanosoma brucei* editosome. *Mol. Cell* 11:1525–1536.

Frech GC and Simpson L. (1996) Uridine insertion into preedited mRNA by a mitochondrial extract from *Leishmania tarentolae*: stereochemical evidence for the enzyme cascade model. *Mol. Cell Biol.* 16:4584–4589.

Gao G and Simpson L. (2003) Is the *Trypanosoma brucei* REL1 RNA ligase specific for U-deletion RNA editing and is the REL2 RNA ligase specific for U-insertion editing? *J. Biol. Chem.* 278:27570–27574.

Garcıa de la Torre J, Llorca O, Carrascosa JL and Valpuesta JM. (2001) HYDROMIC: prediction of hydrodynamic properties of rigid macromolecular structures obtained from electron microscopy images. *Eur. Biophys. J.* 30:457–462.

Golas MM, Böhm C, Sander B, Effenberger K, Brecht M, Stark H and Göringer HU. (2009) Snapshots of the RNA editing machine in trypanosomes captured at different assembly stages in vivo. *EMBO J.* 28:766–778.

Göringer HU, Brecht M, Böhm C and Kruse E. (2008) RNA editing accessory factors—the example of mHel61p. In: Goringer HU, ed. *RNA Editing, Nucleic Acids and Molecular Biology*, vol. 20. Heidelberg: Springer Publishing, 165–179.

Göringer HU, Koslowsky DJ, Morales TH and Stuart K. (1994) The formation of mitochondrial ribonucleoprotein complexes involving gRNA molecules in *Trypanosoma brucei*. *Proc. Natl. Acad. Sci. U.S.A.* 91:1776–1780.

Göringer HU. (2012) "Gestalt," Composition and function of the *Trypanosoma brucei* editosome. *Annu. Rev. Microbiol.* 66:65-82.

Hajduk S and Ochsenreiter T. (2010) RNA editing in kinetoplastids. *RNA Biol.* 7:229-236.

Hans J, Hajduk SL and Madison-Antenucci S. (2007) RNA editing- associated protein 1 null mutant reveals link to mitochondrial RNA stability. *RNA* 13:881–889.

Hashimi H, Zíkova A, Panigrahi AK, Stuart K and Lukes J. (2008) TbRGG1, an essential protein involved in kinetoplastid RNA metabolism that is associated with a novel multiprotein complex. *RNA* 14:970–980.

Hauser R, Pypaert M, Häusler T, Horn EK and Schneider A. (1996) In vitro import of proteins into mitochondria of *Trypanosoma brucei* and *Leishmania tarentolae*. *J. Cell Sci.* 109:517–523.

Hayman ML and Read LK. (1999) *Trypanosoma brucei* RBP16 is a mitochondrial Y-box family protein with guide RNA binding activity. *J. Biol. Chem.* 274:12067–12074.

Hermann T, Schmid B, Heumann H and Göringer HU. (1997) A three-dimensional working model for a guide RNA from *Trypanosoma brucei*. *Nucl. Acids Res.* 25:2311–2318.

Igo RP Jr, Palazzo SS, Burgess ML, Panigrahi AK and Stuart K. (2000) Uridylate addition and RNA ligation contribute to the specificity of kinetoplastid insertion RNA editing. *Mol. Cell Biol.* 20:8447–8457.

Igo RP Jr, Weston DS, Ernst NL, Panigrahi AK, Salavati R and Stuart K. (2002) Role of uridylate-specific exoribonuclease activity in *Trypanosoma brucei* RNA editing. *Eukaryot. Cell* 1:112–118.

Kable ML, Seiwert SD, Heidmann S and Stuart K. (1996) RNA editing: a mechanism for gRNA-specified uridylate insertion into precursor mRNA. *Science* 273:1189–1195.

Kang X, Rogers K, Gao G, Falick AM, Zhou S and Simpson L. (2005) Reconstitution of uridine-deletion precleaved RNA editing with two recombinant enzymes. *Proc. Natl. Acad. Sci. U.S.A.* 102:1017–1022.

Kastner B, Fischer N, Golas MM, Sander B, Dube P, Boehringer D, Hartmuth K, Deckert J, Hauer F and Wolf E, et al. (2008) GraFix: sample preparation for single particle electron cryomicroscopy. *Nat. Methods* 5:53–55.

Köller J, Müller UF, Schmid B, Missel A, Kruft V, Stuart K and Göringer HU. (1997) *Trypanosoma brucei* gBP21: an arginine-rich mitochondrial protein that binds to guide RNA with high affinity. *J. Biol. Chem.* 272:3749–3757.

Köller J, Nörskau G, Paul AS, Stuart K and Göringer HU. (1994) Different *Trypanosoma brucei* guide RNA molecules associate with an identical complement of mitochondrial proteins in vitro. *Nucl. Acids Res.* 22:1988–1995.

Law JA, O'Hearn S and Sollner-Webb B. (2007) In *Trypanosoma brucei* RNA editing, TbMP18 (band VII) is critical for editosome integrity and for both insertional and deletional cleavages. *Mol. Cell Biol.* 27:777–787.

Leung SS and Koslowsky DJ. (2001) Interactions of mRNAs and gRNAs involved in trypanosome mitochondrial RNA editing: structure probing of an mRNA bound to is cognate gRNA. *RNA* 7:1803–1816.

Liu J, Reedy MC, Goldman YE, Franzini-Armstrong C, Sasaki H, Tregear RT, Lucaveche C, Winkler H, Baumann BA and Squire JM, et al. (2004) Electron tomography of fast frozen, stretched rigor fibers reveals elastic distortions in the myosin crossbridges. *J. Struct. Biol.* 147:268–282.

Madison-Antenucci S and Hajduk SL. (2001) RNA editing associated protein 1 is an RNA binding protein with specificity for preedited mRNA. *Mol. Cell* 7:879–886.

Madison-Antenucci S, Grams J and Hajduk SL. (2002) Editing machines: the complexities of trypanosome RNA editing. *Cell* 108:435–8.

Madison-Antenucci S, Sabatini RS, Pollard VW and Hajduk SL. (1998) Kinetoplastid RNA-editing-associated protein 1 (REAP-1): a novel editing complex protein with repetitive domains. *EMBO J.* 17:6368–6376.

Maslov DA and Simpson L. (1992) The polarity of editing within a multiple gRNA-mediated domain is due to formation of anchors for upstream gRNAs by downstream editing. *Cell* 70:459–467.

McManus MT, Shimamura M, Grams J and Hajduk SL. (2001) Identification of candidate mitochondrial RNA editing ligases from *Trypanosoma brucei*. *RNA* 7:167–175.

Miller MM and Read LK. (2003) *Trypanosoma brucei*: functions of RBP16 cold shock and RGG domains in macromolecular interactions. *Exp. Parasit.* 105:140–148.

Missel A and Göringer HU. (1994) *Trypanosoma brucei* mitochondria contain RNA helicase activity. *Nucl. Acids Res.* 22:4050–4056.

Missel A, Souza AE, Nörskau G and Göringer HU. (1997) Gene disruption of a mitochondrial DEAD box protein in *Trypanosoma brucei* affects edited mRNAs. *Mol. Cell Biol.* 17:4895–4903.

Müller UF and Göringer HU. (2002) Mechanism of the gBP21-mediated RNA/RNA annealing reaction: matchmaking and charge reduction. *Nucl. Acids Res.* 30:447–455.

Müller UF, Lambert L and Göringer HU. (2001) Annealing of RNA editing substrates facilitated by guide RNA binding protein gBP21. *EMBO J.* 20:1394–1404.

Niemann M, Brecht M, Schlüter E, Weitzel K, Zacharias M and Göringer HU. (2008) TbMP42 is a structure sensitive ribonuclease that likely follows a metal ion catalysis mechanism. *Nucl. Acids Res.* 36:4465–4473.

Niemann M, Kaibel H, Schlüter E, Weitzel K, Brecht M and Göringer HU. (2009) Kinetoplastid RNA editing involves a 3' nucleotidyl phosphatase activity. *Nucl. Acids Res.* 37:1897–1906.

Ochsenreiter T and Hajduk SL. (2006) Alternative editing of cytochrome c oxidase III mRNA in trypanosome mitochondria generates protein diversity. *EMBO Rep.* 7:1128–1133.

Ochsenreiter T, Anderson S, Wood ZA and Hajduk S. (2008) Alternative RNA editing produces a novel protein involved in mitochondrial DNA maintenance in trypanosomes. *Mol. Cell Biol.* 28:5595–5604.

Ochsenreiter T, Cipriano M and Hajduk SL. (2008) Alternative mRNA editing in trypanosomes is extensive and may contribute to mitochondrial protein diversity. *PLoS One* 3:e1566.

Panigrahi AK, Ernst NL, Domingo GJ, Fleck M, Salavati R and Stuart KD. (2006) Compositionally and functionally distinct editosomes in *Trypanosoma brucei*. *RNA* 12:1038–1049.

Panigrahi AK, Schnaufer A and Stuart KD. (2007) Isolation and compositional analysis of trypanosomatid editosomes. *Methods Enzymol.* 424:3–24.

Panigrahi AK, Schnaufer A, Carmean N, Igo RP Jr, Gygi SP, Ernst NL, Palazzo SS, Weston DS, Aebersold R and Salavati R, et al. (2001) Four related proteins of the *Trypanosoma brucei* RNA editing complex. *Mol. Cell Biol.* 21:6833–6840.

Pelletier M and Read LK. (2003) RBP16 is a multifunctional gene regulatory protein involved in editing and stabilization of specific mitochondrial mRNAs in *Trypanosoma brucei*. *RNA* 9:457–468.

Pelletier M, Miller MM and Read LK. (2000) RNA-binding properties of the mitochondrial Y-box protein RBP16. *Nucl. Acids Res.* 28:1266–1275.

Peris M, Simpson AM, Grunstein J, Liliental JE, Frech GC and Simpson L. (1997) Native gel analysis of ribonucleoprotein complexes from a *Leishmania tarentolae* mitochondrial extract. *Mol. Biochem. Parasitol.* 85:9–24.

Pollard VW, Harris ME and Hajduk SL. (1992) Native mRNA editing complexes from *Trypanosoma brucei* mitochondria. *EMBO J.* 11:4429–4438.

Radermacher M, Wagenknecht T, Verschoor A and Frank J. (1987) Three-dimensional reconstruction from a single-exposure, random conical tilt series applied to the 50S ribosomal subunit of *Escherichia coli*. *J. Microsc.* 146:113–136.

Reifur L and Koslowsky DJ. (2008) *Trypanosoma brucei* ATPase subunit 6 mRNA bound to gA6-14 forms a conserved three-helical structure. *RNA* 14:2195–2211.

Rigaut G, Shevchenko A, Rutz B, Wilm M, Mann M and Séraphin B. (1999) A generic protein purification method for protein complex characterization and proteome exploration. *Nature Biotech.* 17:1030–1032.

Rogers K, Gao G and Simpson L. (2007) Uridylate-specific 3' 5'- exoribonucleases involved in uridylate-deletion RNA editing in trypanosomatid mitochondria. *J. Biol. Chem.* 282:29073–29080.

Rusché LN, Cruz-Reyes J, Piller KJ and Sollner-Webb B. (1997) Purification of a functional enzymatic editing complex from *Trypanosoma brucei* mitochondria. *EMBO J.* 16:4069–4081.

Rusché LN, Huang CE, Piller KJ, Hemann M, Wirtz E and Sollner-Webb B. (2001) The two RNA ligases of the *Trypanosoma brucei* RNA editing complex: cloning the essential band IV gene and identifying the band V gene. *Mol. Cell Biol.* 21:979–989.

Sabatini R and Hajduk SL. (1995) RNA ligase and its involvement in guide RNA/mRNA chimera formation. Evidence for a cleavage-ligation mechanism of *Trypanosoma brucei* mRNA editing. *J. Biol. Chem.* 270:7233–7240.

Salavati R, Ernst NL, O'Rear J, Gilliam T, Tarun S Jr and Stuart K. (2006) KREPA4, an RNA binding protein essential for editosome integrity and survival of *Trypanosoma brucei*. *RNA* 12:819–831.

Sander B, Golas MM, Makarov EM, Brahms H, Kastner B, Lührmann R and Stark H. (2006) Organization of core spliceosomal components U5 snRNA loop I and U4/U6 Di-snRNP within U4/U6.U5 Tri-snRNP as revealed by electron cryomicroscopy. *Mol. Cell* 24:267–278.

Sbicego S, Alfonzo JD, Estevez AM, Rubio MA, Kang X, Turck CW, Peris M and Simpson L. (2003) RBP38, a novel RNA-binding protein from trypanosomatid mitochondria, modulates RNA stability. *Eukaryot. Cell* 2:560–568.

Schmid B, Riley GR, Stuart K and Göringer HU. (1995) The secondary structure of guide RNA molecules from *Trypanosoma brucei*. *Nucl. Acids Res.* 23:3093–3102.

Schnaufer A, Ernst NL, Palazzo SS, O'Rear J, Salavati R and Stuart K. (2003) Separate insertion and deletion subcomplexes of the *Trypanosoma brucei* RNA editing complex. *Mol. Cell* 12:307–319.

Schnaufer A, Wu M, Park YJ, Nakai T, Deng J, Proff R, Hol WG and Stuart KD. (2010) A protein–protein interaction map of trypanosome ~20S editosomes. *J. Biol. Chem.* 285:5282–5295.

Schumacher MA, Karamooz E, Zikova A, Trantirek L and Lukes J. (2006) Crystal structures of *T. brucei* MRP1/MRP2 guide-RNA binding complex reveal RNA matchmaking mechanism. *Cell* 126:701–711.

Seiwert SD and Stuart K. (1994) RNA editing: transfer of genetic information from gRNA to precursor mRNA in vitro. *Science* 266:114–117.

Seiwert SD, Heidmann S and Stuart K. (1996) Direct visualization of uridylate deletion in vitro suggests a mechanism for kinetoplastid RNA editing. *Cell* 84:831–841.

Sigworth FJ. (1998) A maximum-likelihood approach to single-particle image refinement. *J. Struct. Biol.* 122:328–339.

Simpson L, Aphasizhev R, Lukes J and Cruz-Reyes J. (2010) Guide to the nomenclature of kinetoplastid RNA editing: a proposal. *Protist.* 161:2–6.

Stuart KD, Schnaufer A, Ernst NL and Panigrahi AK. (2005) Complex management: RNA editing in trypanosomes. *Trends Biochem. Sci.* 30:97–105.

Trotter JR, Ernst NL, Carnes J, Panicucci B and Stuart K. (2005) A deletion site editing endonuclease in *Trypanosoma brucei*. *Mol. Cell* 20:403–412.

Vanhamme L, Perez-Morga D, Marchal C, Speijer D, Lambert L, Geusken M, Alexandre S, Ismaïli N, Göringer HU and Benne R, et al. (1998) *Trypanosoma brucei* TBRGG1, a mitochondrial oligo(U)-binding protein that colocalizes with an in vitro RNA editing activity. *J. Biol. Chem.* 273:21825–21833.

Wang B, Ernst NL, Palazzo SS, Panigrahi AK, Salavati R and Stuart K. (2003) TbMP44 is essential for RNA editing and structural integrity of the editosome in *Trypanosoma brucei*. *Eukaryot. Cell* 2:578–587.

Yu LE and Koslowsky DJ. (2006) Interactions of mRNAs and gRNAs involved in trypanosome mitochondrial RNA editing: structure probing of a gRNA bound to its cognate mRNA. *RNA* 12:1050–1060.

RESEARCH AIM

First evidence for a RNA editing reaction of mitochondrial mRNAs in African trypanosomes was published more than 25 years ago by Rob Benne and colleagues. Since then the contributing molecular components, the basal reaction mechanism as well as the inventory and global structure of the catalytic machinery have been identified. However, despite that knowledge many biomolecular details of the editing reaction cycle are still unknown. This includes many biophysical attributes of the RNA processing reaction, in addition to stoichiometric aspects of the interaction of the participating molecular components as well as regulatory details of RNA editing within the cell-cycle of the parasitic organism.

In **Chapter One,** I present real time binding experiments of different full length substrate mRNAs to 20S editosomes in order to characterize the thermodynamic and kinetic parameters of the mRNA/editosome interaction. The binding data are used to calculate the number of 20S editosomes bound per mRNA and I present a first visualization of the RNA binding site using transmission electron microscopy.

Chapter Two includes a structural characterization of the editosome machinery by Atomic Force Microscopy (AFM). I present a kinetic analysis of the interaction of substrate RNAs with 20S editosomes, which culminates in the identification of a so far unknown catalytic activity of the 20S editosome.

Chapter Three – RNA editing has been shown to be regulated between the two main life cycle stages of the parasite. Whether RNA editing is also regulated within the cell-cycle of the parasite is not known. Here I present data to determine the RNA activity in mitochondrial lysates derived from different cell cycle-phases of synchronized trypanosome cells.

Chapter Four – RNA editing is typically analyzed *in vitro* at dilute reaction conditions. However, the reaction takes place within the mitochondria of African trypanosomes, which represents a severly colume-occupied or "crowded" environment. Since molecular crowding has been shown to affect the equilibrium and kinetic of macromolecular reactions, I present a biophysical and biochemical analysis of the RNA editing reaction at different molecular crowding conditions.

“There are two typos of people in this world: those who can edit and those who can’t.”

– Jarod Kintz

Chapter One

Trypanosoma brucei 20S editosomes have one RNA substrate-binding site

Editing of mitochondrial pre-mRNAs in African trypanosomes generates full-length transcripts by the site-specific insertion and deletion of U nucleotides. The reaction is catalyzed by a 0.8 MDa multienzyme complex, the editosome. Although the binding of substrate pre-edited mRNAs and cognate gRNAs represents the first step in the reaction cycle, the biochemical and biophysical details of the editosome/RNA interaction are not understood. Here we show that editosomes bind full-length substrate mRNAs with nanomolar affinity in a nonselective fashion. The complexes do not discriminate - neither kinetically nor thermodynamically - between different mitochondrial pre-mRNAs or between edited and unedited versions of the same transcript. They also bind gRNAs and gRNA/pre-mRNA hybrid RNAs with similar affinities and association rate constants. Gold-labeling of editosome-bound RNA in combination with transmission electron microscopy (TEM) identified a single RNA binding site per editosome.

Introduction

RNA editing is required for the expression of the majority of mitochondrial genes in African trypanosomes. The reaction is characterized by the site-specific insertion and/or deletion of U nucleotides thereby converting cryptic pre-mRNAs into translatable transcripts (reviewed in Hadjuk and Ochsenreiter, 2010; Aphasizhev and Aphasizheva, 2011). RNA editing involves a specific class of small, non-coding RNAs known as guide RNAs (gRNAs). The molecules function as "quasi" templates in the reaction and "guide" the U-insertion/deletion reaction by basepairing to the pre-edited mRNA molecules (Blum et al., 1990). Both subtypes of the reaction (U-insertion/deletion) start with the endonucleolytic cleavage of the pre-mRNA. In U-insertion-type RNA editing, a terminal uridylyl transferase (TUTase) then catalyzes the addition of U's (Ernst et al., 2003; Aphasizhev et al., 2003) to the 3' end of the 5'-pre-mRNA cleavage fragment. In the case of the U-deletion reaction, unpaired Us are removed by a U nucleotide-specific exonuclease (exoUase) (Igo et al., 2002; Aphasizhev and Simpson, 2001). Finally, the processed mRNA fragments, are ligated by RNA ligases (McManus et al., 2001; Huang et al., 2001; Rusché et al., 2001; Gao and Simpson, 2003). Next to these core activities additional, so-called accessory activities have been identified. This includes matchmaking-type RNA/RNA annealing factors (Müller et al., 2001; Blom et al., 2001; Müller and Göringer, 2002; Aphasizhev et al., 2003a; Ammerman et al., 2008; Sbicego et al., 2003; Kala and Salavati, 2010) as well as RNA helicases (Missel et al., 1997; Li et al., 2011).

The key enzymes of the editing reaction cycle are assembled in a high molecular mass protein complex termed the editosome. Editosomes provides a reaction platform for the processing reaction (reviewed in Aphasizhev and Aphasizheva, 2011, Göringer et al., 2011; Göringer, 2012). The complexes have been isolated from steady state detergent extracts of African trypanosomes and have been visualized by transmission electron microscopy (TEM) and cryo-EM (Golas et al., 2009). The structural studies revealed two classes of high molecular mass complexes with apparent S-values of 20S and 35-40S (Golas et al., 2009). 20S and 35-40S editosomes have calculated molecular mass of 0.8 MDa and 1.6 MDa (Golas et al., 2009). 20S editosomes are composed of two globular subdomains (Golas et al., 2009), whereas 35-40S editosomes have a slightly convex platform extending into head-like and foot-like protuberances (Golas et al., 2009). While a three-dimensional alignment of the 20S and 35-40S complexes demonstrated that 20S complexes represent a major part of the 35-40S complexes, the difference between the two complexes lies in the presence/absence of bound substrate RNA. RNA binding converts 20S editosomes into 35-40S editosomes. Although 20S editosomes have been shown to bind short, synthetic substrate RNAs with nanomolar affinity (Golas et al., 2009) unfortunately, the molecular details of the editosome/RNA interaction are only marginally understood. Neither, the number of RNA binding sites per editosome, nor kinetic, thermodynamic and/or selectivity and specificity issues have been addressed systematically. The situation is further complicated by the fact that compositionally different editosomes seem to exist in transgenic trypanosomes (Carnes et al., 2008; Carnes et al., 2011) and that the complexes can associate with multiple RNA ligands: pre-edited, partially edited and fully edited mRNAs as well as gRNAs and cognate gRNA/pre-mRNA pairs.

Here we present an analysis of the RNA binding characteristics of native *T.*

brucei 20S editosomes. We show high affinity RNA binding without discrimination between mRNA, gRNA and mRNA/gRNA hybrid molecules and without discrimination between different mitochondrial transcripts, or edited and unedited version of the same transcript. We further demonstrate that 20S editosomes have a single RNA binding site, while multiple editosomes can interact with one RNA molecule. Lastly, we show that both subtypes of the editing reaction are catalyzed within a single, bifunctional reaction center.

Materials and Methods

Preparation of editosomes

20S editosomes were isolated from mitochondrial vesicle preparations of procyclic stage *T. brucei* cells. The following strains were used: Lister 427 (Cross, 1975) and the transgenic cell line 29-13-TbMP42/TAP (Golas et al., 2009). Parasite cells were harvested at late log phase and disrupted by N_2 cavitation at isotonic conditions (Hauser et al., 1996). Mitochondrial vesicles were isolated by differential centrifugation and used to prepare mitochondrial detergent extracts by incubation with 0.6% (v/v) Nonidet-P40 in editing buffer (EB): 20 mM HEPES/KOH pH 7.5, 30 mM KCl, 10 mM $Mg(OAc)_2$, 0.5 mM DTT. 20S editosomes were enriched by isokinetic ultracentrifugation in linear 10–35% (v/v) glycerol gradients (Göringer et al., 1994). TAP-tagged 20S editosomes were isolated from spin-cleared mitochondrial detergent extracts by consecutive IgG and calmodulin affinity chromatography followed by isokinetic ultracentrifugation in linear 10–35% (v/v) glycerol gradients. All editosome preparations were tested for their gRNA-dependent U insertion/U deletion *in vitro* RNA editing activity (Igo et al., 2000; Igo et al., 2002). The protein composition of TbMP42/TAP editosomes has been described by Golas et al., 2009.

RNA oligonucleotide synthesis and biotinylation

RNA oligonucleotides were synthesized by solid phase phosphoramidite chemistry using 2'-*O*-triisopropylsilyloxymethyl-protected monomers. The U insertion substrate RNAs were 5'-mRNA fragment: GGAAGUAGAGAGUAGG, 3'-mRNA fragment: AUUGGAGUUAUAG-NH_2, and gRNA: CUAUAACCCGAUAAACC UACGUCUCAUACUUCC. The U deletion substrate RNAs were 5'-mRNA fragment: GGAAAGGGAAAGUUGUGAUUUU, 3'-mRNA fragment: GCGAGUUAUAGAA UA-NH_2, and gRNA: GGUUCUAUAACUCG CUCACAACUUUCCCUUUCC. 5'-biotinylated oligoribonucleotides were synthesized using 2-aminoethoxyethoxyethanol-linked biotinylated phosphoramidites. Synthetic pre-mRNA/gRNA hybrid molecules were generated in EB by incubating equimolar concentrations of both RNAs at 65 °C for 5 min and cooling to room temperature at a rate of 1 °C/min.

RNA transcription

Unedited (UE) and fully edited (FE) A6 (344 nucleotides/762 nucleotides), UE and FE apocytochrome *b* (Cyb) (1080 nucleotides/1113 nucleotides), and never edited cytochromoxidase subunit I (COI) (1647 nucleotides) transcripts were PCR-amplified from *T. brucei* Lister 427 cDNA preparations. PCR products were cloned into pBS SK^- and sequenced. RNAs were synthesized by run-off transcription from linear DNA plasmid templates using T7 RNA polymerase following standard procedures. Guide RNA gA6-14 was *in vitro* transcribed as in Schmid et al., 1995. All of the transcripts were gel electrophoretically purified, eluted from the gel slices, and EtOH-precipitated. RNA folding was performed in EB by heating to 75 °C (5 min) and cooling to room temperature at 1 °C/min.

Substrate RNA competition of *in vitro* RNA editing

Precleaved RNA editing *in vitro* insertion and deletion assays were conducted as described (Igo et al., 2000; Igo et al., 2002) using preannealed, synthetic pre-mRNA/gRNA hybrid RNAs. The reactions were initiated by a 5 min preincubation at 27 °C with 20S editosomes in EB in the presence of 0.5 mM ATP and 40 µM UTP. Competitor pre-mRNA/gRNA hybrid RNA was added (up to a 380-fold molar excess) and incubated for an additional 2 h at 27 °C. The reactions were terminated by phenol extraction, EtOH-precipitated, and analyzed in denaturing (8M urea), 15% (w/v) polyacrylamide gels followed by phosphorimaging.

Surface plasmon resonance

gRNAs, pre-edited, and edited mRNAs were 3'-oxidized at 4 °C overnight in the dark in 10 mM $NaIO_4$, 50 mM NaOAc pH 4.8, 10 mM $MgCl_2$, 100 mM NaCl (Odom et al., 1980). The samples were desalted by size exclusion chromatography and EtOH-precipitated. RNAs were covalently attached to the surface of an amino silane-derivatized microcuvette in coupling buffer (100 mM $Na_xH_yPO_4$ pH 7.0, 150 mM NaCl, 50 mM $NaBH_3CN$) for 3 h at 27 °C. Binding was monitored in real time as a shift in the resonant angle. The data were fitted by nonlinear regression, and k_{diss} and k_{ass} values were determined by plotting observed on rates ($k_{on(obs)}$ as a function of the complex concentration ($k_{on(obs)} = k_{ass}$ [RNA/20S complex] + k_{diss}). Equilibrium dissociation constants (K_d) were calculated as $K_d = k_{diss}/k_{ass}$. The number of binding sites was calculated based on the equation $K_aR_{max} - R_{eq}K_a = R_{eq}/[20S]$. A plot of R_{eq} *versus* $R_{eq}/[20S]$ yields a slope of $-K_a$ with a *x* intercept of R_{max} and a *y* intercept of K_aR_{max}. RNA/editosome half-lives ($t_{1/2}$) were determined as $t_{1/2} = \ln 2/k_{diss}$.

Streptavidin gold labeling and transmission EM

20S editosome preparations were dialyzed to remove glycerol and incubated with synthetic 5'-biotinylated (bio) substrate RNAs (bio gRNA, bio pre-edited mRNA, or gRNA/bio pre-edited mRNA hybrid molecules) in EB in a 1:1 molar ratio (27 °C, 60 min). Editosome-bio RNA complexes were allowed to adhere to carbon films and were further incubated with streptavidin-derivatized 6-nm gold particles (room temperature, 30 min). Following an additional 20 min incubation with 2% (w/v) uranyl acetate in H_2O, the streptavidin-decorated editosome-bio RNA complexes were transferred onto 400 mesh square copper grids and sandwiched with another carbon film. Air-dried specimens were analyzed by transmission electron microscopy at 50 keV, and pictures were taken at 85,000x magnification. The images were processed using ImageJ (Abramoff et al., 2004). The images were smoothed to reduce noise and false colored by applying the ImageJ interactive three-dimensional surface plot plug-in.

Results

20S editosomes bind mitochondrial RNAs indiscriminately

T. brucei 20S editosomes have been shown to bind short (≤30 nucleotides), synthetic oligoribonucleotides that mimic substrate gRNA and pre-mRNA molecules as well as short, antiparallel gRNA/pre-mRNA hybrid RNAs with nanomolar affinity (Golas et al., 2009). To analyze the binding of 20S editosomes to their natural substrates, we examined their interaction with full-length mRNA and gRNA molecules. For that we generated a set of mitochondrial mRNAs that are edited to a different extent. We cloned the UE and FE versions of the ATPase subunit 6 (A6) transcript, which undergoes editing throughout its entire primary sequence (447 U insertions and 28 U deletions) (Bhat et al.,

1990). Furthermore, we cloned the UE and FE versions of the Cyb transcript, which contains a single editing domain at its 5'-end (34 U insertions) (Feagin et al., 1987), and lastly we used the COI transcript, which is never edited. To derive quantitative data we performed real time binding experiments using a surface plasmon resonance based-readout system. Fig. 1A shows representative

thermore, we showed that Cyb-UE transcripts and the never edited COI transcript interact with 20S editosomes with K_d values of 2.9 and 8.6 nM, indicating that pan-edited pre-mRNAs, pre-mRNAs that are edited to a lower extent, and never edited transcripts are bound with similar affinities. Experiments with A6-FE and Cyb-FE resulted in K_d values of 3.6 and 12 nM with calculated half-lives

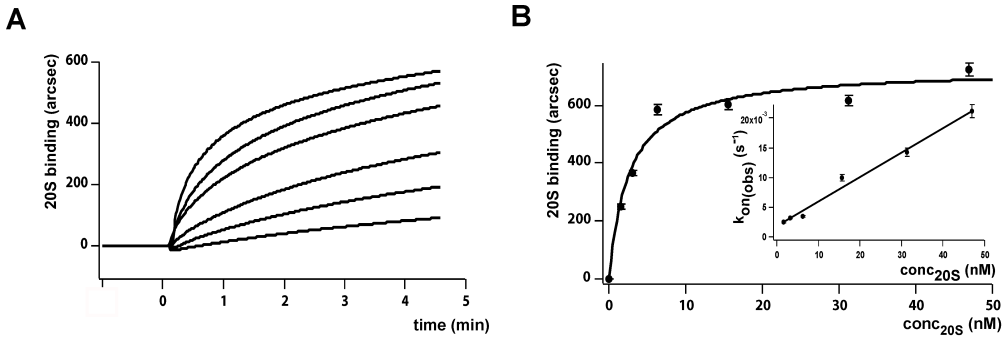

C

RNA	length (nt)	K_d (nM)	k_{ass} (M^{-1} s^{-1})	k_{diss} (s^{-1})	$t_{1/2}$ (min)
COI	1647	8.6	4.3×10^5	3.7×10^{-3}	3.1
A6-UE	344	5	4.1×10^5	2.1×10^{-3}	5.5
A6-FE	762	3.6	7.7×10^5	2.8×10^{-3}	4.1
Cyb-UE	1080	2.9	4.2×10^5	1.2×10^{-3}	9.6
Cyb-FE	1113	12	6.0×10^5	7.2×10^{-3}	1.6
A6-UE/gRNA	344/70	5.5	4.4×10^5	2.4×10^{-3}	4.8
gRNA	70	6.5	7.6×10^5	4.9×10^{-3}	2.4

Figure 1. Real time surface Plasmon resonance monitoring of the binding of 20S editosomes to mitochondrial RNAs. (A) Sensograms of the concentration dependent binding of 20S editosomes to A6-UE mRNA (*top to bottom*: 50, 30, 15, 6, 3, and 2 nM editosomes). (B) Corresponding binding curve of the 20S/A6-UE association. (Inset) Plot of $k_{on(obs)} = f(conc_{20S})$ for the calculation of k_{on} and k_{diss}. The error bars represent relative errors as percentages. (C) Summary of the binding characteristics of the 20S/RNA interaction for different mitochondrial transcripts.

binding isotherms of 20S editosomes to surface immobilized A6-UE mRNA. The two binding partners interact in a concentration dependent fashion. Binding is complete within 3–4 min and is characterized by an association rate constant (k_{ass}) of 4.1×10^5 $M^{-1}s^{-1}$ and a macroscopic equilibrium dissociation constant (K_d) of 4.9 nM (Fig. 1B). Identical experiments with full-length gRNA gA6-14 and gA6-14 hybridized to A6-UE resulted in K_d values of 6.5 and 5.5 nM. This indicates high affinity binding and confirms that 20S editosomes do not discriminate between full-length mRNA, full-length gRNA, and full-length mRNA/gRNA hybrid molecules. Fur-

($t_{1/2}$) for the different complexes varying between 2 and 10 min. Taken together (Fig. 1C and Suppl. Fig. 1), the determined association rate constants (k_{ass}) vary by a factor of 2, the k_{diss} values vary by a factor of 6, and the corresponding macroscopic K_d values vary by a factor of 4. This indicates that 20S editosomes by and large interact with different RNA species in a kinetically and thermodynamically nondiscriminative fashion.

Multiple 20S editosomes can bind to a single pre-mRNA

The different 20S/RNA binding isotherms can be further analyzed to de-

termine the number of 20S binding sites/RNA substrate molecule (suppl. Fig. 2 and Table 1). For gRNA gA6-14 (70 nucleotides), A6-UE (344 nucleotides), and the A6-UE/gRNA hybrid molecule (344/70 nucleotides) we derived ≤1 bound editosome per RNA molecule. For Cyb-FE (1113 nucleotides) and Cyb-UE (1080 nucleotides), we identified two interaction sites and the never edited COI transcript (1647 nucleotides) was bound by four editosomes. This demonstrates that multiple editosomes can bind to a single mRNA and further suggests that the editosome/mRNA interaction is characterized by a defined spatial arrangement of ≤470 nucleotides of RNA per 20S particle.

RNA	length (nt)	20S/RNA
COI	1647	3.7 ≈ 4
A6-UE	344	0.6 ≈ 1
A6-FE	762	1.9 ≈ 2
Cyb-UE	1080	2.1 ≈ 2
Cyb-FE	1113	2
A6-UE/gRNA	344/70	1.1 ≈ 1
gRNA	70	0.2 ≈ 1

Table 1 Summary of the binding site data for all tested RNAs: A6: ATPase subunit 6; Cyb: apocytochrome b; COI: cytochrome oxidase I; gRNA: guide RNA; UE: unedited; FE: fully edited.

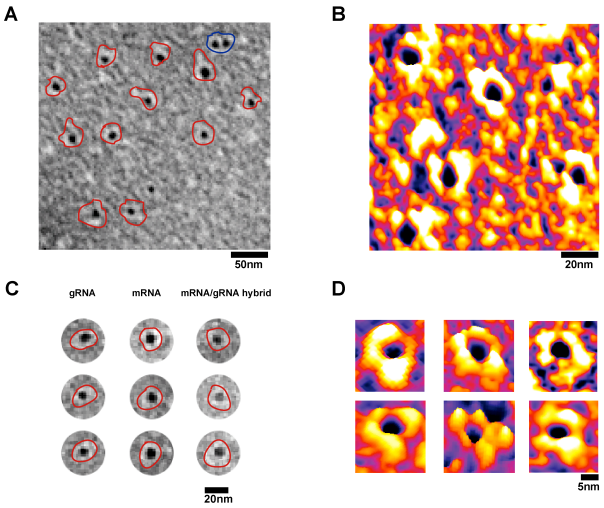

Figure 2. (A) Transmission electronmicrograph of 20S editosomes (*red circles*) with bound gold-derivatized mRNA/gRNA hybrid RNAs. The complexes are characterized by one bound gold cluster (average diameter of 6 nm), which indicates one RNA-binding site. The complex circled in *blue* is an aggregate of two editosomes. (B) False color image of several gold-derivatized editosome-RNA complexes. (C) Individual gold-labeled editosome-RNA complexes for all three RNA ligands: gRNA, pre-mRNA and gRNA/pre-mRNA hybrid RNA. (D) False color images of individual gold-labeled editosome-RNA complexes. Please note that *B* and *D* do not represent three-dimensional images.

20S editosomes have one RNA-binding site

As a follow up, these data raised the question of the number of RNA-binding site(s) per 20S editosome. To address this issue, we directly visualized editosome-bound RNA by gold labeling in combination with transmission electron microscopy. Affinity-purified 20S complexes were incubated with 5'-biotin-derivatized, synthetic oligoribonucleotides mimicking gRNA, pre-mRNA, and gRNA/pre-mRNA hybrid RNAs. After binding we localized the biotin-modified RNAs with the help of streptavidin-derivatized gold cluster with a mean diameter of 6 nm. Fig. 2 (A and B) shows representative electronmicrographs of gold-labeled mRNA/gRNA hybrid molecules bound to 20S editosomes. Fig. 2C shows individual gold-labeled editosome-RNA complexes derived from experiments with all three RNA species (gRNA, pre-mRNA, and gRNA/mRNA hybrid RNAs). The complexes are characterized by dimensions of 21 x 26 nm (Golas et al., 2009), and as expected, the bound gold cluster covers approximately one fourth of the surface area of the individual particles (Fig. 2D). For each RNA binding experiment, we analyzed 10^3 editosome-RNA complexes. Approximately 97% of the complexes showed one bound gold cluster indicating that editosomes have a single substrate RNA-binding site. This result has the following consequences: First, it implicates that editing substrate RNAs should compete for the editosome-binding site, and second, it suggests that

the two types of editing reactions (U deletion and U insertion) might be catalyzed within a single, bifunctional reaction center.

20S editosomes have a bifunctional reaction center

To test this hypothesis we conducted substrate RNA competition experiments in combination with *in vitro* RNA editing activity assays (Igo et al., 2000; Igo et al., 2002). The experiments are based on the rationale that a prebound insertion type RNA editing substrate should be competed out of its binding site by an excess of deletion type RNA substrate (and *vice versa*). Fig. 3 shows the result. As anticipated, both the U deletion editing activity as well as the U insertion activity can be inhibited by increasing amounts of the "reciprocal" editing substrate. In both cases half-maximal inhibition was achieved at a ≤10-fold molar excess of competitor RNA, which verifies that the different substrate RNAs act as archetypical competitive inhibitors. Furthermore it shows that the identified substrate-binding site is at or in close proximity to the catalytically active reaction center of the editosome.

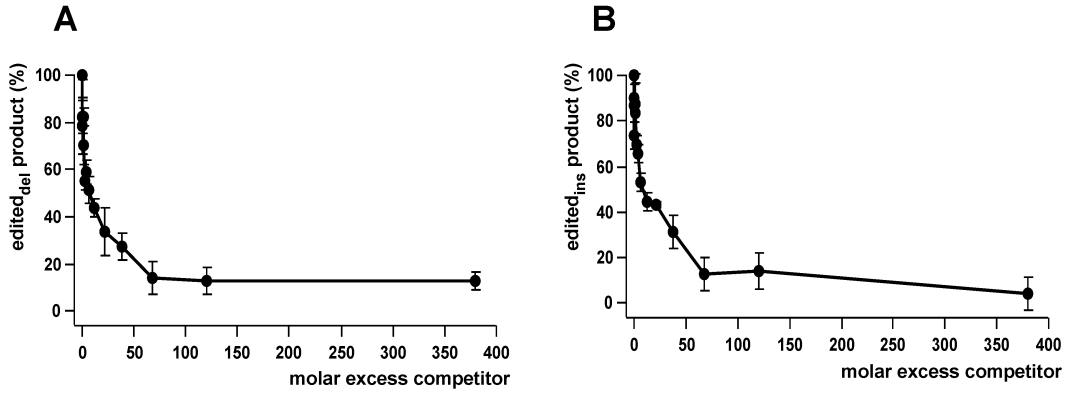

Figure 3. Substrate RNA competition experiments. Pre-cleaved *in vitro* insertion- and deletion-RNA editing assays (Igo et al., 2000; Igo et al., 2002) were performed using pre-annealed radioactively labeled gRNA/pre-mRNA substrate RNAs. Reactions were carried out in the presence of increasing amounts (≤380-fold molar excess) of non-radioactive competitor gRNA/pre-mRNA hybrid RNAs in a reciprocal fashion (U-deletion editing was competed with a U-insertion RNA substrate and *vice versa*). Edited product formation was measured and plotted as a function of the molar excess of competitor RNA. (A) Pre-cleaved U-deletion editing (competed with a U-insertion RNA). (B) Pre-cleaved U-insertion editing (competed with a U-deletion RNA). Half-maximal inhibition for both editing reactions is at ≤10nM competitor RNA. Error bars indicate relative errors (%).

Discussion

20S editosomes are the catalytic machinery of the RNA editing reaction. They represent high molecular mass, "protein-only" assemblies that contain all key activities to convert pre-edited transcripts into edited mRNAs. A crucial step in the reaction cascade is the binding of pre-edited mRNAs and gRNAs to form "substrate RNA-loaded" editosomes. Here we analyzed the thermodynamic and kinetic characteristics as well as the molecularity of the editosome/RNA interaction in detail. 20S editosomes have previously been shown to bind short, synthetic gRNA, pre-mRNA and gRNA/pre-mRNA hybrid oligonucleotides with nanomolar affinity (K_d) (Golas et al., 2009). In the present study we used a panel of "*in vivo*-sized" substrate RNAs (70-1647 nt). We determined that full length mRNAs, gRNAs and mRNA/gRNA hybrid RNAs interact with editosomes with similar (nanomolar) K_d's and almost identical association and dissociation rate constants (k_{ass}/k_{diss}). Furthermore, we showed that editosomes do not discriminate between transcripts that are extensively (A6) or moderately edited (Cyb), or between pre-edited and edited versions of the same transcript. Even never edited

mRNAs (COI) bind with nanomolar affinity. Despite the high affinity of the different 20S/RNA complexes, the lack of substrate specificity demonstrates that editosomes can interact with RNA molecules in a non-selective fashion and it further shows that RNA binding is not restricted to exclusively RNA editing substrate RNAs. This suggests an additional, perhaps in parts even RNA editing-independent function of the editosome (see chapter two). Whether that reflects the situation *in vivo* remains to be tested. Given the fact that the RNA editing machinery has been shown to interact with various gRNA- and mRNA-containing ribonucleoprotein complexes it seems plausible that some level of discrimination can be achieved by binding protein-associated RNAs rather than "naked" RNA molecules. Potential candidates are the identified mitochondrial RNA binding and mRNA-stabilizing proteins and complexes as well as chaperone-type RNA annealing factors and RNA helicases (reviewed in Aphasizhev and Aphasizheva, 2011; Hernandez et al., 2010; Acestor et al., 2009; Pusnik and Schneider, 2012).

We also found no evidence for discrimination between transcripts that undergo insertion-type editing only and transcripts that undergo both, insertion- and deletion-type RNA editing. This raised the questions whether editosomes have one or multiple reaction centers, and whether the two different editing reactions are catalyzed by the same or by separate (sub)complexes with separate RNA binding sites. Using transmission electron microscopy we were able to demonstrate that editosomes have only one substrate RNA binding site. All three RNA classes - mRNAs, gRNAs and mRNA/gRNA hybrids – bind to a single binding domain on the surface of the complex. Only in 3% of the examined particles we identified ≥2 RNA binding sites. However, these cases could be characterized as aggregates of two or more 20S complexes.

Importantly, the identified RNA binding domain is the interaction site for both types of RNA editing substrates. U-deletion as well as U-insertion pre-mRNA/gRNA model substrates interact with the very same 20S binding site and as a consequence can act as competitive inhibitors in a reciprocal fashion. Since that also leads to an inhibition of the *in vitro* editing activity this further demonstrates that the identified substrate binding domain is structurally linked or located near the catalytically-active center of the editosome. It also shows that the two types of editing reactions are catalyzed within a single, bifunctional reaction center. These data find additional support in the fact that individual gRNAs can guide both, deletion and insertion editing within one editing domain (Maslov and Simpson, 1992).

Lastly, while editosomes have only one RNA binding site, we identified multiple interaction sites of editosomes per RNA molecule. Using SPR-based real time binding experiments we verified that long substrate RNAs (A6-FE, Cyb-FE, Cyb-UE, COI) can be occupied with multiple editosomes with a calculated mean spacing of the particles in the range of 300-500 nt/20S complex.

Taken together, the data suggest that editosomes bind substrate RNAs with high affinity in a non-discriminative fashion with one RNA-binding site. Editosomes can execute both U-insertions and U-deletions on the same pre-edited mRNA, depending on the RNA domain that is in physical contact with the complex.

References

Abramoff MD, Magelhaes PJ and Ram SJ. (2004) Image processing with ImageJ. *J. Biophotonics Int.* 11:36–42.

Acestor N, Panigrahi AK, Carnes J, Zíková A and Stuart KD. (2009) The MRB1 complex functions in kinetoplastid RNA processing. *RNA* 15:277–286.

Ammerman ML, Fisk JC and Read LK. (2008) gRNA/pre-mRNA annealing and RNA chaperone activities of RBP16. *RNA* 14:1069–1080.

Aphasizhev R and Aphasizheva I. (2011) Uridine insertion/deletion editing in trypanosomes. A playground for RNA-guided information transfer. *Wiley Interdiscip. Rev. RNA* 2:669–685.

Aphasizhev R and Simpson L. (2001) Isolation and characterization of a U-specific 3'-5'-exonuclease from mitochondria of *Leishmania taren-tolae. J. Biol. Chem.* 276: 21280–21284.

Aphasizhev R, Aphasizheva I and Simpson L. (2003) A tale of two TUTases. *Proc. Natl. Acad. Sci. U.S.A.* 100:10617–10622.

Aphasizhev R, Aphasizheva I, Nelson RE and Simpson L. (2003a) A 100-kD complex of two RNA-binding proteins from mitochondria of *Leishmania tarentolae* catalyzes RNA annealing and interacts with several RNA editing components. *RNA* 9:62–76.

Bhat GJ, Koslowsky DJ, Feagin JE, Smiley BL and Stuart K. (1990) An extensively edited mitochondrial transcript in kinetoplastids encodes a protein homologous to ATPase subunit 6. *Cell* 61:885–894.

Blom D, Burg J, Breek CK, Speijer D, Muijsers AO and Benne R. (2001) Cloning and characterization of two guide RNA-binding proteins from mitochondria of *Crithidia fasciculata*. gBP27, a novel protein, and gBP29, the orthologue of *Trypanosoma brucei* gBP21. *Nucl. Acids Res.* 29:2950–2962.

Blum B, Bakalara N and Simpson L. (1990) A model for RNA editing in kinetoplastid mitochondria. "Guide" RNA molecules transcribed from maxicircle DNA provide the edited information. *Cell* 60:189–198.

Carnes J, Soares CZ, Wickham C and Stuart K. (2011) Endonuclease associations with three distinct editosomes in *Trypanosoma brucei*. *J. Biol. Chem.* 286:19320–19330.

Carnes J, Trotter JR, Peltan A, Fleck M and Stuart K. (2008) RNA editing in *Trypanosoma brucei* requires three different editosomes. *Mol. Cell. Biol.* 28:122–130.

Cross GA. (1975) Identification, purification and properties of clonespecific glycoprotein antigens constituting the surface coat of *Trypanosoma brucei*. *Parasitol.* 71:393–417.

Ernst NL, Panicucci B, Igo RP Jr, Panigrahi AK, Salavati R and Stuart K. (2003) TbMP57 is a 3' terminal uridylyl transferase (TUTase) of the *Trypanosoma brucei* editosome. *Mol. Cell* 11:1525–1536.

Feagin JE, Jasmer DP and Stuart K. (1987) Developmentally regulated addition of nucleotides within apocytochrome *b* transcripts in *Trypanosoma brucei*. *Cell* 49:337–345.

Gao G and Simpson L. (2003) Is the *Trypanosoma brucei* REL1 RNA ligase specific for U-deletion RNA editing, and is the REL2 RNA ligase specific for U-insertion editing? *J. Biol. Chem.* 278:27570-27574.

Golas MM, Böhm C, Sander B, Effenberger K, Brecht M, Stark H and Göringer HU. (2009) Snapshots of the RNA editing machine in trypanosomes captured at different assembly stages *in vivo*. *EMBO J.* 28:766–778.

Göringer HU. (2012) 'Gesalt,' Composition and function of the *Trypanosoma brucei* editosome. *Annu. Rev. Microbiol.* 66:65-82.

Göringer HU, Katari VS and Böhm C. (2011) The structural landscape of native editosomes in African trypanosomes. *Wiley Interdiscip. Rev. RNA* 2:395–407.

Göringer HU, Koslowsky DJ, Morales TH and Stuart K. (1994) The formation of mitochondrial ribonucleoprotein complexes involving guide RNA molecules in *Trypanosoma brucei*. *Proc. Natl. Acad. Sci. U.S.A.* 91:1776–1780.

Hajduk S and Ochsenreiter T. (2010) RNA editing in kinetoplastids. *RNA Biol.* 7:229–236.

Hauser R, Pypaert M, Häusler T, Horn EK and Schneider A. (1996) *In vitro* import of proteins into mitochondria of *Trypanosoma brucei* and *Leishmania tarentolae*. *J. Cell Sci.* 109:517–523.

Hernandez A, Madina BR, Ro K, Wohlschlegel JA, Willard B, Kinter MT and Cruz-Reyes J. (2010) REH2 RNA helicase in kinetoplastid mitochondria. Ribonucleoprotein complexes and essential motifs for unwinding and guide RNA (gRNA) binding. *J. Biol. Chem.* 285:1220–1228.

Huang CE, Cruz-Reyes J, Zhelonkina AG, O'Hearn S, Wirtz E, and Sollner-Webb B. (2001) Roles for

ligases in the RNA editing complex of *Trypanosoma brucei*: band IV is needed for U-deletion and RNA repair. *EMBO J.* 20:4694-4704.

Igo RP Jr, Palazzo SS, Burgess ML, Panigrahi AK and Stuart K. (2000) Uridylate addition and RNA ligation contribute to the specificity of kinetoplastid insertion RNA editing. *Mol. Cell. Biol.* 20:8447–8457.

Igo RP Jr, Weston DS, Ernst NL, Panigrahi AK, Salavati R and Stuart K. (2002) Role of uridylate-specific exoribonuclease activity in *Trypanosoma brucei* RNA editing. *Eukaryot. Cell* 1:112–118.

Kala S and Salavati R. (2010) OB-fold domain of KREPA4 mediates high-affinity interaction with guide RNA and possesses annealing activity. *RNA* 16:1951–1967.

Li F, Herrera J, Zhou S, Maslov DA and Simpson L. (2011) Trypanosome REH1 is an RNA helicase involved with the 3'-5' polarity of multiple gRNA-guided uridine insertion/deletion RNA editing. *Proc. Natl. Acad. Sci. U.S.A.* 108:3542–3547.

Maslov DA and Simpson L. (1992) The polarity of editing within a multiple gRNA-mediated domain is due to formation of anchors for upstream gRNAs by downstream editing. *Cell* 70:459–467.

McManus MT, Shimamura M, Grams J and Hajduk SL. (2001) Identification of candidate mitochondrial RNA editing ligases from *Trypanosoma brucei. RNA* 7:167–175.

Missel A, Souza AE, Nörskau G and Göringer HU. (1997) Disruption of a gene encoding a novel mitochondrial DEAD-box protein in *Trypanosoma brucei* affects edited mRNAs. *Mol. Cell. Biol.* 17:4895– 4903.

Müller UF and Göringer HU. (2002) Mechanism of the gBP21-mediated RNA/RNA annealing reaction. Matchmaking and charge reduction. *Nucl. Acids Res.* 30:447–455.

Müller UF, Lambert L and Göringer HU. (2001) Annealing of RNA editing substrates facilitated by guide RNA-binding protein gBP21. *EMBO J.* 20:1394–1404.

Odom OW Jr, Robbins DJ, Lynch J, Dottavio-Martin D, Kramer G and Hardesty B. (1980) Distances between 3' ends of ribosomal ribonucleic acids reassembled into *Escherichia coli* ribosomes. *Biochem.* 19:5947–5954.

Pusnik M and Schneider A. (2012) A trypanosomal pentatricopeptide repeat protein stabilizes the mitochondrial mRNAs of cytochrome oxidase subunits 1 and 2. *Eukaryot. Cell* 11:79–87.

Rusché LN, Huang CE, Piller KJ, Hemann M, Wirtz E and Sollner- Webb B. (2001) The two RNA ligases of the *Trypanosoma brucei* RNA editing complex. Cloning the essential band IV gene and identifying the band V gene. *Mol. Cell. Biol.* 21:979–989.

Sbicego S, Alfonzo JD, Estévez AM, Rubio MA, Kang X, Turck CW, Peris M and Simpson L. (2003) RBP38, a novel RNA-binding protein from trypanosomatid mitochondria, modulates RNA stability. *Eukaryot. Cell* 2:560–568.

Schmid B, Riley GR, Stuart K and Göringer HU. (1995) The secondary structure of guide RNA molecules from *Trypanosoma brucei*. *Nucl. Acids Res.* 23:3093–3102.

Supplementary material

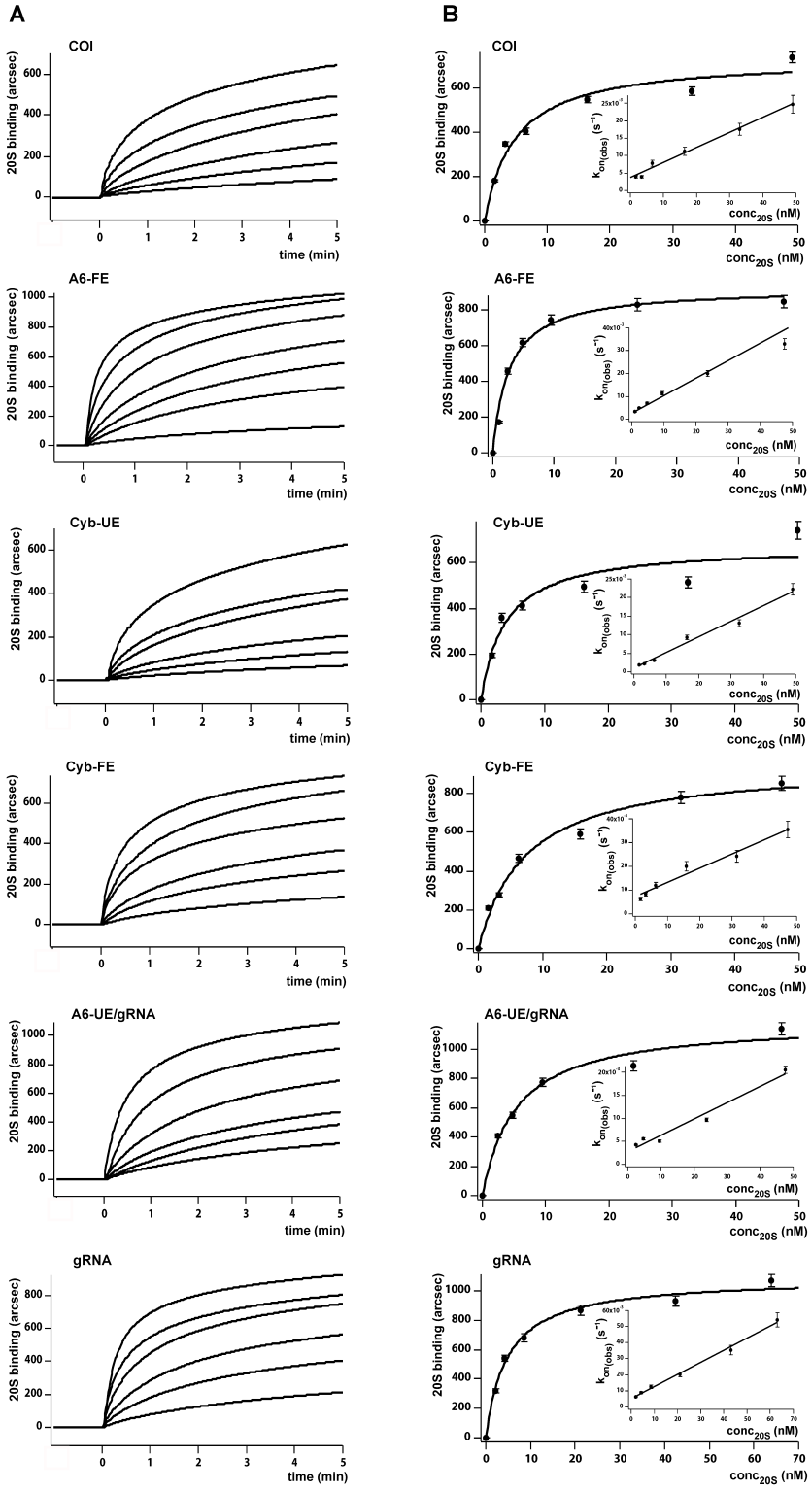

Suppl. Fig. 1 Real time surface plasmon resonance monitoring of the binding of 20S editosomes to different mitochondrial RNAs. (A) Sensograms of the concentration dependent binding (50mM, 30mM, 15mM, 6mM, 3mM, 2nM *top to bottom*) of 20S editosomes to: COI mRNA, A6-FE mRNA, Cyb-UE mRNA, Cyb-FE mRNA, A6-UE/gRNA hybrid RNA and gRNA. (B) Corresponding binding curves for the different 20S/RNA interactions. Inserts: Plot of $k_{on(obs)} = f(conc_{20S})$ for the calculation of k_{on} and k_{diss}. A6: ATPase subunit 6; Cyb: apocytochrome b; COI: cytochrome oxidase I; gRNA: guide RNA; UE: unedited; FE: fully edited. Error bars are relative errors in percent.

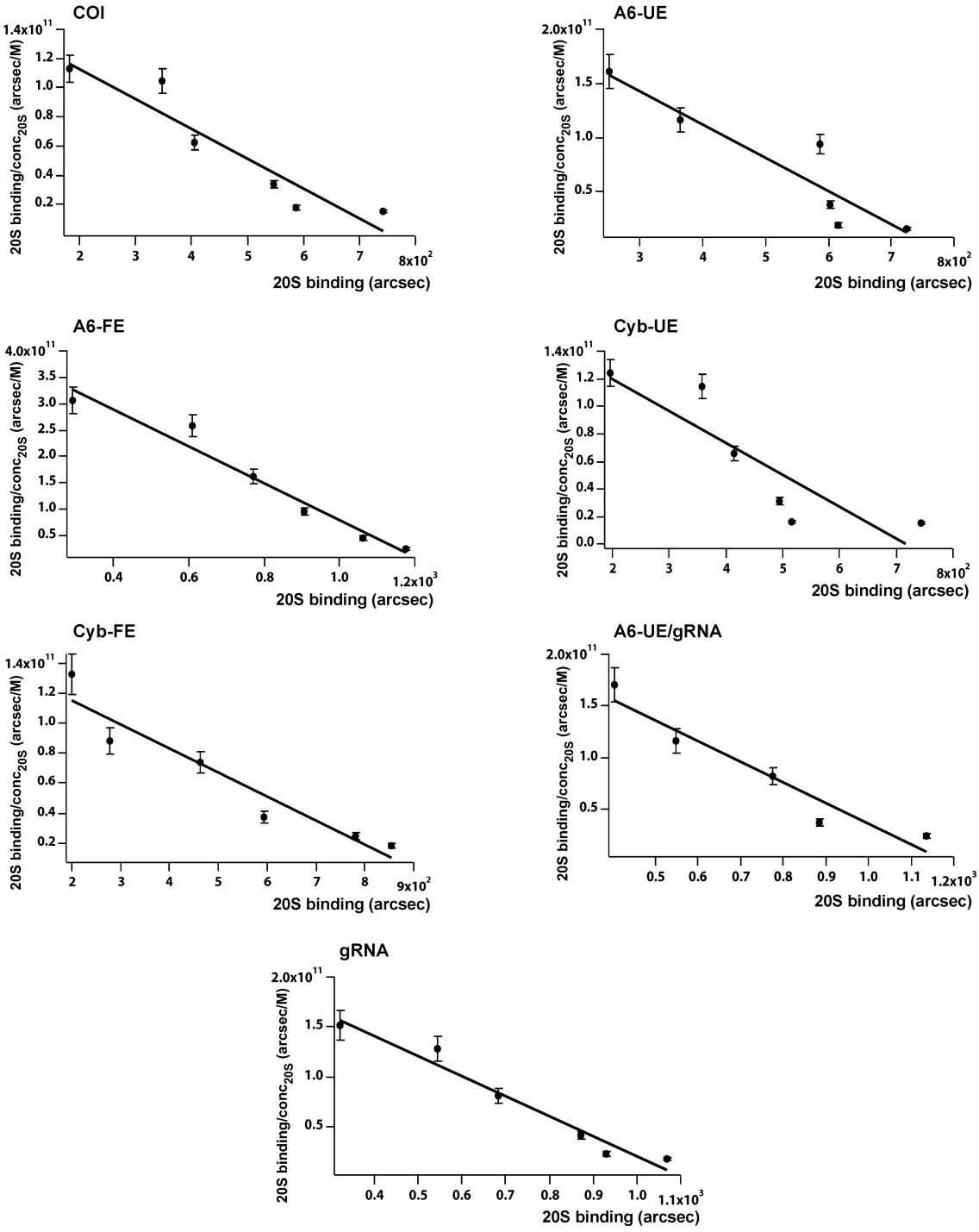

Suppl. Fig. 2 Binding site analysis. Scatchard analysis for the binding of 20S editosomes to surface immobilized RNA molecules to determine the number of RNA binding sites. A6: ATPase subunit 6; Cyb: apocytochrome b; COI: cytochrome oxidase I; gRNA: guide RNA; UE: unedited; FE: fully edited. Error bars are relative errors in percent.

“Editing might be a bloody trade, but knives aren’t the exclusive property of butchers. Surgeons use them too.”

– Blake Morrison

Chapter Two

Trypanosoma brucei 20S editosomes execute RNA unwinding activity

Non-translatable pre-mRNA molecules of mitochondrial genes in African trypanosomes are edited to generate mature transcripts. The process is characterized by the site-specific insertion and deletion of exclusively uridylate (U) nucleotides and is catalyzed by a macromolecular complex, the editosome. To initiate the editing reaction cycle, pre-edited substrate mRNAs have to bind to the catalytic machinery. Unfortunately, the editosome/RNA interaction is only marginally understood. Here we present a first visualization of individual pre-mRNA/editosome complexes using atomic force microscopy (AFM). We demonstrate that editosomes have one RNA binding site and that multiple editosomes can interact with a single pre-mRNA molecule. Furthermore, we identified a so far unknown activity of the editing machinery: editosomes execute a chaperone-type RNA unwinding activity.

Introduction

The majority of mitochondrial transcripts in African trypanosomes are substrates of a posttranscriptional modification reaction that converts non-translatable RNAs into mature transcripts. The reaction is characterized by the site-specific insertion and/or deletion of exclusively U nucleotides and as such it can be classified as an archetypical RNA editing reaction (reviewed in Hajduk and Ochsenreiter, 2010; Aphasizhev and Aphasizheva, 2011). The process involves small non-coding RNAs known as guide RNAs (gRNAs), which function as templates in the process (Blum et al., 1990). RNA editing is catalyzed by a multi-enzyme protein machinery, the editosome (reviewed in Aphasizhev and Aphasizheva, 2011; Göringer et al., 2011; Göringer, 2012). The complexes act as a reaction platform for the individual steps of the reaction cycle and contain all necessary catalytic activities.

Native, steady state isolates of editosomes have been visualized by transmission electronmicroscopy (TEM) and by cryo-EM (Golas et al., 2009; Kastner et al., 2008). The data identified the presence of two classes of high molecular mass assemblies (Golas et al., 2009) with well-defined, compact shapes and distinct structural features including surface areas of different electron density. A sedimentation analysis characterized the two particles as high molecular mass assemblies with apparent S-values of 20S and 35–40S (Golas et al., 2009). 35–40S editosomes have a calculated molecular mass of 1.6 MDa (Golas et al., 2009) and are associated with endogenous RNA including pre-mRNA and gRNA (Pollard et al., 1992; Corell et al., 1996; Golas et al., 2009). By contrast, 20S complexes are “protein-only” assemblies with a calculated molecular mass of 0.8 MDa (Rusché et al., 1997; Golas et al., 2009). They consist of 13-20 individual polypeptides (reviewed in Hadjuk and Ochsenreiter, 2010). A three-dimensional alignment of the 20S and 35-40S complexes revealed that 20S editosomes represent an integral part of the 35-40S complexes, which identified the binding of substrate RNA as a key determinant for the interconversion of the two complexes (Golas et al., 2009). In line with that observation, isolated 35–40S complexes are inactive to bind and process synthetic pre-mRNA molecules because their RNA binding site is occupied with endogenous RNAs (Golas et al., 2009). By contrast, 20S complexes are competent to bind and faithfully edit synthetic, pre-edited mRNAs in a gRNA-dependent fashion (Igo et al., 2000; Igo et al., 2002; Carnes and Stuart, 2007).

In order to visualize the editosome/pre-mRNA interaction, here we use atomic force microscopy (AFM) to picture the RNA binding reaction using a panel of "*in vivo*-sized", full length transcripts. The data confirm that 20S editosomes have one RNA binding site (see chapter one) and that multiple editosomes can bind to a single pre-mRNA molecule. Furthermore, the data reveal a so far unknown biochemical activity of the editing machinery: Following RNA binding, 20S editosomes unwind the bound RNA by a chaperone-type RNA unwinding activity.

Materials and Methods

Preparation of editosomes

20S editosomes were isolated from mitochondrial vesicle preparations of procyclic stage *T. brucei* cells. The following strains were used: Lister 427 (Cross, 1975) and the transgenic cell line 29-13-TbMP42/TAP (Golas et al., 2009). Parasite cells were harvested at late log phase and disrupted by N_2 cavitation at isotonic conditions (Hauser et al., 1996). Mitochondrial vesicles were isolated by differential centrifugation and used to prepare mitochondrial detergent ex-

tracts by incubation with 0.6% (v/v) Nonidet-P40 in editing buffer (EB): 20 mM HEPES/KOH pH 7.5, 30 mM KCl, 10 mM $Mg(OAc)_2$, 0.5 mM DTT. 20S editosomes were enriched by isokinetic ultracentrifugation in linear 10–35% (v/v) glycerol gradients (Göringer et al., 1994). TAP-tagged 20S editosomes were isolated from spin-cleared mitochondrial detergent extracts by consecutive IgG and calmodulin affinity chromatography followed by isokinetic ultracentrifugation in linear 10–35% (v/v) glycerol gradients. All editosome preparations were tested for their gRNA-dependent U insertion/U deletion *in vitro* RNA editing activity (Igo et al., 2000; Igo et al., 2002). The protein composition of TbMP-42/TAP editosomes has been described by Golas et al., 2009.

RNA synthesis

Unedited (UE) and fully edited (FE) A6 (344 nucleotides/762 nucleotides), UE and FE apocytochrome *b* (Cyb) (1080 nucleotides/1113 nucleotides), and never edited cytochromoxidase subunit I (COI) (1647 nucleotides) transcripts were PCR-amplified from *T. brucei* Lister 427 cDNA preparations. PCR products were cloned into pBS SK^- and sequenced. RNAs were synthesized by run-off transcription from linear DNA plasmid templates using T7 RNA polymerase following standard procedures. Guide RNA gA6-14 was *in vitro* transcribed as in Schmid et al., 1995. Radioactive RNA preparations were generated by *in vitro* transcription in the presence of α-[^{32}P]ATP (specific activity, 3000 Ci/mmol). All of the transcripts were gel electrophoretically purified, eluted from the gel slices, and EtOH precipitated. RNA folding was performed in EB by heating to 75 °C (5 min) and cooling to room temperature at 1 °C/min.

RNA unfolding

^{32}P-labeled pre-mRNA (2 nM) was incubated with 0–40 nM 20S editosomes at 27 °C for 0–60 min followed by structure-specific enzymatic probing at limiting enzyme concentrations. RNA cleavage was performed with 60 units/mL RNase T1 or 3 units/mL cobra venom RNase V1 for 2 min at room temperature. The samples were analyzed in urea-containing (8 M), 6% (w/v) polyacrylamide gels followed by phosphorimaging.

Atomic force microscopy (AFM*)*

Editosomes were dialyzed in EB to remove glycerol and incubated with substrate RNAs (pre-mRNA, gRNA, and pre-mRNA/gRNA hybrids) in a 1:1 molar stoichiometry (60 min at 27 °C). Editosome/RNA complexes were deposited onto freshly cleaved mica and allowed to adhere for 5 min. The mica was washed (3 x 1 mL of EB) and dried in a mild stream of N_2. The images were taken in tapping mode in air using silicon cantilevers with a nominal spring constant of 2 N/m and a resonance frequency of approximately 70 kHz. All of the images were scanned at a frequency of 1 Hz and were analyzed using the MFP-3D software. Apparent particle volumes (V_{app}) were calculated as $V_{app} = \pi h(w)^2/6$ (where h is height, and w is width), assuming oblate spheroid shapes of the complexes (Minh et al., 2009). Contour length measurements were performed by manually tracing using MFP-3D and fitting of the contour length histogram to a Gaussian distribution.

Results

Atomic force microscopy of native editosomes

As a first experiment we analyzed affinity-purified (TAP tagged) editosome preparations in the absence of exogenously added RNA. Fig. 1A shows a representative result. As anticipated from the published EM data (Golas et al., 2009) TAP-tagged editosome preparations contain both 20S and 35–40S complexes. Both particles are characterized

by a well defined, roundish appearance and can be distinguished by their diameter and height (Fig. 1, B and C). 20S complexes have a mean diameter of 24.4 nm and an average height of 4 nm (Fig. 1B). 35–40S particles have a mean diameter of 49.3 nm and an average height of 7 nm (Fig. 1C). These numbers deviate from the published EM-based measurements (Golas et al., 2009) and are likely influenced by two phenomena: (i) flattening of the complexes during the AFM analysis (Minh et al., 2009; Matsuura et al., 2006; Mikamo-Satoh et al., 2009) and (ii) shrinking of the particles caused by dehydration on the mica surface (Moreno-Herrero et al., 2003; Santos et al., 2011). Nevertheless, the dimensions can be used to calculate apparent volumes (V_{app}) for the complexes, which revealed Gaussian distributions with an average volume of 3–4 x 10^3 nm^3 for the 20S editosome and 6–7 x 10^3 nm^3 for the 35–40S editosome (Fig. 1, D and E). In agreement with recently published data (Kuznetsov et al., 2010), AFM of pure RNA preparations showed that the molecules are highly folded. Fig. 1F illustrates as an example a preparation of the A6-UE transcript. The molecules appear as a monodisperse population of small roundish structures with diameters varying between 7 and 20 nm (mean diameter, 13 nm) and an average height of ≤2 nm (Fig. 1G).

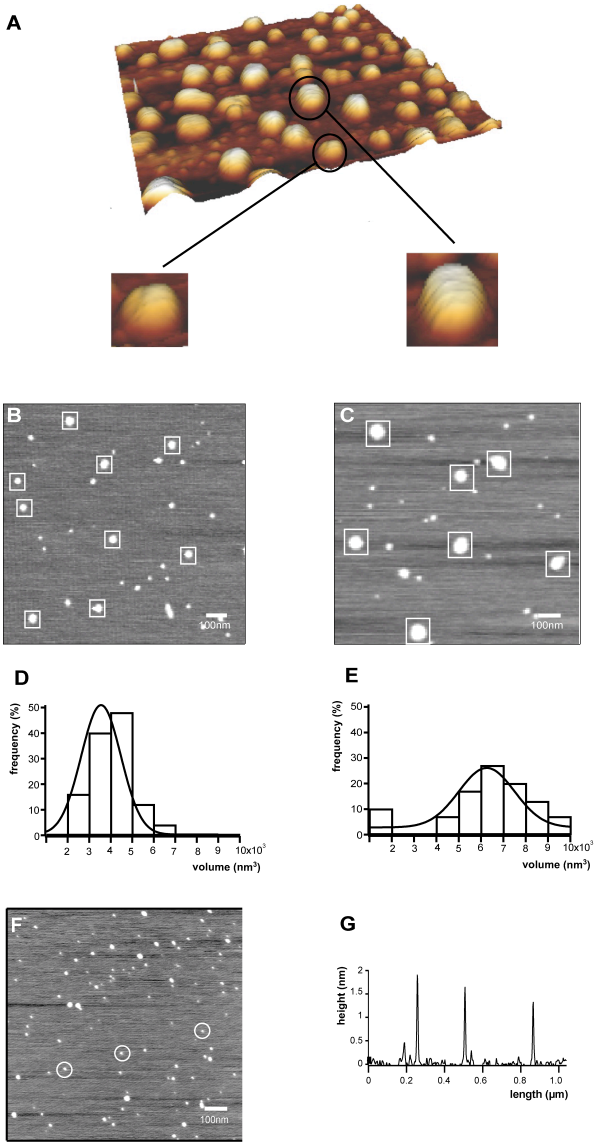

Figure 1. AFM of native editosomes and substrate RNAs. (A) Three-dimensional AFM image of an affinity-purified (TAP-tagged) editosome preparation deposited on a mica surface. The isolate contains both 20 and 35–40S editosomes. Two individual complexes of each kind are encircled and outcropped (*left panel*, 20S editosome; *right panel*, 35–40S editosome). (B) AFM image (height view) of purified 20S editosomes. Individual complexes (*white squares*) have a mean diameter of 24.4 nm (B) and an average volume of 3–4 x 10^3 nm^3 (D). (C) AFM image (height view) of purified 35–40S editosomes. The particles have a mean diameter of 49.3 nm (C) and a mean volume of 6–7 x 10^3 nm^3 (E). (F) AFM image (height view) of A6-UE mRNA on mica. The RNAs appear as round structures with an average diameter of 13 nm and an average height of ≤2 nm. (G) Height trace of the three encircled A6-UE mRNA molecules in F.

Atomic force microscopy of editosome-RNA complexes

For the visualization of individual editosome-RNA complexes, we incubated the two reactants at equimolar concentrations for 0–60 min. Fig. 2 shows representative experiments using the transcripts A6-UE, A6-FE, Cyb-UE, and COI. At zero incubation time, the two reactants are well separated and can be distinguished by their characteristic dimensions (Fig. 2A). After 5 min (Fig. 2B) binding can be detected, which surprisingly is accompanied by an unfolding of the RNA structure (see *inset* in Fig. 2B). The highly folded RNAs (Fig. 1F) are opened up through the interaction with

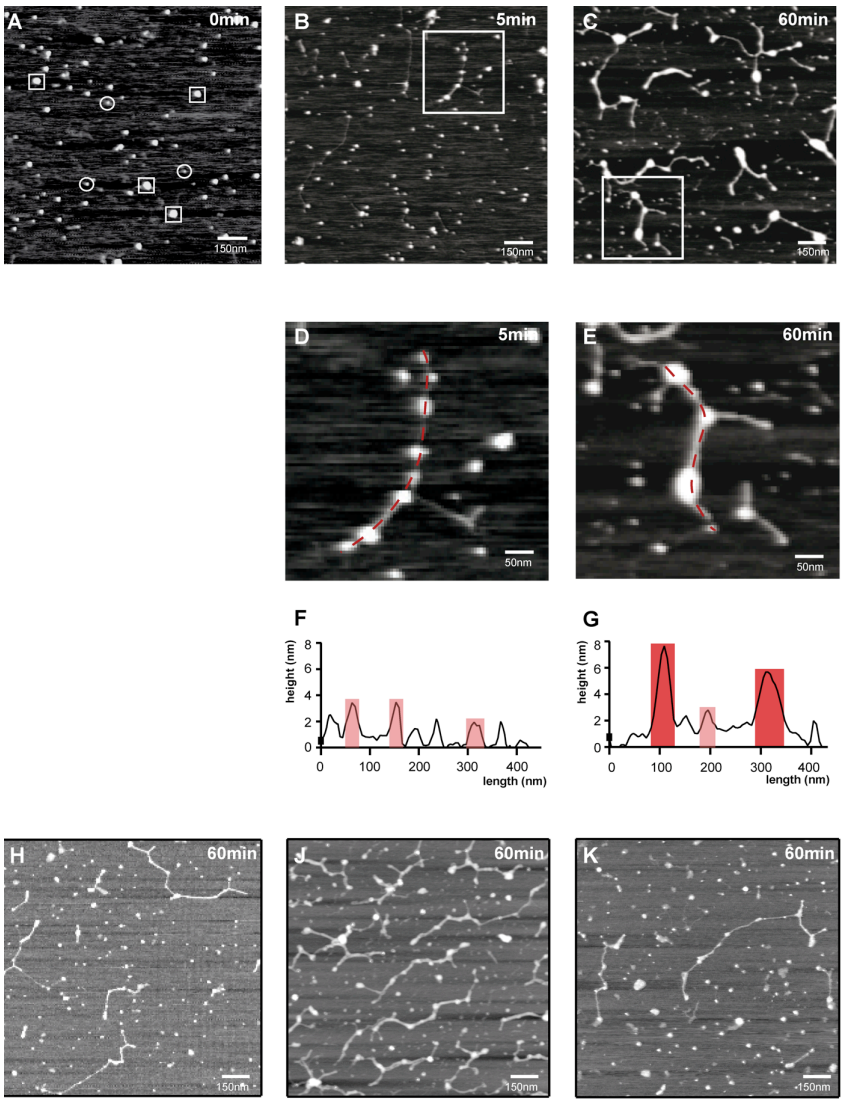

Figure 2. AFM of editosome-RNA complexes. (A-C) AFM images of 20S editosomes (*small squares*) incubated with A6-UE mRNA (*circles*) for 0, 5, and 60 min. (D) Enlargement of the highlighted (*large square*) editosome-A6-UE mRNA complex in B. The image shows a single A6-UE mRNA molecule bound by multiple editosomes. (E) Enlargement of the highlighted (*large square*) editosome-A6-UE mRNA complex in C. The image shows the formation of editosome multimers/aggregates on a single A6-UE mRNA after 60 min of incubation. (F and G) Contour length measurements (stippled lines) of the complexes shown in D and E. *Red*, 20S editosomes; *dark red*, editosome multimers; *no highlighting*, higher order RNA structure elements. (H, J, and K) AFM images of editosome-RNA complexes for different pre-mRNAs after 60 min of incubation: COI (H), Cyb-UE (J), and A6-FE (k).

20S editosomes, and the reaction increases over time (Fig. 2C). Furthermore, more than one editosome interacts with a fully unfolded mRNA molecule. Fig. 2 (D and F) shows a representative example of an A6-UE mRNA-editosome complex after 5 min of incubation. Multiple 20S particles (on average 2–3) are bound to one A6-UE transcript and are distributed over the entire length of the RNA. No preferential binding sites were identified, confirming the non-sequence-specific binding of RNA by 20S editosomes. After 60 min, RNA-associated structures with dimensions even greater than that of a 20S editosome were observed (Fig. 2, E and G). These structures likely represent editosome multimers (likely dimers and trimers). All tested mRNAs (Fig. 2, H, J and K) were substrates of the unwinding reaction although with different kinetic (after 60 min): Cyb-UE>A6-UE>COI=A6-FE. This likely reflects the different higher order foldings, *i.e.*, thermodynamic stabilities of the various RNAs.

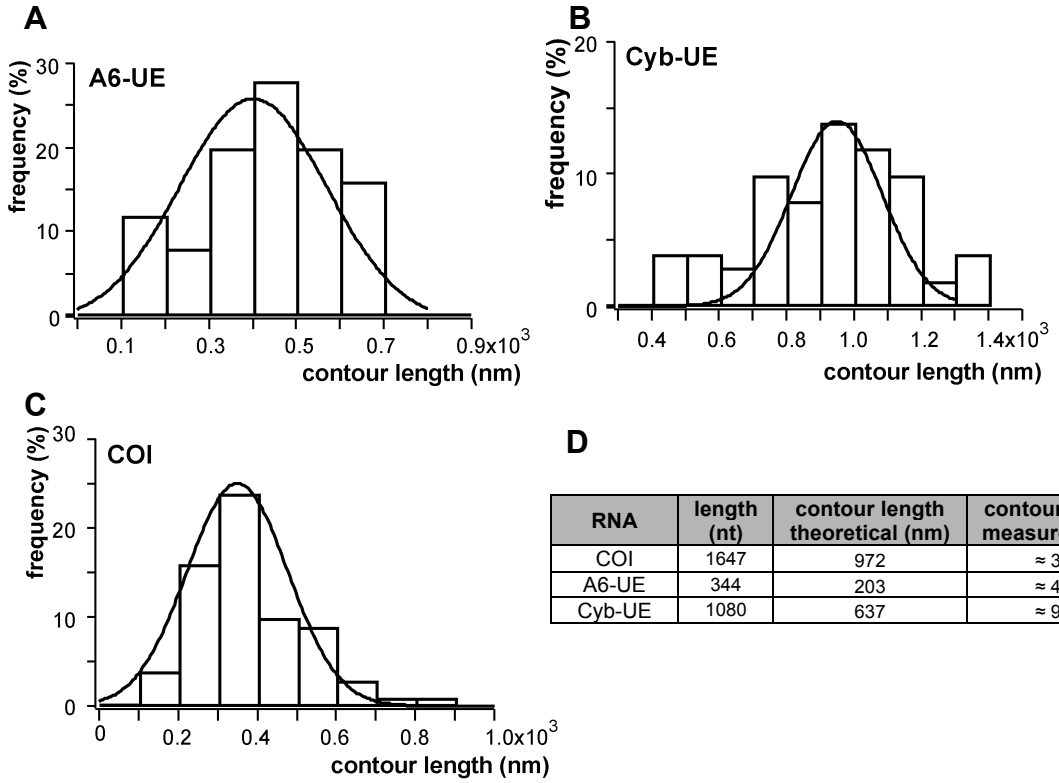

D

RNA	length (nt)	contour length theoretical (nm)	contour length measured (nm)
COI	1647	972	≈ 341
A6-UE	344	203	≈ 431
Cyb-UE	1080	637	≈ 956

Figure 3. AFM-based RNA contour lengths measurements. Messenger RNA preparations of A6-UE (A), Cyb-UE (B) and COI (C) were incubated with 20S editosomes for 60min to induce RNA unwinding. Unwound RNAs were visualized by AFM and outlines of 30-60 individual RNAs were manually traced using MFP-3D (Asylum Research, USA) to measure their contour length. The resulting contour length histograms were fitted to a Gaussian distribution. (D) Theoretical and measured contour lengths for the three different mRNAs.

Measuring the contour length of three of the transcripts (COI, A6-UE, and Cyb-UE) after 60 min identified that the A6-UE and Cyb-UE transcripts were fully unfolded, whereas the COI mRNA was resolved to only approximately 30% of its theoretical length (Fig. 3). The average thickness of an unfolded RNA strand was determined as ≤2 nm in line with previously published data (Hansma et al., 1996).

20S editosomes execute RNA unwinding activity

To confirm the editosome-driven RNA unfolding reaction, we measured RNA unfolding by biochemical means. The assay is based on the rationale that opening up the higher order structure of an RNA should make the molecule RNase susceptible. For that, we generated radioactively labeled mRNA preparations, which were incubated with 20S editosomes in the presence of structure-specific RNases. The reaction was performed at limiting enzyme conditions to ensure that in the absence of editosomes, all input RNA remained undigested during the incubation. Fig. 4 shows a representative experiment using the A6-UE transcript as an example. The RNA was hydrolyzed with RNase T1 (Fig. 4A), which degrades RNA 3' of single-stranded G-residues, as well as with cobra venom RNase V1 (Fig. 4D), which cleaves base-paired nucleotides. The generated cleavage products were separated in denaturing polyacrylamide gels, and the percentage of degradation was determined. Incubation of 2 nM A6-UE mRNA with increasing concentrations (0–40 nM) of 20S editosomes for 60 min

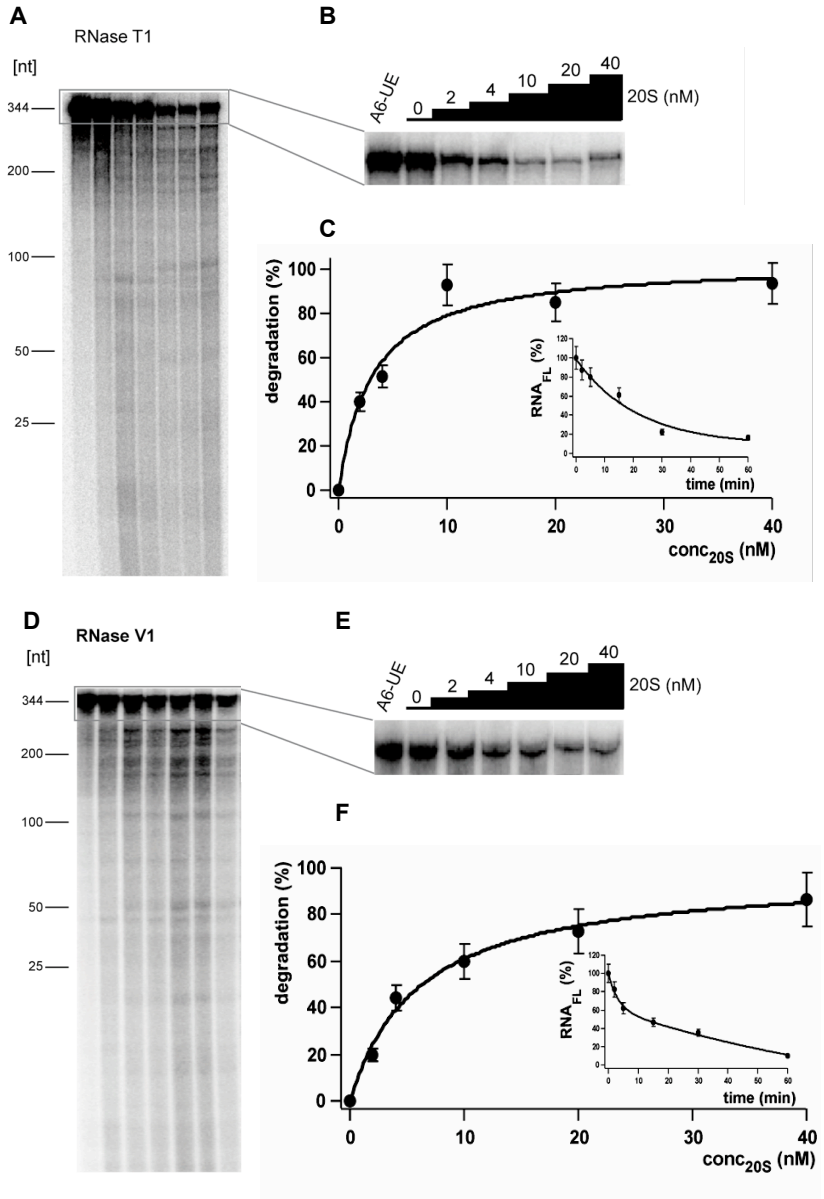

Figure 4. Editosome-driven RNA unwinding. Autoradiograms of 32P-labeled A6-UE mRNA after incubation with increasing concentrations of 20S editosomes (0–40 nM) are shown. RNA unwinding was monitored by structure-specific RNase digestion using RNase T1 (A) and RNase V1 (D). Nonsaturated exposures of the full-length mRNA(344 nucleotides) are shown in B and E. Shown is a plot of the percentage of degradation as a function of the 20S editosome concentration. (C) RNase T1 digestion. (F) RNase V1 digestion. (Insets) Kinetic of the editosome-dependent RNA unwinding reaction. *FL*, full-length. The *error bars* show the relative errors as percentages.

at 27 °C led to an increased degradation of the RNA by the two ribonucleases (Fig. 4, B and E). The degradation follows a general decay function (Fig. 4, C and F), and the RNase T1 digestion is ≥90% complete at an editosome concentration of ≥10 nM. The RNase V1 digest requires 40 nM editing complex to achieve the same result. Half-maximal degradation is accomplished at approximately 5 nM editosomes in both experiments (Fig. 4, C and F). The *insets* in Fig. 4 (C and F) show the results of two time course experiments. The degradation follows a decay kinetic with half-maximal degradation after approximately 15 min and approximately 80–90% degradation after 60 min in both cases. As expected for a RNA chaperone type activity (Rajkowitsch et al., 2007), the reaction does not require exogenous ATP.

Discussion

U-insertion/U–deletion-type RNA editing is catalyzed by a high molecular mass protein complex the 20S editosome. Key step in the process is the initial binding of pre-edited substrate RNAs to the catalytic machinery, which converts 20S editosomes to 35-40S complexes. Using Atomic Force Microscopy (AFM), we visualized steady state isolates of native editosome preparations and confirmed the presence of both, "RNA-free" 20S complexes as well as "RNA-loaded" 35-40S complexes. The two particles are characterized by a roundish appearance and can be distinguished by their diameter and height. Upon incubation of 20S editosomes with different substrate mRNAs we were able to confirm that the complexes bind RNA in a nonselective fashion at a single RNA binding site (see chapter one). No evidence of a preferential binding domain in any of the tested pre-mRNAs was found. However, we identified that multiple editosomes can interact with a single RNA molecule. Editosome dimers, trimers and even assemblies of higher complexities were observed after 60min of incubation. The significance of these "multimeric" complexes awaits further testing.

Additionally, the AFM experiments revealed a so far unknown biochemical activity of the editing machinery: RNA binding is followed by RNA unwinding, which resolves the higher order structure of editosome-bound RNAs. This implies that 20S editosomes execute a chaperone-type RNA unwinding activity. Biochemical unfolding experiments confirmed the presence of the activity and demonstrated that the reaction features defined stoichiometric and kinetic characteristics. RNA contour length measurement further demonstrated that some of the bound transcripts (A6-UE – 344 nt; Cyb-UE – 1080 nt) were fully unfolded (after 60 min), while others (COI – 1647 nt) were only partially resolved (app. 30%). This likely reflects a dependence on the length and/or thermodynamic stability of the bound RNAs. RNA chaperones are proteins that recognize substrate RNA with a broad specificity. They play a role in a multitude of biological processes (reviewed in Rajkowitsch et al., 2007; Herschlag, 1995) and modulate RNA folding to generate biochemically active RNA conformations. Generally, the binding of a chaperone protein destabilizes "incorrectly" folded RNA elements and therefore, within the context of the editing reaction, the most likely function of the activity is to resolve the highly structured conformations of editosome-bound pre-edited transcripts. Misfolded and/or conformationally trapped RNAs have been shown to be rate limiting in other RNA-guided biochemical processes (Thirumalai et al., 2001; Russell and Herschlag, 2001; Russell et al., 2002) and as consequence, it seems plausible that the editing machinery exhibits a catalytic activity to side step this potential roadblock. Whether the activity contributes to other editing-specific reaction steps such as the presentation of anchor sequences or the unfolding of gRNA secondary structure elements (Hermann et al., 1997; Reifur and Koslowsky, 2008) cannot be deduced from the data here. However, based on the observation that never edited mRNAs are substrates of the unwinding reaction, it seems conceivable that the activity represents a rather promiscuous feature of the editing machinery. The reaction possibly contributes to other mitochondrial RNA-driven processes and thus, provides a rationale for the above described lack of substrate specificity.

Which of the protein component(s) of the editosome mediates the unfolding activity is an open question. Importantly, the activity is intrinsic to the 20S editosome and thus is different from the

various accessory RNA structure-modulating activities that have been identified within the context of the editing cycle (reviewed in Göringer et al., 2008). Therefore, all so far functionally unassigned editosomal proteins represent potential candidates. However, of special importance are the six OB (oligonucleotide/oligosaccharide binding)-fold proteins of the 20S complex (Stuart et al., 2005). OB-fold proteins in other RNA-based biochemical systems have been shown to provide RNA chaperone-type activities (reviewed in Rajkowitsch et al., 2007; Kwon et al., 2007) and TbMP24/KREPA4, one of the editosomal OB-fold proteins, has recently been identified to execute RNA annealing activity (Kala and Salavati, 2010). Within that context the yeast exosome core protein Rrp44 is of special interest (Lorentzen et al., 2008; Bonneau et al., 2009). Rrp44 has been shown to catalyze RNA unwinding and the activity was structurally attributed to a multimeric OB-fold domain. Evidence for a heteromultimeric association of five of the editosomal OB-fold proteins has recently been published (Park et al., 2012), which makes this hypothetical "OB-fold core" a prime candidate for the unwinding activity of the 20S editosome.

Taken together, the presented data support the following scenario (Fig. 5): mitochondrial RNA molecules bind with high affinity to a single RNA binding site of the 20S editosome. Both types of editing substrate RNAs (insertion/deletion) interact with the same binding site suggesting a bifunctional reaction center of the editing machinery. RNA binding is followed by RNA unwinding. The activity is intrinsic to 20S editosomes and unfolds higher order RNA structure elements thereby resolving structural roadblocks. Ultimately the activity facilitates the interaction of multiple editosomes with one pre-mRNA. The unwinding activity is promiscuous, which suggests that editosomes may contribute their unwinding function to other RNA-driven mitochondrial pathways in trypanosomes.

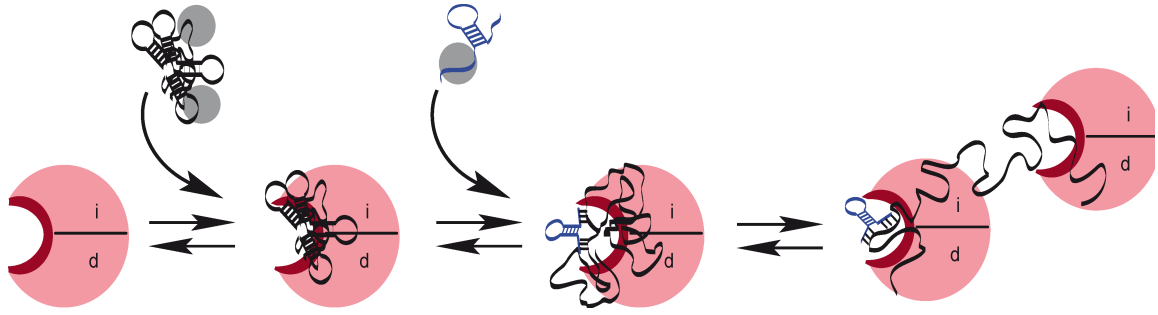

Figure 5. Cartoon of the binding characteristics and downstream events of the editosome/RNA interaction. 20S editosomes (*red spheres*) bind substrate RNAs with high affinity. The interacting RNAs (pre-mRNAs, *black*; gRNAs, *blue*) likely bind in the form of ribonucleoprotein complexes (*gray spheres*), and the interaction takes place at a single RNA-binding site (*dark red*). Upon binding, an editosome-intrinsic RNA unwinding activity catalyzes the unwinding of the bound RNAs, which ultimately enables multiple editosomes to bind to one pre-mRNA. *i*, insertion; *d*, deletion subdomain of the 20S editosome.

References

Aphasizhev R and Aphasizheva I. (2011) Uridine insertion/deletion editing in trypanosomes. A playground for RNA-guided information transfer. *Wiley Interdiscip. Rev. RNA* 2:669–685.

Blum B, Bakalara N and Simpson L. (1990) A model for RNA editing in kinetoplastid mitochondria. "Guide" RNA molecules transcribed from maxicircle DNA provide the edited information. *Cell* 60:189–198.

Bonneau F, Basquin J, Ebert J, Lorentzen E and Conti E. (2009) The yeast exosome functions as a macromolecular cage to channel RNA substrates

for degradation. *Cell* 139:547–559.

Carnes J and Stuart K. (2007) Uridine insertion/deletion editing activities. *Methods Enzymol.* 424:25-54.

Corell RA, Read LK, Riley GR, Nellissery JK, Allen TE, Kable ML, Wachal MD, Seiwert SD, Myler PJ and Stuart KD. (1996) Complexes from *Trypanosoma brucei* that exhibit deletion editing and other editing-associated properties. *Mol. Cell. Biol.* 16:1410-1418.

Cross GA. (1975) Identification, purification and properties of clonespecific glycoprotein antigens constituting the surface coat of *Trypanosoma brucei*. *Parasitol.* 71:393–417.

Ernst NL, Panicucci B, Igo RP Jr, Panigrahi AK, Salavati R and Stuart K. (2003) TbMP57 is a 3' terminal uridylyl transferase (TUTase) of the *Trypanosoma brucei* editosome. *Mol. Cell* 11:1525–1536.

Golas MM, Böhm C, Sander B, Effenberger K, Brecht M, Stark H and Göringer HU. (2009) Snapshots of the RNA editing machine in trypanosomes captured at different assembly stages *in vivo*. *EMBO J.* 28:766–778.

Göringer HU. (2012) 'Gesalt,' Composition and function of the *Trypanosoma brucei* editosome. *Annu. Rev. Microbiol.* 66:65-82.

Göringer HU, Brecht M, Böhm C and Kruse E. (2008) RNA editing accessory factors. The example of mHel61p. In *RNA Editing, Nucleic Acids and Molecular Biology* (Göringer, H. U., ed) pp. 165–179, Springer, Heidelberg.

Göringer HU, Katari VS and Böhm C. (2011) The structural landscape of native editosomes in African trypanosomes. *Wiley Interdiscip. Rev. RNA* 2:395–407.

Göringer HU, Koslowsky DJ, Morales TH and Stuart K. (1994) The formation of mitochondrial ribonucleoprotein complexes involving guide RNA molecules in *Trypanosoma brucei*. *Proc. Natl. Acad. Sci. U.S.A.* 91:1776–1780.

Hajduk S and Ochsenreiter T. (2010) RNA editing in kinetoplastids. *RNA Biol.* 7:229–236.

Hauser R, Pypaert M, Häusler T, Horn EK and Schneider A. (1996) *In vitro* import of proteins into mitochondria of *Trypanosoma brucei* and *Leishmania tarentolae*. *J. Cell Sci.* 109:517–523.

Hermann T, Schmid B, Heumann H and Göringer HU. (1997) A three-dimensional working model for a guide RNA from *Trypanosoma brucei*. *Nucl. Acids Res.* 25:2311-2318.

Herschlag D. (1995) RNA chaperones and the RNA folding problem. *J. Biol. Chem.* 270:20871–20874.

Igo RP Jr, Palazzo SS, Burgess ML, Panigrahi, AK and Stuart K. (2000) Uridylate addition and RNA ligation contribute to the specificity of kinetoplastid insertion RNA editing. *Mol. Cell. Biol.* 20:8447–8457.

Igo RP Jr, Weston DS, Ernst NL, Panigrahi AK, Salavati R and Stuart K. (2002) Role of uridylate-specific exoribonuclease activity in *Trypanosoma brucei* RNA editing. *Eukaryot. Cell* 1:112–118.

Kala S and Salavati R. (2010) OB-fold domain of KREPA4 mediates high-affinity interaction with guide RNA and possesses annealing activity. *RNA* 16:1951–1967.

Kastner B, Fischer N, Golas MM, Sander B, Dube P, Boehringer D, Hartmuth K, Deckert J, Hauer F and Wolf E, et al. (2008) GraFix: sample preparation for single particle electron cryomicroscopy. *Nat. Methods* 5:53–55.

Kuznetsov YG, Dowell JJ, Gavira JA, Ng JD and McPherson. (2010) A Biophysical and atomic force microscopy characterization of the RNA from satellite tobacco mosaic virus. *Nucl. Acids Res.* 38:8284–8294.

Kwon SH, Lee IH, Kim NY, Choi DH, Oh YM and Bae SH. (2007) Translation initiation factor eIF1A possesses RNA annealing activity in its oligonucleotide-binding fold. *Biochem. Biophys. Res. Commun.* 361:681–686.

Lorentzen E, Basquin J, Tomecki R, Dziembowski A and Conti E. (2008) Structure of the active subunit of the yeast exosome core, Rrp44. Diverse modes of substrate recruitment in the RNase II nuclease family. *Mol. Cell* 29:717–728.

Matsuura T, Tanaka H, Matsumoto T and Kawai T. (2006) Atomic force microscopic observation of *Escherichia coli* ribosomes in solution. *Biosci. Biotechnol. Biochem.* 70:300–302.

Mikamo-Satoh E, Takagi A, Tanaka H, Matsumoto T, Nishihara T and Kawai T. (2009) Profiling of gene-dependent translational progress in cell-free protein synthesis by real-space imaging. *Anal. Biochem.* 394:275–280.

Minh PN, Devroede N, Massant J, Maes D and

Charlier D. (2009) Insights into the architecture and stoichiometry of Escherichia coli PepA*DNA complexes involved in transcriptional control and site-specific DNA recombination by atomic force microscopy. *Nucl. Acids Res.* 37:1463–1476.

Moreno-Herrero F, Colchero J and Baró AM. (2003) DNA height in scanning force microscopy. *Ultramicroscopy* 96:167–174.

Park YJ, Pardon E, Wu M, Steyaert J and Hol WG. (2012) Crystal structure of a heterodimer of editosome interaction proteins in complex with two copies of a cross-reacting nanobody. *Nucl. Acids Res.* 40:1828–1840.

Pollard VW, Harris ME and Hajduk SL. (1992) Native mRNA editing complexes from *Trypanosoma brucei* mitochondria. *EMBO J.* 11:4429-4439.

Rajkowitsch L, Chen D, Stampfl S, Semrad K, Waldsich C, Mayer O, Jantsch MF, Konrat R, Bläsi U and Schroeder R. (2007) RNA chaperones, RNA annealers and RNA helicases. *RNA Biol* 4:118–130.

Reifur L and Koslowsky DJ. (2008) *Trypanosoma brucei* ATPase subunit 6 mRNA bound to gA6-14 forms a conserved three-helical structure. *RNA* 14:2195–2211.

Rusché LN, Cruz-Reyes J, Piller KJ and Sollner-Webb. (1997) Purification of a functional enzymatic editing complex from *Trypanosoma brucei* mitochondria. *EMBO J.* 16:4069-4081.

Russell R and Herschlag D. (2001) Probing the folding landscape of the *Tetrahymena* ribozyme. Commitment to form the native conformation is late in the folding pathway. *J. Mol. Biol.* 308:839–851.

Russell R, Zhuang X, Babcock HP, Millett IS, Doniach S, Chu S and Herschlag D. (2002) Exploring the folding landscape of a structured RNA. *Proc. Natl. Acad. Sci. U.S.A.* 99:155–160.

Santos S, Barcons V, Christenson HK, Font J and Thomson NH. (2011) The intrinsic resolution limit in the atomic force microscope: implications for heights of nano-scale features. *PLoS One* 6, e23821.

Schmid B, Riley GR, Stuart K and Göringer HU. (1995) The secondary structure of guide RNA molecules from *Trypanosoma brucei*. *Nucl. Acids Res.* 23:3093–3102.

Stuart KD, Schnaufer A, Ernst NL and Panigrahi AK. (2005) Complex management: RNA editing in trypanosomes. *Trends Biochem. Sci* 30, 97–105.

Thirumalai D, Lee N, Woodson SA and Klimov D. (2001) Early events in RNA folding. *Annu. Rev. Phys. Chem.* 52:751–762.

“The difference between the right word and the nearly right word is the same as the difference between lightning and the lightning bug.”

– Mark Twain

Chapter Three

U-insertion/deletion RNA editing is not cell-cycle regulated

The life cycle of African trypanosomes involves the cyclic transmission between a mammalian host and an insect vector. U-insertion/deletion-type RNA editing has been suggested to play a major role in the regulation of mitochondrial gene expression in the two life cycle stages based on the observation that steady state levels of some edited mRNAs vary dramatically between the two stages. Here we investigate the possibility that RNA editing is regulated during the cell cycle of trypanosomes. Insect-stage *Trypanosoma brucei* were synchronized with 0.2mM hydroxyurea and used to isolate 20S editosomes from G1- and G2-cell cycle phase-enriched parasites. The isolates were separately tested for their U-insertion and U-deletion RNA editing activity using synthetic pre-mRNA /gRNA substrate RNAs. Editosomes from both cell cycle stages showed editing activity. No difference, neither qualitatively nor quantitatively was observed between the G1- and G2-isolates and both complexes were able to conduct the two editing reactions (U-insertion/U-deletion) in an identical fashion. The experiments demonstrate that U-insertion/deletion-type RNA editing in African trypanosomes is not cell-cycle regulated.

Introduction

Trypanosoma brucei is a protozoan parasite that contains a single large mitochondrion. Its mitochondrial DNA is concentrated within a portion of the mitochondrion called the kinetoplast DNA (kDNA). It is organized as a concatenated network of two types of circular DNA molecules – minicircle and maxicircle DNA (reviewed in Liu et al., 2005). Maxicircles are homogenous in size (25 kbp) with a copy number of 25-50 molecules per trypanosome. Minicircles are about 1 kbp in size. A single kDNA network contains about an estimated number of 10,000 minicircles, which can be grouped into 250 different minicircle classes (Hajduk and Sabatini, 1998). Maxicircle gene products include rRNAs and subunits of respiratory complexes (reviewed in Liu et al., 2005). Twelve of the maxicircle transcripts are posttranscriptionally modified to form functional mRNAs. The process is known as "RNA editing". Editing is characterized by the site-specific insertion/deletion of U nucleotides (reviewed in Hajduk and Ochsenreiter, 2010; Aphasizhev and Aphasizheva, 2011). The reaction is a guided process that involves small non-coding RNAs known as "guide RNAs" (gRNA). They are in majority encoded on the minicircles. Guide RNAs function as "quasi" templates by forming hybrids with the pre-edited mRNAs and dictate the number of Us to be inserted and/or deleted during the editing cycle (Blum et al., 1990, Blum and Simpson, 1990).

The editing reaction is catalyzed by a high molecular mass protein complex, the editosome (reviewed in Göringer, 2012). Recent studies revealed that editosomes bind substrate-RNAs with nanomolar affinity (Golas et al., 2009; Böhm et al., 2012). They have one substrate-RNA binding site (Böhm et al., 2012) and catalyze both editing reactions within a single, bifunctional reaction center (Böhm et al., 2012). The reactions are executed *via* a cleavage-ligase mechanism that involves enzymatic activities such as ribonuclease (Igo et al., 2002; Aphasizhev and Simpson, 2001), terminal uridylyltransferace (TUTase) (Ernst et al., 2003; Aphasizhev et al., 2003), RNA ligase (McManus et al., 2001; Huang et al., 2001; Rusché et al., 2001; Gao and Simpson, 2003) and perhaps nucleotidyl phosphatase activity (Niemann et al., 2008). Several accessory factors have been shown to contribute in the editing process, such as matchmaking-type RNA/RNA annealing factors (Müller et al., 2001; Blom et al., 2001; Müller and Göringer, 2002; Aphasizhev et al., 2003; Ammerman et al., 2008; Sbicego et al., 2003; Kala and Salavati, 2010) and RNA helicases (Missel et al., 1997; Li et al., 2011).

The parasite's life cycle is characterized by the cyclic transmission between a mammalian host and an insect vector (reviewed in McKean, 2003; Kramer, 2012). The life cycle stages are known as bloodstream form (BF) and procyclic form (PF) trypanosomes (reviewed in Kramer 2012). The source for ATP in the PFs' is through mitochondrial oxidative phosphorylation and BFs' use almost exclusively gylcolysis (Bringaud et al., 2006). RNA editing takes place in both developmental stages. Certain transcripts are edited in either of the developmental stages, whereas others are edited in both stages (Table 1) (reviewed in Hajduk and Sabatini, 1998). However, it has been suggested that polyadenylation of RNAs plays an important role in modulating the rates of RNA turnover (Ryan et al., 2003). The poly(A) tail lengths has been correlated with the edited status of the RNA (Kao and Read, 2005). They are regulated throughout the life cycle of trypanosomes (Bhat et al., 1992; Read et al.,

1994). Edited transcripts have longer poly(A) tails than unedited transcripts and this may influence mitochondrial gene expression since polyadenylation can regulate cytoplasmic gene expression in eukaryotes (Bhat et al., 1992).

gene	no. of uridines		edited size (nt)	life cycle
	added	deleted		
Cyb	34	0	1151	PF
A6	447	28	811	PF/BF
COI	0	0		unedited
COII	4	0	663	PF
COIII	547	41	969	PF/BF
ND1	0	0		unedited
ND3	210	13	452	unknown
ND4	0	0		unedited
ND5	0	0		unedited
ND7	553	89	1238	5' PF/BF, 3' BF
ND8	259	46	574	BF
ND9	345	20	649	BF
S12	132	28	325	BF
MURF1	0	0		unedited
MURF2	26	4	1111	PF/BF
CR3	148	13	299	BF
CR6	325	40	567	BF

Table 1 List of mRNAs that are edited in *T. brucei*. Number of uridines added and/or deleted during RNA editing . PF: procyclic form; BS: bloodstream form. Cyb: apocytochrome b; A6: ATPase subunit 6; CO: cytochrome oxidase (subunits I-III); ND: NADH dehydrogenase (subunits 1, 3-5, 7-9); S12: ribosomal protein S12; MURF: maxicircle unidentified reading frame; CR: C-rich reading frame. For ND7: the 5' of the transcript is edited in PF and BF, whereas 3' of the transcripts is edited only in the BF (reviewed in Hajduk and Sabatini, 1998).

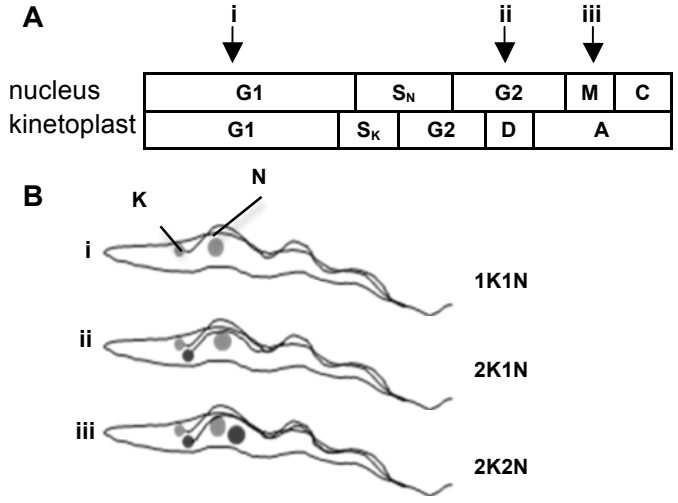

Figure 1. The *T. brucei* cell cycle. (A) Linear map of the cell cycle representing G1, $S_{K/N}$, G2, D/M, A/C periods for the kinetoplast (K) and nucleus (N). D: the period in which kinetoplast division occurs, M: mitosis, A: period when cell contains two kinetoplasts (2K), C: cytokinesis. (B) Schematic representation of trypanosomes at different time points within the cell cycle (McKean, 2003). (i): G1-phase; the cell contains one kinetoplast and one nucleus (1K1N) (light- and dark grey circle); (ii) G2-phase; the cell contains two kinetoplasts and one nucleus (2K1N)

RNA editing within different phases of the cell cycle has been addressed in *Leishmania tarentolae* (Carrillo et al., 2001). In the *leishmania* system, RNA editing is cell cycle dependent. However, the variations between fully edited to unedited transcripts are only 1.3- to 2.0-fold. Such a regulatory role of RNA editing within different phases of the cell cycle has not been addressed for *T. brucei*. The *T. brucei* cell cycle involves a periodic S-phase for the kinetoplast in addition to nuclear G1, S, G2, M-phases (Ploubidou et al., 1999). The kinetoplast also undergoes replication and division during the cell cycle (Fig. 1). Synthesis of the kinetoplast (kDNA) and the nuclear

DNA start very close together but kDNA synthesis finishes before the nuclear DNA (Woodward and Gull, 1990). A division period (D) and a period (A) when the cell contains two kinetoplasts (2K) can be defined (Woodward and Gull, 1990).

Here we analyze whether RNA editing is regulated within the cell cycle of the parasite. We test the RNA editing activity of 20S editosomes enriched from the G1- and G2-phases of the cell cycle *in vitro*. The cells are synchronized with hydroxyurea (HU) (Chowdhury et al., 2008). HU inhibits the ribonucleotide reductase during the DNA synthesis by interacting with the enzyme's free tyrosyl radical (Reichard and Ehrenberg, 1983) without affecting other metabolic processes (Galanti et al., 1994). Both, U-insertion/deletion-type RNA editing assays are performed using synthetic pre-mRNA/gRNA substrate RNAs (Igo et al., 2000; Igo et al., 2002). Our results confirm that editosomes are present in both cell cycle phases and that they are able to catalyze both types of the editing reaction. U-insertion/deletion RNA editing is not cell cycle regulated.

Materials and Methods

Synchronization and mitochondrial vesicle preparation

Procyclic stage *Trypanosoma brucei* cells (Cross, 1975) were cultured to a cell density of 2.5-3.0 x 10^6 cells/ml in 5 L SDM 79 medium (Brun and Schönenberger, 1979) at 27 °C. The cells were synchronized with 0.2 mM hydroxyurea (HU) (Chowdhury et al, 2008) for 12 h, followed by HU removal and culturing the cells in fresh SDM 79 medium. Approximately, 6.5 x 10^9 cells were harvested at G1- and G2- phase after assessing for synchrony by flow cytometry. The cells were disrupted at isotonic conditions by nitrogen cavitation (Hauser et al., 1996) and mt-vesicles were isolated by differential centrifugation. Detergent extracts of the vesicles were generated by incubation with 1% (v/v) Triton X-100 (2x critical micelle concentration (CMC)) in editing buffer (EB: 20 mM HEPES/KOH pH 7.5; 30 mM KCl; 10 mM $Mg(OAc)_2$) containing 1 mM DTT; 1 mM PMSF; 1 µg/mL leupeptin; 10 µg/mL trypsin inhibitor. Editosomes were enriched in 2 mL linear 10-35% (v/v) glycerol gradients (Göringer et al., 1994) by isokinetic ultracentrifugation and fractionated.

Oligonucleotide synthesis

RNA oligonucleotides were synthesized by automated solid phase synthesis using 2´-O-triisopropylsilyoxymethyl (TOM) protected phosphoramidites in a 50 nmole synthesis scale. Yields varied between 95-97 %. RNA oligonucleotides were dissolved in 10 mM Tris/HCl pH 7.5, 1 mM EDTA and stored at -20 °C. Concentrations were determined by UV absorbance measurements at 260 nm. The following sequences were synthesized: U-insertion RNA editing 5'CL18: GGAAGUAUGAGACGUAGG, 3'CL-13: AUU GGAGUUAUAG, $gRNA_{(ins)}$: CUAUAACUCCG AUAAACCUACGUCUCAUACUUCC. U-dele tion RNA editing: 5'CL22: GGAAAGGGAA AGUUGUGAUUUU, 3'CL15: GCGAGUUAU AGAAUA, $gRNA_{(del)}$: GGUUCUAUAACUCG CUCACAACUUCCCUUUCC.

FACS measurements

Cells were harvested by centrifugation at 1200 g for 5 min at 4 °C, fixed in 70 % (v/v) ethanol and stained with propidium iodide (PI) in 500 µL (50 µg/mL PI in PBS; 0.5 µg/mL RNase A) in the dark for 10 min on ice. Flow cytometry measurements were done with excitation at 536 nm and emission at 617 nm and the integration of the peaks were used to quantify the G1- and G2-phase distribution of the cell cycle.

DAPI staining and microscopy
Cells were harvested by centrifugation at 1200 g for 10 min at 4 °C, fixed in 70 % (v/v) ethanol, and stained with 4´, 6-Diamidino-2-phenylindol (DAPI) (1 mg/mL) in PBS at RT in the dark for 15 min. Cells were washed with PBS and analyzed microscopically for kinetoplasts (1K/2K) and nuclei (1N/2N) configuration.

Radioactive labeling of 5' cleavage fragment
RNAs were [^{32}P]-labeled at their 5'-ends using γ-[^{32}P]-ATP (specific activity: 3000 Ci/mmol). Reactions were catalyzed using T4 polynucleotide kinase (10 U) and contained 50 pmol of RNA and 50 µCi γ-[^{32}P]-ATP in 50 mM Tris/HCl pH 7.6, 10 mM $MgCl_2$, and 5 mM DTT. Reactions were incubated at 37 °C for 90 min. Labeled RNAs were purified in 12% (w/v) denaturing polyacrylamide gels followed by gel excision, gel extraction and ethanol precipitation.

***In vitro* RNA editing**
In vitro RNA editing assays were performed as in Igo et al., 2000 and Igo et al., 2002 using [^{32}P]-labeled (5'CL18 /5'CL22) substrate RNAs (specific activity: 8x10^5 cpm/pmol). Messenger RNAs (mRNAs) and cognate gRNAs were annealed by heating at 70 °C for 5 min and cooling down to 25 °C at a rate of 1 °C/min. Editing reactions were executed in 30 µL with 1 µg editosomes in EB containing 0.2 mM DTT, 0.5 mM ATP and 40 µM UTP (for insertion assay only) at 27 °C for 2 h. The products and intermediates were resolved in 18% (w/v) polyacrylamide gels containing 8 M urea. Gels were visualized by phosphorimaging and analyzed densitometrically.

Results
Synchronization of procyclic stage *T. brucei*
RNA editing has been suggested to play a major role in the regulation of mitochondrial gene expression based on the observation that steady state levels of some edited mRNAs vary dramatically between the two life cycle stages. Here we investigated the possibility that RNA editing is regulated during the cell cycle of African trypanosomes. Cells were synchronized and editosomal complexes from the G1- and G2-phases of the cell cycle were analyzed for their RNA editing activity using synthetic RNA editing substrates. Procyclic stage *T. brucei* (Cross, 1975) cells in the mid log-phase were incubated with 0.2 mM HU for 12 h, followed by washing and culturing the cells in the absence of HU. Cells treated with HU arrest in the late S-phase and, after removal of HU resume growth and divide synchronously for at least one cell cycle (Chowdhury et al., 2008). The enrichment of G1- and G2-phases during cell cycle was monitored by flow cytometry (Fig. 2A). At the start of synchronization (T0), 70% of the cells were in the G1-phase and 30% in the G2-phase. After 12 h of incubation with HU (T12), cells arrested in the late S-phase. Before the cells could traverse to the G2-phase, they had a lag phase for about 1 h (T13). Two hours after the removal of HU (T14), 80% of the synchronized cells traversed to the G2-phase and at 15 h (T15), 35% of the synchronized cells entered the G1-phase of the next cell cycle. After 5 h (T17) of removal of HU, 70% of the cells were in the G1-phase and 30% were in G2-phase of the next cell cycle. At this time point, the cell distribution was identical to the starting conditions of the synchronization experiment (T0).

To validate the flow cytometric analysis, the synchronization was monitored by assaying the percentage of cells

according to the kinetoplasts/nuclei configuration by DAPI staining. As shown in Fig. 2B, 2C, at 0 h (T0), 80% of the cells are 1K1N, 15% 2K1N and 5% 2K2N. After HU removal (T12), 70% of

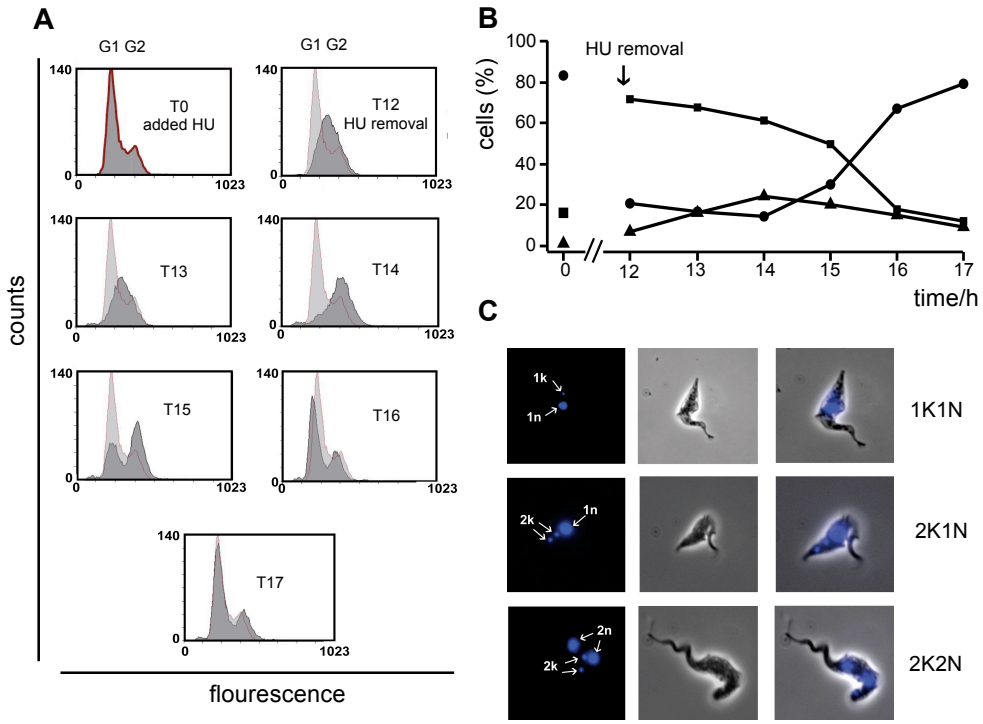

Figure 2. Synchronization of procyclic *T. brucei* with hydroxyurea (HU). (A) Cells were treated with 0.2mM HU for 12h, followed by HU removal, stained with propidium iodide and analyzed by flow cytometry. The peaks represent G1- and G2- phases of the cell cycle. T0: addition of HU (start of synchronization), T12: HU removal after 12 h, T13-T17: incubation after removal of HU. The T0 trace shown in red is used as an overlay. (B) Kinetoplasts and nuclei configuration. Cells were stained with DAPI and 500 cells were analyzed at each time point. Circles: 1K1N, squares: 2K1N, triangles: 2K2N. (C) Cells stained with DAPI representing different kinetoplasts and nuclei configurations.

synchronized cells are 2K1N, 20% 1K1N and 10% 2K2N. At the 14 h (T14) time point, 60% are 2K1N, 20% 2K2N and 20% 1K1N. At the next cell cycle, at 15 h (T15), 50% of the cells contained 2K1N, 30% 1K1N and 20% 2K2N and at 17h (T17), the majority (75%) of cells were in the G1-phase of the next cell cycle with 1K1N and 25% with 2K1N/2K2N. The data demonstrate that the nuclei/kinetoplasts configurations are identical with the flow cytometric analysis.

In vitro U-insertion/deletion-type RNA editing

In vitro U-insertion- and -deletion-type RNA editing assays were performed according to Igo et al., 2000 and Igo et al., 2002 with editosome complexes enriched from cells in the G1- and G2-phases. As substrate mRNAs, synthetic versions of the first editing site of the subunit 6 of the mitochondrial ATPase (A6) from *T. brucei* were used. The system either monitors the site-specific insertion of 3 U-nucleotides or the deletion of 4 U's (Fig. 3A) in the presence of cognate gRNA molecules. The data reveal that editosomes from the G1- and G2-phases catalyze both editing reactions. The generated products and intermediates were resolved electrophoretically and quantified (Fig. 3B). The data are shown in Fig. 4. 35% of the input RNA are converted into edited products. No difference, neither qualitatively, nor quantitatively was observed between the two enriched complexes from G1- and G2-phases of the cell cycle.

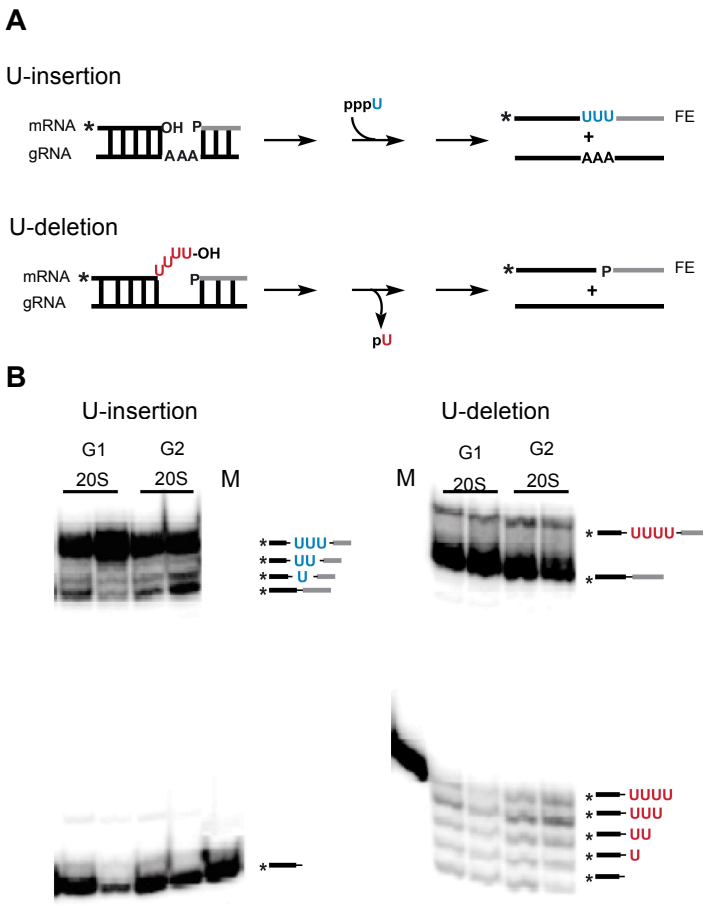

Figure 3. *In vitro* U-insertion/dele-tion-type RNA editing. (A) Sche-matic illustration of U-inser-tion/deletion-type RNA editing pathway. mRNA/gRNA hybrid RNAs are incubated with 20S editosomes, which harbor the basic enzymes to catalyze -reaction. Depending on the cognate gRNA, the system monitors either the insertion of 3 Us (blue) or the deletion of 4 Us (red). Products (FE) and intermediates obtained can be resolved electrophoretically. FE: fully edited product. (*): radioactive label. (B) *In vitro* RNA editing was performed by incubating substrate RNAs with 20S editosomes from G1- and G2-cell cycle phases. Products and intermediates (represented on the right of the autoradiographs) were resolved electrophoretically and densitometrically quantified. Inserted and deleted Us are represented in blue and red. M: mock (absence of 20S editosomes).

Discussion

RNA editing converts non-translatable transcripts into mature RNAs by the site-specific insertion and/or deletion of uridines. The process takes place in both developmental stages (BF and PF) of the parasite. 20S editosomes catalyze both types of the reactions. The variations in transcript abundance in both developmental stages have been suggested to reflect a regulatory role of RNA editing. However, a cell cycle-dependent regulatory role of RNA editing has not been addressed in *T. brucei.* Here, we analyzed whether the U-insertion/deletion RNA editing of 20S editosomes is regulated between the G1- and G2-phases of the cell cycle. 20S editosomes were harvested from G1- and G2-phase-synchronized cells. Synchronization of the cells was performed according to

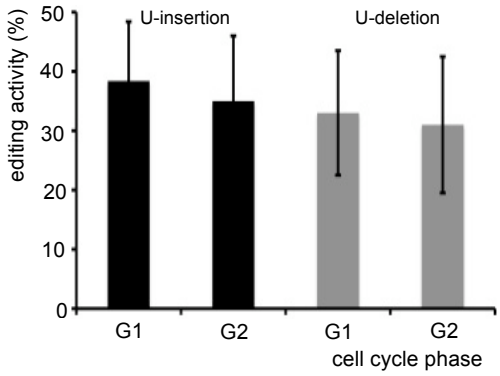

Figure 4. U-insertion/deletion RNA editing activity of 20S editosomes. 20S editing activity in % plotted against G1- and G2- cell cycle phases (SD in %).

Chowdhury et al., 2008. Cells arrested in the S-phase when treated with HU for 12 h. The data reveal that cells in G1-phase contained one kinetoplast and one nucleus (1K1N) and in G2-phase contained 2K1N and/or 2K2N. This demonstrates that the inhibition is at the nuclear S-phase but not at the kinetoplast S-phase and suggests that kinetoplast division can proceed despite the arrest of the nuclear S-phase (Ploubidou et al., 1999; Siegel et al., 2008).

The data further demonstrate that 20S editosomes from G1- and G2-phases of the cell cycle can catalyze both, U-insertion and U-deletion reactions *in vitro*. This suggests that the editing machinery is present in both the cell cycle phases, which is in line with the observation that pre-mRNAs and gRNAs are not required for the formation of the editing complex (Domingo et al., 2003). Dyskinetoplastid (Dk) trypanosomes survive as BF but not as PF (Schnaufer et al., 2002). They lack maxicircles but contain editosomes and require the expression of proteins forming editosome complexes for their survival (Domingo et al., 2003). Editosome from dyskinetoplasts can catalyze the reactions *in vitro* (Domingo et al., 2003). Therefore, the data support that the proteins forming the editosome complexes are expressed in both G1- and G2-phases of the cell cycle. No difference, neither qualitatively, nor quantitatively was observed between the isolated editosomal complexes from G1- and G2-phases of the cell cycle. The data show that the editosome-catalyzed U-insertion/deletion reaction is not cell cycle regulated.

In the related *leishmania* system, RNA editing has been shown to be regulated within the cell cycle (Carrillo et al., 2001). Here, the ratios of fully edited (FE) to unedited (UE) transcripts varied between 1.3- to 2.0-fold. The variation of ratios of the four (MURF2; COIII; Cyb and ND7) tested transcripts increased in the S+G2-phases and decreased in M-phase. Unfortunately, the experiments lack (i): controls i.e. never edited transcript and (ii): a statistical treatment that confirms the significance of the variation. The expression of β-F1-ATPase mRNA with similar variation was considered not significant (Martinez-Diez et al., 2006). Therefore, the small variation might be due post-editing processes that arise as a function of different stabilities of the edited transcripts during cell cycle. Polyadenylation of RNAs plays an important role in modulating the rates of RNA turnover (Ryan et al., 2003). It is regulated throughout the life cycle of trypanosomes (Bhat et al., 1992; Read et al., 1994). Edited transcripts have longer poly(A) tails than unedited transcripts. It has been shown that the absence of poly(A) tails leads to degradation of the partially/fully edited RNAs *in vitro* more rapidly than their unedited counter parts and *verse vice* in their presence (Kao and Read, 2005). Though, direct evidence for an influence of the poly(A) tail length is uncertain in trypanosomes (Schnaufer et al., 2002), but it is known that poly(A) tail regulates mRNA stability and translation efficiency in other systems (reviewed in Jackson and Standart, 1990; Bachvarova, 1992; Wormington, 1993).

References

Ammerman ML, Fisk JC and Read LK. (2008) gRNA/pre-mRNA annealing and RNA chaperone activities of RBP16. *RNA* 14:1069–1080.

Aphasizhev R and Aphasizheva I. (2011) Uridine insertion/deletion editing in trypanosomes: a playground for RNA-guided information transfer. *Wiley Interdiscip. Rev. RNA* 2:669-685.

Aphasizhev R and Simpson L. (2001) Isolation and characterization of a U-specific 3'-5'-exonuclease from mitochondria of *Leishmania tarentolae*. *J. Biol. Chem.* 276:21280-21284.

Aphasizhev R, Aphasizheva I, Nelson RE, Gao G, Simpson AM, Kang X, Falick AM, Sbicego S and Simpson L. (2003) Isolation of a U-insertion/deletion editing complex from *Leishmania tarentolae* mitochondria. *EMBO J.* 22:913-924.

Aphasizhev R, Aphasizheva I, Nelson RE and Simpson L. (2003) A 100-kD complex of two RNA-binding proteins from mitochondria of *Leishmania tarentolae* catalyzes RNA annealing and interacts with several RNA editing components. *RNA* 9:62–76.

Bachvarova RF. (1992) A maternal tail of poly(A): The long and the short of it. *Cell* 69:895-897.

Bhat GJ, Souza AE, Feagin JE and Stuart K. (1992) Transcript-specific developmental regulation of polyadenylation in *Trypanosoma brucei* mitochondria. *Mol. Biochem. Parasitol.* 52:231-240.

Blom D, Burg J, Breek CK, Speijer D, Muijsers AO and Benne R. (2001) Cloning and characterization of two guide RNA-binding proteins from mitochondria of *Crithidia fasciculata*. gBP27, a novel protein, and gBP29, the orthologue of *Trypanosoma brucei* gBP21. *Nucl. Acids Res.* 29:2950–2962.

Blum B and Simpson L. (1990) Guide RNAs in kinetoplastid mitochondria have a non encoded 3' oligo (U) tail involved in recognition of the pre-edited region. *Cell* 62:391–397.

Blum B, Bakalara N and Simpson L. (1990) A model for RNA editing in kinetoplastid mitochondria: "guide" RNA molecules transcribed from maxicircle DNA provide the edited information. *Cell* 60:189-198.

Böhm C, Katari VS, Brecht M and Göringer HU. (2012) *Trypanosoma brucei* 20S editosomes have one RNA substrate-binding site and execute RNA unwinding activity. *J. Biol. Chem.* 287:26268-26277.

Bringaud F, Riviere L and Couston V. (2006) Energy metabolism of trypanomastids: adaptation to available carbon sources. *Mol. Biochem. Parasitol.* 149:1-9.

Brun R and Schönenberger M. (1979) Cultivation and in vitro cloning or procyclic culture forms of *Trypanosoma brucei* in a semi-defined medium. Short communication. *Acta Tropica, J*. 36:289–292.

Carrillo R, Thiemann OH, Alfonzo JD and Simpson L. (2001) Uridine insertion/del-etion RNA editing in *Leishmania tarentolae* mitochondria shows cell cycle dependence. *Mol. Biochem. Parasitol.* 113:175-181.

Chowdhury AR, Zhao Z and Englund PT. (2008) Effect of hydroxyurea on procyclic *trypanosoma brucei*: an unconventional mechanism for achieving synchronous growth. *Eukayot. Cell* 7:425-428.

Cross GA. (1975) Identification, purification and properties of clone specific glycoprotein antigens constituting the surface coat of *Trypanosoma brucei*. *Parasitol*. 71:393–417.

Domingo GJ, Palazzo SS, Wand B, Pannicucci B, Salavati R and Stuart KD. (2003) Dyskinetoplastic *Trypanosoma brucei* contain functional editing complexes. *Eukaryot. Cell* 2:569-577.

Ernst NL, Panicucci B, Igo Jr. Jr. RP, Panigrahi AK, Salavati R and Stuart K. (2003) TbMP57 is a 3' terminal uridylyl transferase (TUTase) of the *Trypanosoma brucei* editosome. *Mol. Cell* 11:1525-1536.

Galanti N, Dvorak JA, Grenet J and McDaniel JP. (1994) Hydroxyurea-induced synchrony of DNA replication in the kinetoplastida. *Exper. Cell Res.* 214:225-230.

Gao G and Simpson L. (2003) Is the *Trypanosoma brucei* REL1 RNA ligase specific for U-deletion RNA editing, and is the REL2 RNA ligase specific for U-insertion editing? *J. Biol. Chem.* 278:27570-27574.

Golas MM, Böhm C, Sander B, Effenberger K, Brecht M, Stark H and Göringer HU. (2009) Snapshots of the RNA editing machine in trypanosomes captured at different assembly stages *in vivo*. *EMBO J*. 28:766-778.

Göringer HU. (2012) 'Gesalt,' Composition and function of the *Trypanosoma brucei* editosome. *Annu. Rev. Microbiol.* 66:65-82.

Göringer HU, Koslowsky DJ, Morales TH and Stuart K. (1994) The formation of mitochondrial ribonucleoprotein complexes involving guide RNA molecules in *Trypanosoma brucei*. *Proc. Natl. Acad. Sci. U.S.A.* 91:1776–1780.

Hajduk SL and Sabatini RS. (1998) Mitochondrial mRNA editing in kinetoplpastid protozoa. In Modification and editing of RNA, ASM press, Washington D.C. :377-392.

Hajduk S and Ochsenreiter T. (2010) RNA editing in kinetoplastids. *RNA Biol.* 7:229-236.

Hauser R, Pypaert M, Häusler T, Horn EK and Schneider A. (1996) In vitro import of proteins into mitochondria *Trypanosoma brucei* and *Leishmania tarentolae*. *J. Cell Sci.* 109:517-523.

Huang CE, Cruz-Reyes J, Zhelonkina AG, O'Hearn S, Wirtz E and Sollner-Webb B. (2001) Roles for ligases in the RNA editing complex of *Trypanosoma brucei*: band IV is needed for U-deletion and RNA repair. *EMBO J.* 20:4694-4704.

Igo RP Jr, Palazzo SS, Burgess ML, Panigrahi AK and Stuart K. (2000) Uridylate addition and RNA ligation contribute to the specificity of kinetoplastid insertion RNA editing. *Mol. Cell. Biol.* 20:8447–8457.

Igo RP Jr, Weston DS, Ernst NL, Panigrahi AK, Salavati R and Stuart K. (2002) Role of uridylate-specific exoribonuclease activity in *Trypanosoma brucei* RNA editing. *Eukar*. *Cell* 1:112-118.

Jackson RJ and Standart N. (1990) Do the poly(A) tail and 3' untranslated region control mRNA translation? *Cell* 62:15-24

Kala S and Salavati R. (2010) OB-fold domain of KREPA4 mediates high-affinity interaction with guide RNA and possesses annealing activity. *RNA* 16:1951–1967.

Kao CY and Read LK. (2005) Opposing effects of polyadenylation on the stability of edited and unedited mitochondrial RNAs in *Trypanosoma brucei*. *Mol. Cell. Biol.* 25:1634-1644.

Kramer S. (2012) Developmental regulation of gene expression in the absence of transcriptional control: The case of kinetoplastids. *Mol. Biochem. Parasitol.* 181:61-72.

Li F, Herrera J, Zhou S, Maslov DA and Simpson L. (2011) Trypanosome REH1 is an RNA helicase involved with the 3'-5' polarity of multiple gRNA-guided uridine insertion/deletion RNA editing. *Proc. Natl. Acad. Sci. U.S.A.* 108:3542–3547.

Liu B, Liu Y, Motyka SA, Agbo Eddy EC and Englund PT. (2005) Fellowships of the rings: he replication of kinetoplast DNA. *TRENDS Parasitol.* 21:363-369.

Martinez-Diez M, Santamaria G, Ortega AD Cuezva JM. (2006) Biogenesis and dynamics of mitochondria during the cell cycle: Significance of 3' UTRs. *PLoS ONE* doi: 10.1371/journal.pone.0000107.

McKean P. (2003) Coordination of cell cycle and cytokinesis in *Trypanosoma brucei*. *Curr. Opin. Microbiol.* 6:600-607.

McManus MT, Shimamura M, Grams J and Hajduk SL. (2001) Identification of candidate mitochondrial RNA editing ligases from *Trypanosoma brucei. RNA* 7:167–175.

Missel A, Souza AE, Nörskau G and Göringer HU. (1997) Disruption of a gene encoding a novel mitochondrial DEAD-box protein in *Trypanosoma brucei* affects edited mRNAs. *Mol. Cell. Biol.* 17:4895– 4903.

Müller UF and Göringer HU. (2002) Mechanism of the gBP21-mediated RNA/RNA annealing reaction. Matchmaking and charge reduction. *Nucleic Acids Res.* 30:447–455.

Müller UF, Lambert L and Göringer HU. (2001) Annealing of RNA editing substrates facilitated by guide RNA-binding protein gBP21. *EMBO J.* 20:1394–1404.

Niemann M, Kaibel H, Schlüter E, Weitzel K, Brecht M and Göringer HU. (2009) Kinetoplastid RNA editing involves a 3' nucleotidyl phosphatase activity. *Nucl. Acids Res.* 37:1897–1906.

Ploubidou A, Robinson AR, Docherty RC, Ogbadoyi EO and Gull K. (1999) Evidence of novel cell cycle checkpoints in trypanosomes: kinetoplast segregation and cytokinesis in the absence of mitosis. *J. Cell Sci.* 112:4641-4650.

Read LK, Stankey KA, Fish WR, Muthiani AM and Stuart K. (1994) Developmental regulation of RNA editing and polyadenylation in four life cycle stages of *Trypanosoma congolense. Mol. Biochem. Parasitol.* 68:297-306.

Reichard P and Ehrenberg A. (1983) Ribonucleotide reductase - a radical enzyme. *Science* 221:514-519.

Rusché LN, Huang CE, Piller KJ, Hemann M, Wirtz E and Sollner-webb B. (2001) The two RNA ligases of the *Trypanosoma brucei* RNA editing complex: Cloning the essential band IV gene and identifying the band V gene. *Mol. Cell. Biol.* 21:979-989.

Ryan CM, Militello KT and Read LK. (2003) Polyadenylation regulates the stability of *Try-*

pabosoma brucei mitochondrial RNAs. *J. Biolog. Chem.* 278:32753-32762.

Sbicego S, Alfonzo JD, Estévez AM, Rubio MA, Kang X, Turck CW, Peris M and Simpson L. (2003) RBP38, a novel RNA-binding protein from trypanosomatid mitochondria, modulates RNA stability. *Eukaryot. Cell* 2:560–568.

Schnaufer A, Domingo GJ and Stuart K. (2002) Natural and induced kinetoplastic trypanomastids: how to live without mitochondrial DNA. *Intl. J. Parasitol.* 32:1701-1084.

Siegel TN, Hekstra DR and Cross GAM. (2008) Analysis of the *trypanosoma brucei* cell cycle by quantitative DAPI imaging. *Mol. Biochem. Parasitol.* 160:171-174.

Woodward R and Gull K. (1990) Timing of nuclear and kinetoplast DNA replication and early morphological events in the cell cycle of *trypanosoma brucei*. *J. Cell Sci.* 95:49-57.

Wormington M. (1993) Poly(A) and translation: development and control. *Curr. Opin. Cell Biol.* 5:950-954

“A fact is a simple statement that everyone believes. It is innocent, unless found guilty. A hypothesis is a novel suggestion that no one wants to believe. It is guilty, untill found effective.”

– Edward Teller

Chapter Four

Molecular crowding inhibits U-insertion/deletion RNA editing *in vitro* – consequences for the *in vivo* reaction

Mitochondrial pre-mRNAs in African trypanosomes are edited to generate functional transcripts. The reaction is typified by the insertion and deletion of U nucleotides and is catalyzed by a macromolecular complex, the editosome. Editosomes bind pre-edited mRNA/gRNA pairs and the reaction can be recapitulated *in vitro* by using pre-mRNA- and gRNA-mimicking oligoribonucleotides together with enriched editosome preparations. Although the *in vitro* assay has been instrumental in unraveling the basic steps of the editing cycle it is performed at dilute solvent conditions. This ignores the fact that editing takes place inside the highly "crowded" mitochondria. Here we investigate the effects of molecular crowding on RNA editing. By using neutral, macromolecular cosolutes we generate defined dilute, semidilute and crowded solvent properties and we demonstrate different thermodynamic stabilities of the pre-mRNA/gRNA hybrid RNAs at these conditions. Crowded conditions stabilize the RNAs by -30kJ/mol. Furthermore, we show that the rate constants for the association and dissociation (k_{ass}/k_{diss}) of substrate RNAs to editosomes decrease, ultimately inhibiting the *in vitro* reaction. The data demonstrate that the current RNA editing *in vitro* system is sensitive to molecular crowding, which suggests that the *in vivo* reaction cannot rely on a diffusion-controlled, collision-based mechanism. Possible non-diffusional reaction pathways are discussed.

Introduction

Chemical reactions in living systems take place in aqueous solutions that contain high concentrations of macromolecules. Intracellular concentrations can reach up to 400 g/L thereby generating "crowded" or "volume-occupied" solvent conditions (reviewed in Minton, 2001; Zhou et al., 2008; Elcock, 2010). Although no individual macromolecular species is present at a high concentration, together all macromolecules can occupy up to 30% of the total cell volume and thus, physically occupy a significant fraction of the cell (Ellis, 2001). In general, macromolecular crowding enhances biomolecular interactions and reactions that ultimately cause a reduction of the total excluded volume. This includes the formation of macromolecular complexes, the binding of macromolecules to surface sites as well as aggregation and folding/unfolding phenomena of nucleic acids and proteins (Zhou et al., 2008). Furthermore, volume exclusion affects the equilibrium and kinetic of macromolecular reactions with two opposing effects: while it increases the rate of slow, transition-state-limited association reactions, it decreases the rate of fast, diffusion-limited association reactions (Minton, 2001; Zhou et al., 2008).

Volume-occupied solvent conditions can be generated *in vitro* by using high concentrations of chemically neutral, macromolecular cosolutes such as polyethylene glycol (PEG), Ficoll, dextran or bovine serum albumin (BSA) (reviewed in Minton, 2001; Chebotareva et al., 2004). The different compounds can be used to generate dilute, semidilute as well as crowded solvent properties depending on their "crossover polymer concentration" (Φ^*) (De Gennes, 1979; Kozer and Schreiber, 2004; Kozer et al., 2007). Φ^* is a function of the number of monomers per polymer (N) ($\Phi^* = N^{-4/5}$) and it represents the concentration (in w/w %) at which the polymer molecules start to form porous, network-like structures. At dilute conditions ($\Phi < \Phi^*$), the polymers can be viewed as flexible, coiled spheres with a defined radius of gyration (R_g). At semidilute conditions ($\Phi \approx \Phi^*$), the coils begin to overlap forming random networks with a mean mesh size ξ. ξ is a function of the polymer concentration (Φ) ($\xi \approx \Phi^{-3/4}$) (Kozer et al., 2007) and a further increase of Φ generates crowded solvent conditions ($\Phi > \Phi^*$), which are characterized by a dense entanglement and interpenetration of the polymer coils (Wang et al., 2010) (Fig. 1).

Despite the fact that macromolecular crowding has been shown to impact a large number of biological processes involving proteins and protein complexes (reviewed in Zhou, 2008; Batra et al., 2009; Zhou and Qin, 2013), its effect on nucleic acids especially on the structure, stability and function of RNA molecules is less studied. Multiple attributes of a crowded solution can affect the equilibrium between a properly folded, functional RNA and its unfolded, non-functional conformation(s). This includes a change in the chemical potential of the RNA due to a reduction of the available volume. The degree of volume exclusion is a consequence of the size of all macromolecules in the solution and depending on the number of interactions it is highly nonlinear with concentration (Minton, 1998). In addition, crowding can impact the activities of ions in the solution thereby modulating one of the dominating forces of macromolecular folding. While small molecule osmolytes have been shown to destabilize RNA secondary structure and in some cases RNA 3D-structure due to unfavorable surface interactions (Lambert and Draper, 2007; Pincus et al., 2008; Lambert et al., 2010), high molecular mass crowding reagents stabilize

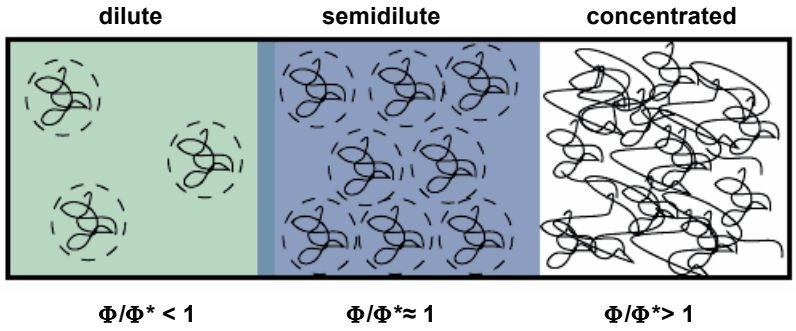

Figure 1. Schematic representation of dilute, semidilute and crowded cosolute properties according to Wang et al., 2010. Crowding reagents such as PEG or dextran can be approximated as elastic, coiled spheres (dashed circles). The polymers change their behavior in solution as a function of concentration. The character of the polymer-induced interaction changes significantly as one goes from dilute (green) to semidilute (blue) to crowded conditions (white). Dilute conditions ($\Phi<\Phi^*$) are characterized by polymer concentrations (Φ) below the critical cross-over concentration (Φ^*) and thus the cosolute molecules are well separated from each other. In the semidilute regime ($\Phi\approx\Phi^*$) the polymers start to overlap and form network-like structures. At crowded conditions ($\Phi>\Phi^*$) the polymer density is very high and the molecules become intricately entangled. For linear polymers, Φ^* can be approximated as $\Phi^*=N^{-4/5}$ (De Gennes, 1979; Kozer and Schreiber, 2004).

folded RNA (and DNA) conformations entropically due to the excluded volume effect (Karimata et al., 2004; Nakano et al., 2004; Kilburn et al., 2010). This holds also true for large ribonucleoprotein (RNP) complexes such as ribosomes: the association of the two ribosomal subunits can be stimulated by chemically inert cosolutes (Zimmerman and Trach, 1988). Furthermore, the catalytic activity of the hammerhead ribozyme is enhanced in the presence of crowding reagents (Nashimoto, 2000; Karimata et al., 2006; Nakano et al., 2009) as is the hairpin/pseudoknot transition of the human telomerase RNA (Denesyuk and Thirumalai, 2011). Similarly, the formation of DNA (and perhaps RNA) three-way junctions (TWJ) (Miyoshi et al., 2009; Muhuri et al., 2009), of G-quadruplex structures (Miyoshi et al., 2002; Fujimoto et al., 2011) and of DNA triple helices (Spink and Chaires, 1995) are favored in crowded solutions. Next to the excluded volume effect, hydration has been identified as a crucial factor for the stability of RNA molecules in crowded solutions with opposite effects on the stabilities of RNA tertiary and secondary structures (Nakano et al., 2009; Koumoto et al., 2008; Pramanik et al., 2011). Neutral cosolutes can stabilize the water release reaction of RNA 3D-folds while at the same time disfavor the water-uptake reaction of Watson-Crick base pairs (Nakano et al., 2009).

RNA editing describes a posttranscriptional modification reaction of mitochondrial pre-mRNAs that is characterized by the site-specific insertion and deletion of exclusively U nucleotides (nts) (for a review see Aphasizhev and Aphasizheva, 2011). The reaction takes place within the single mitochondrion of trypanosomes, which represents the most “crowded” intracellular environment of eukaryotic cells. Intramitochondrial macromolecular concentrations can reach up to 560 g/L (Srere, 1980; Harve et al., 2010). Editing is catalyzed by a macromolecular machinery, the 20S editosome (reviewed in Göringer, 2012). The multi-enzyme complex has a calculated molecular mass of 0.8 MDa and has been visualized by cryo-electron microscopy (EM) and atomic force microscopy (AFM) (Golas et al., 2009; Böhm et al., 2012). Key players in the reaction are a specific class of small, non-coding RNAs known as guide (g)RNAs. gRNAs function as templates in the reaction. They basepair to cognate pre-edited mRNAs and dic-

tate the number of U's to be inserted and/or deleted by way of their primary sequence. Editosomes have a single substrate RNA binding site, which binds the two RNA species with nanomolar affinity (Böhm et al., 2012). The catalytic conversion takes place within a multifunctional reaction centre that executes several enzyme activities: endo/exonuclease, terminal uridylyl transferase, RNA ligase and perhaps nucleotidyl phosphatase (reviewed in Aphasizhev and Aphasizheva, 2011; Göringer, 2012). Thus, the reaction likely requires several dynamic adjustments not only of the RNA substrate molecules (Böhm et al., 2012) but also of the catalytic machinery itself.

Our current understanding of the editing reaction mechanism is derived from an *in vitro* assay system that relies on truncated, cognate pairs of synthetic, pre-edited mRNAs and gRNAs together with enriched 20S editosome preparations (reviewed in Stuart et al., 2004). The complexes are isolated from non-ionic detergent lysates of *Trypanosoma brucei* mitochondria (reviewed in Panigrahi et al., 2007) and the assay depends on the diffusion/collision-based interaction of the RNA reactants with the catalytic machinery. Since the *in vitro* reaction is capable of monitoring the formation of fully edited reaction products and at the same time the formation of reaction intermediates and side products, it has been instrumental in unraveling the individual steps of the reaction cycle. However, at the same time the assay is characterized by a number of unexplained limitations. This includes the questions whether the reaction is diffusionally or transition-state controlled and whether the catalytic machinery acts processively or distributively. Although a single gRNA is able to edit several editing sites *in vivo*, *in vitro* only a single site can be converted. Also, while most mitochondrial pre-mRNAs require the successive action of multiple gRNAs, *in vitro* the action of only one gRNA can be addressed. One obvious inadequacy of the assay is that it is carried out at dilute solvent conditions, which differ significantly from the above-described "crowded" *in vivo* situation. Here we ask the question whether editing is affected by volume-occupied solvent conditions? We use neutral macromolecular co-polymers to generate defined dilute, semidilute and crowded solvent conditions and examine three different aspects of the editing reaction: First, we analyze the thermodynamic stability of synthetic gRNA/pre-mRNA substrate RNAs at volume-occupied solvent conditions; second, we monitor the kinetic and thermodynamic characteristics of the binding reaction of 20S editosomes to substrate gRNA/pre-mRNA hybrid RNAs and third, we measure the catalytic conversion of pre-edited mRNAs to edited RNAs in crowded solutions.

Materials and Methods

Crowding agents

The following crowding reagents were used: polyethylene glycol (PEG)200, PEG300, PEG400, PEG2000, PEG4000 as well as Ficoll400, Dextran150 and bovine serum albumin (BSA). Relevant physical parameters of the different compounds are listed in suppl. Table 1: molecular mass distribution, number of monomers/polymer (N), crossover polymer concentration (Φ*), polymer length/persistence length ratio (L/Lp) and viscosity (h). Depending on the individual Φ*-values the reagents were used to generate dilute (Φ < Φ*), semidilute (Φ ≈ Φ*) and crowded solvent conditions (Φ > Φ*) covering a Φ/Φ* range of 0-4.9.

Oligoribonucleotide synthesis and radioactive labeling

RNA oligonucleotides were synthesized by automated solid phase phosphoramidite chemistry using 2´-O-triisopropylsilyoxy-methyl (TOM) protected phos-

phoramidites (synthesis scale 50 nmoles). Purified RNA oligonucleotides were dissolved in 10 mM Tris/HCl pH 7.5, 1 mM EDTA and stored at -20 °C. Concentrations were determined by UV absorbance measurements at 260 nm. The following sequences were synthesized: Insertion RNA editing -5'CL18: GGAAGU AUGAGACGUAGG, 3'C-L13: AUUGGAGUU AUAG, $gRNA_{ins}$: CUAUAACUCCGAUAAAC CUACGCUCAUACUUCC. Deletion RNA editing 5'CL22: GGAAAGGGAAAGUUGUG AUUUU, 3'CL15: GCGAGUUAUAGAAUA, $gRNA_{del}$: GGUUCUAUAACUCGCUCACAAC UUUCCCUUCC. RNAs were 5' [^{32}P]-labeled using T4 polynucleotide kinase (10 U) and γ-[^{32}P]-ATP (specific activity: 3000 Ci/mmol) as a substrate. A typical reaction contained 50 pmol RNA and 50 µCi γ-[^{32}P]-ATP in 50 mM Tris/HCl pH 7.6, 10 mM $MgCl_2$, 5 mM DTT and was incubated at 37 °C for 90 min. Radioactively labeled RNAs were purified in 12% (w/v) denaturing polyacrylamide gels followed by gel excision, gel extraction and ethanol precipitation.

Editosome enrichment

Insect-stage *Trypanosoma brucei* cells of strain Lister 427 (Cross, 1975) were propagated in SDM-79 medium (Brun and Schönenberger, 1979). Ten litre cultures were grown to late log phase equivalent to a cell density of $1x10^7$ cells/mL. Cells were disrupted at isotonic conditions by N_2-cavitation (Hauser et al., 1996) and mitochondrial (mt) vesicles were isolated by differential centrifugation. Detergent lysates of the mt-vesicles were generated by incubation with 1% (v/v) Triton X-100 (2x critical micelle concentration (CMC)) in editing buffer (EB: 20 mM HEPES/KOH pH 7.5, 30 mM KCl, 10 mM $Mg(OAc)_2$) containing 1 mM DTT, 1 mM PMSF, 1 µg/mL leupeptin and 10 µg/mL trypsin inhibitor. Editosomes were enriched by isokinetic ultracentrifugation in linear 10-35% (v/v) glycerol gradients (Göringer et al., 1994) and fractionated. Editosome-containing fractions (app. S value: 20-24S; refractive indices 1.355–1.360) were pooled. Protein concentrations varied between 0.15-0.2 mg/mL. Samples were frozen in liquid N_2 and stored at -20 °C.

***In vitro* RNA editing**

In vitro RNA editing assays were performed as in Igo et al., 2000 and Igo et al., 2002 using [^{32}P]-labeled substrate RNAs (specific activity: $8x10^5$ cpm/pmol). Cognate gRNAs and mRNAs were annealed by heating at 70 °C for 5 min and cooling to 25 °C at a rate of 1 °C/min. Reactions were performed using 0.5 µg enriched 20S editosomes with 100 fmol of annealed substrate RNAs, 0.2 mM DTT, 0.5 mM ATP and 40 µM UTP (for insertion assay only) in EB at 27 °C for 2 h. Edited RNAs were resolved in 18% (w/v) polyacrylamide gels containing 8M urea, visualized by phosphorimaging and analyzed densitometrically. RNA editing activities (EA) were normalized to the activity in the absence of crowding reagent ($\Phi/\Phi^* = 0$) and plotted as a function of the molecular crowder (MC) concentration ($\log_{EA} = f(conc_{MC})$).

UV hyperchromicity measurements

Absorbance versus temperature profiles (melting curves) of RNA substrates were recorded at 260 nm using a thermoelectrically controlled UV-spectrophotometer in 50 mM sodium cacodylate pH 6.5, 150 mM NaCl and 2 mM $MgCl_2$. Measurements were performed in the presence of low and high molecular mass PEG's (PEG200, PEG300, PEG400, PEG2000, PEG4000) at Φ/Φ^* ratios of 0.3-4.9 (Table 1). The temperature was scanned at a heating rate of 1 °C/min at temperatures between 20 °C and 90 °C. Absorbance values were recorded with an average time of 0.5 s and data were collected every 0.1 °C. T_m-values were determined from derivative plots of absorbance *versus* temperature dA_{260}/dT

=f(T) and the half maximum of fraction folded (α) *versus* temperature plots generated by correcting the melting curves for upper and lower baselines (Breslauer, 1994). ΔH and ΔS-values were determined from van't Hoff plots of ln(*K*) *versus* 1000/T(K) with the slope representing $-\Delta H/R$ and the y-intercept $\Delta S/R$. ΔG was determined by $\Delta G = \Delta H - T\Delta S = RT \times \ln K$.

Surface plasmon resonance (SPR) measurements

Guide RNAs were 3'-oxidized at 4 °C in the dark in 50 mM NaOAc pH 4.8, 10 mM $MgCl_2$, 100 mM NaCl and 10 mM $NaIO_4$ (Odom et al., 1980). Samples were desalted and ethanol precipitated. Oxidized gRNAs were covalently attached to the surface of an amino silane-derivatized microcuvette in 50 mM $NaBH_3CN$ in a buffer containing 100 mM $Na_xH_yPO_4$ pH 7, 150 mM NaCl for 3 h at 27 °C. Coupled gRNAs were annealed to pre-mRNAs for 5 min in EB to generate gRNA/pre-mRNA hybrid RNAs. Binding of 20S editosomes to the gRNA/pre-mRNA hybrids was monitored in real time in the presence of 25% (w/v) PEG400 ($\Phi/\Phi^* = 0.9$) and 20% (w/v) PEG2000 ($\Phi/\Phi^* = 3.3$) as a shift in the resonant angle. k_{diss} and k_{ass} values were determined by plotting observed on rates ($k_{on(obs)}$) as a function of the editosome complex concentration ($k_{on(obs)} = k_{ass} \times [complex] + k_{diss}$). Equilibrium dissociation constants (K_d) were calculated as $K_d = k_{diss}/k_{ass}$. Half-lives of 20S editosome/RNA complexes were determined as $t_{1/2} = \ln 2/k_{diss}$.

Results

Stability of gRNA/pre-mRNA hybrid RNAs at molecular crowding conditions

Crowded intracellular environments are characterized by unique solvent properties such as a reduced number of free water molecules, which has been shown to affect the structure of nucleic acid molecules (Nakano et al., 2009; Pramanik et al., 2011). Depending on the crowding reagent, stabilizing as well as destabilizing effects have been reported (Karimata et al., 2004; Koumoto et al., 2008). U-insertion/deletion-type RNA editing is a RNA processing reaction that takes place within the mitochondria of kinetoplastid organisms. Despite the fact that mitochondria have been identified as the most severely crowded intracellular compartment (Srere, 1980; Harve et al., 2010), editing has only been analyzed at highly dilute solvent conditions. This tempted us to test whether the structure of substrate gRNA/pre-mRNA hybrid RNAs of the editing reaction might be affected by crowded solvent conditions. gRNA/pre-mRNA hybrids adopt a three-helix-junction (THJ) geometry (Reifur and Koslowsky, 2008; Koslowsky et al., 2004), however, the molecules can be mimicked by hybridized, synthetic oligoribonucleotides that consist of only two helical elements. Fig. 2A shows two typical "pre-cleaved" gRNA/pre-mRNA hybrid RNAs specific for a U-insertion- and a U-deletion-type editing reaction. To analyze whether the two "model" editing RNAs become structurally altered at crowded solvent conditions we measured the temperature-dependent helix/coil transitions of the two RNAs in the presence of different crowding reagents at dilute ($\Phi < \Phi^*$), semidilute ($\Phi \approx \Phi^*$) and crowded ($\Phi > \Phi^*$) cosolute conditions. Fig. 2B shows representative UV melting curves of the two gRNA/pre-mRNA pairs in a dilute buffer ($\Phi/\Phi^* = 0$). The two RNAs "melt" with two separate transitions (T_m-1, T_m-2), corresponding to the unfolding of the two RNA helices (Fig. 2A). The melting midpoints are at 54 °C and 77 °C for the U-insertion RNA and at 67 °C and 74 °C for the U-deletion substrate. Fig. 2C shows the same UV-melting profiles in the presence of 20% (w/v) PEG4000 *i.e.* at crowded solvent conditions 5-fold above the crossover polymer fraction

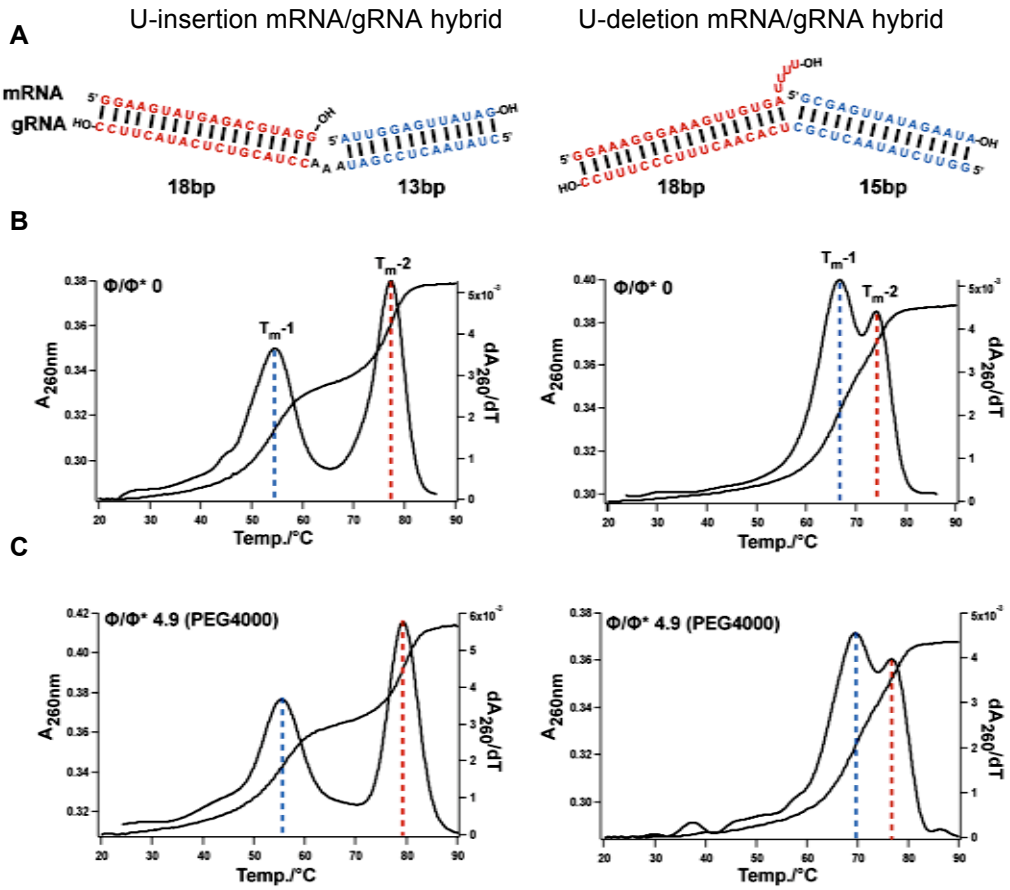

Figure 2. UV melting profiles of synthetic RNA editing substrate RNAs. (A) Schematic representation of the two model pre-mRNA/gRNA hybrid RNAs specific for a U-insertion (left) and a U-deletion (right) RNA editing reaction. Both RNAs consist of two helical domains shown in red and blue. (B) UV melting profiles (A_{260}=f(T)) and 1st derivatives (dA_{260}/dT=f(T)) of the two RNAs at dilute solvent conditions (Φ/Φ*=0) in the absence of PEG. (C) UV melting profiles (A_{260}=f(T)) and 1st derivatives (dA_{260}/dT=f(T)) of the two RNAs at crowded conditions (Φ/Φ*=4.9). Dotted lines indicate the half maximal melting transitions of the two helical domains (blue: T_m-1; red: T_m-2).

(Φ/Φ* = 4.9). At these conditions, all melting transitions in both RNAs are shifted to higher temperatures with ΔT_m's between 1.9 °C and 3.3 °C. This indicates a stabilization of the two RNA molecules. The stabilization calculates to a Gibb's free energy change (ΔΔG) of -31.4 kJ/mol for the U-insertion RNA and -33.7 kJ/mol for the U-deletion hybrid (all thermodynamic parameters are summarized in Tab. 1). Identical results were obtained at a Φ/Φ* ratio of 3 using 20% (w/v) PEG2000 (suppl. Fig. 1). The resulting ΔT_m-values range from 1.7 °C to 3.3 °C (Tab. 1) equivalent to ΔΔG's of -29.4 kJ/mol (U-insertion substrate) and -31.6 kJ/mol (U-deletion RNA).

By contrast, semidilute solvent conditions ranging from Φ/Φ* = 0.3-1.1 (PEG200, PEG300, PEG400) destabilized the two helical elements in both RNAs (suppl. Fig. 1). The corresponding ΔT_m's vary between -0.3°C to -7.3°C equivalent to ΔΔG's of 14 kJ/mol and 60 kJ/mol (Tab. 1). The destabilization is concentration-dependent: a doubling of the PEG concentration results in a 2- to 4-fold reduction of the T_m-values. Furthermore, the destabilization is inversely correlated to the chain length of the PEG molecules. PEG200 is more "destabilizing" than PEG300 and PEG400 by about -2°C/100Da. Fig. 3 summarizes the data by correlating the measured stability changes (ΔΔG) of the two RNAs to the number of monomers/polymer (N) and the concentration of the different PEG's (ΔΔG = f(N/conc)). An increase per monomer stabilizes the U-

U-insertion

	% (w/v)	Φ/Φ*	T_m-1 (°C)	ΔT_m-1 (°C)	T_m-2 (°C)	ΔT_m-2 (°C)	ΔG (kJ/mol)	ΔH (kJ/mol)	ΔS (kJ/mol/K)	ΔΔG (kJ/mol)
w/o PEG	-	0	54.0	-	77.0	-	-293.4	-1103	-2717	-
PEG4000	20	4.9	55.9	1.9	79.5	2.5	-324.8	-1482.3	-3879	-31.4
PEG2000	20	3.3	55.7	1.7	79.5	2.5	-322.9	-1472.8	-3857.3	-29.4
PEG400	30	1.1	50.2	-3.8	75.8	-1.2	-265.7	-926.4	-220	27.7
	15	0.5	53.0	-1.0	76.5	-0.5	-279.7	-980.9	-2325	13.8
PEG300	30	0.8	48.6	-5.4	73.8	-3.2	-248.9	-880.5	-2118	44.5
	15	0.4	52.1	-1.9	75.8	-1.2	-268.9	-988.1	-2412	24.5
PEG200	30	0.6	46.7	-7.3	71.7	-5.3	-241.4	-842	-2014	51.7
	15	0.3	50.5	-3.5	74.4	-2.6	-253.3	-886.8	-2130	41.2

U-deletion

	% (w/v)	Φ/Φ*	T_m-1 (°C)	ΔT_m-1 (°C)	T_m-2 (°C)	ΔT_m-2 (°C)	ΔG (kJ/mol)	ΔH (kJ/mol)	ΔS (kJ/mol/K)	ΔΔG (kJ/mol)
w/o PEG	-	0	66.6	-	74.0	-	-283.8	-969.1	-2303.2	-
PEG4000	20	4.9	69.9	3.3	76.7	2.7	-317.4	-1189.8	-2593.3	-33.7
PEG2000	20	3.3	69.9	3.3	76.2	2.2	-315.4	-1192.8	-2943.1	-31.6
PEG400	30	1.1	65.4	-1.2	71.6	-2.4	-252.3	-762.7	-1715.1	31.4
	15	0.5	66.3	-0.3	73.2	-0.8	-255.1	-754.8	-1678.8	28.7
PEG300	30	0.8	63.2	-3.4	69.3	-4.7	-231.8	-627.7	-1334.2	51.9
	15	0.4	64.8	-1.8	72.0	-2.0	-250.9	-787.3	-1799.1	32.8
PEG200	30	0.6	60.3	-6.3	67.1	-6.9	-223.7	-625.8	-1359.3	60
	15	0.3	63.5	-3.1	70.5	-3.5	-230.3	-588.2	-1228.2	53.5

Table 1. Melting temperatures and thermodynamic parameters (ΔG, ΔH, ΔS) for the helix/coil transition of U-insertion and U-deletion mRNA/gRNA hybrid RNAs in the presence of high and low molecular mass PEG's at dilute, semidilute and crowded solvent conditions (Φ/Φ* varies from 0 to 4.9). Blue: T_m-1; red T_m-2.

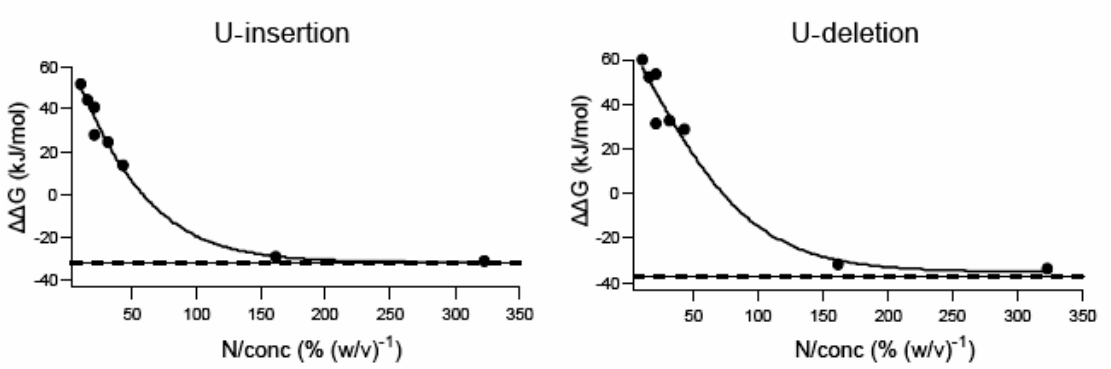

Figure 3. PEG-dependent RNA editing substrate stabilization. Gibb's free energy changes (ΔΔG) of the U-insertion (left) and U-deletion (right) pre-mRNA/gRNA hybrid RNAs in the presence of different polyethylene glycols. N - number of monomers/polymer (see suppl. Table 1); conc – PEG concentration in % (w/v). The dashed lines mark the maximal values of -33kJ/mol for the U-insertion hybrid RNA and -38kJ/mol for the U-deletion RNA.

insertion RNA by -1.2 kJ/mol/N/conc and the U-deletion RNA by -0.9 kJ/mol/N/conc. Maximal stabilization is achieved at -33 kJ/mol for the U-insertion pre-mRNA/gRNA hybrid and at -38 kJ/mol for the U-deletion RNA (Fig. 3).

Editosome/RNA interaction at molecular crowding conditions

Crowding reagents typically increase the viscosity of the solvent thereby influencing the thermodynamic and kinetic characteristics of biomolecular interactions (Minton, 2001; Zhou et al., 2008). As a follow up of the above-described experiments we asked the question whether a "volume-occupied" solvent

regimen affects the binding of editosomes to their substrate RNAs. In order to derive kinetic and thermodynamic data simultaneously, we monitored the editosome/RNA interaction in real time using a plasmon surface resonance (SPR)-based readout system. At dilute buffer conditions ($\Phi/\Phi^* = 0$), the two reactants (20S editosomes and gRNA/pre-mRNA hybrid RNAs) interact in a concentration-dependent fashion (suppl. Fig. 2). The formation of the RNA/editosome complexes is complete within ≤5 min. Fig. 4A shows the corresponding binding curves for a U-insertion-type and a U-deletion-type gRNA/pre-mRNA hybrid RNA. The equilibrium dissociation constants (K_d) for the binding reactions calculate to 6.4 nM (U-insertion RNA) and 6.6 nM (U-deletion RNA) indicating high affinity binding. The association- and dissociation rate constants (k_{ass} and k_{diss}) range between 3.3-4.7 x 10^5 $M^{-1}s^{-1}$ and 2-3 x 10^{-3} s^{-1} and the calculated half-lives ($t_{1/2}$) for the editosome/RNA complexes are 5.8 min (U-insertion RNA) and 3.9 min (U-deletion RNA). All binding characteristics are summarized in Table 2.

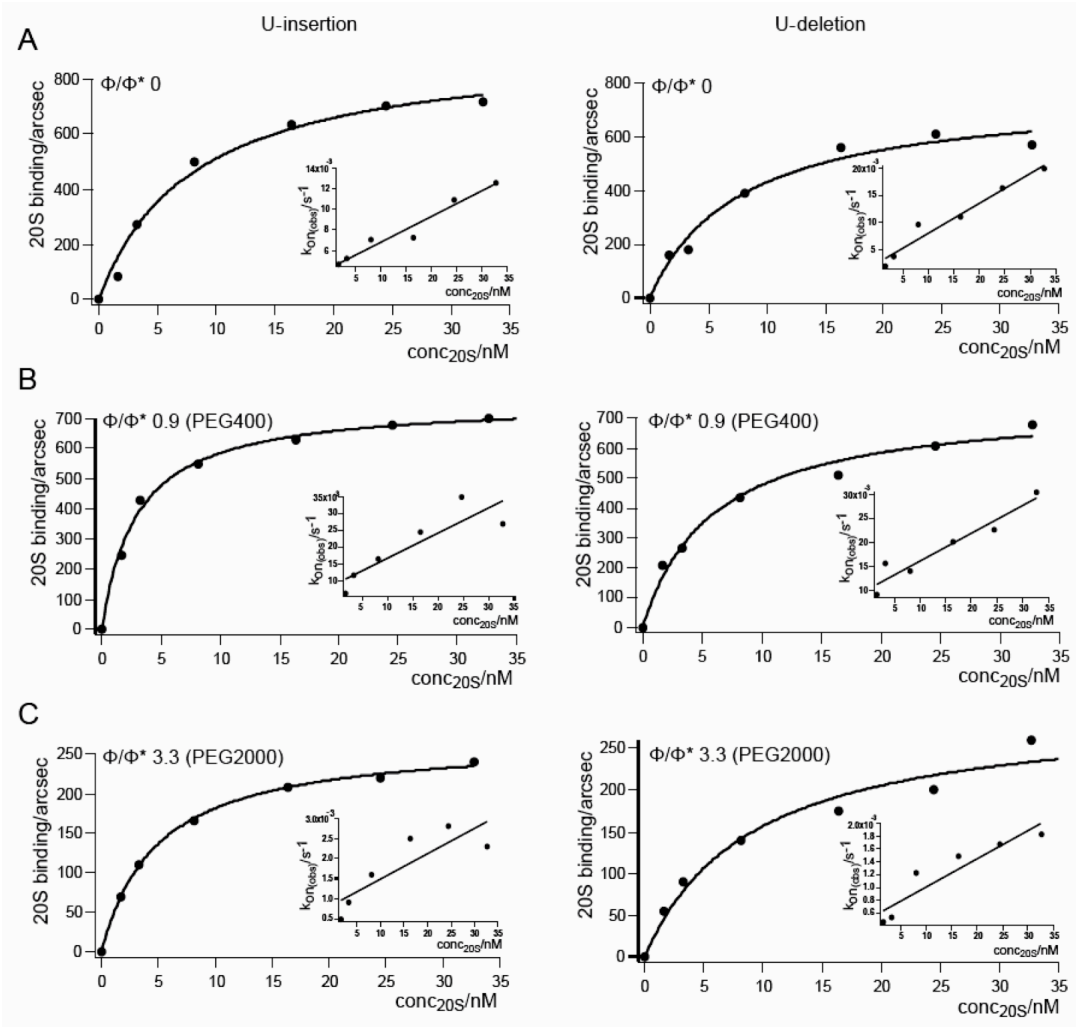

Figure 4. SPR-derived binding curves of 20S editosomes to U-insertion (left) and U-deletion (right) pre-mRNA/gRNA hybrid RNAs. (A) Binding at dilute solvent conditions (Φ/Φ^*=0). (B) Binding at semidilute conditions (Φ/Φ^*=0.9) and (C) at crowded cosolute conditions (Φ/Φ^*=3.3). Inserts: Plots of $k_{on(obs)}$= f($conc_{20S}$) for the calculation of k_{ass} and k_{diss}.

By changing the solvent conditions to a semidilute regimen (Φ/Φ^* = 0.9) the macroscopic K_d's for both RNA/editosome complexes increase to 12 nM (U-insertion) and 18 nM (U-deletion) (Fig. 4B and Table 2). The k_{ass}- and k_{diss}-rate

constants increase up to 5-fold for the U-insertion hybrid and maximally 3-fold for the U-deletion RNA. As a consequence the half-lives ($t_{1/2}$) of the RNA/editosome complexes decrease by a factor ≤5 (1.3 min for the U-insertion substrate; 1.2 min for the U-deletion

	Φ/Φ*	k_{ass} (M^{-1} s^{-1})	k_{diss} (s^{-1})	K_d (nM)	$t_{1/2}$ (min)
U-insertion					
w/o PEG	0	$3.3x10^5$	$2.0x10^{-3}$	6.4	5.8
25% (w/v) PEG400	0.9	$7.5x10^5$	$9.0x10^{-3}$	12.0	1.3
20% (w/v) PEG2000	3.3	$0.4x10^5$	$0.6x10^{-3}$	13.4	20.6
U-deletion					
w/o PEG	0	$4.7x10^5$	$3.0x10^{-3}$	6.6	3.9
25% (w/v) PEG400	0.9	$5.5x10^5$	$10.0x10^{-3}$	18.0	1.2
20% (w/v) PEG2000	3.3	$0.6x10^5$	$0.9x10^{-3}$	12.6	13.6

Table 2. Summary of binding data (k_{ass}, k_{diss}, K_d, $t_{1/2}$) of 20S editosomes to U-insertion and -deletion mRNA/gRNA hybrid RNAs at semidilute (Φ/Φ*=0.9) and crowded (Φ/Φ*=3.3) solvent conditions.

RNA hybrid). By contrast, at crowded solvent conditions (Φ/Φ* = 3.3) the association and dissociation rate constants decrease 3 to 8-fold resulting in a roughly 4-fold longer half-live of the complexes (Fig. 4C and Table 2). Thus, the data demonstrate a vital difference between dilute, semidilute and crowded solvent conditions: the transition from a dilute to a semidilute regimen increases the rate constants for the formation and dissociation of the RNA/editosome complexes while at crowded conditions the rate constants decrease. This affects the half-lives of the complexes in opposite directions suggesting that the reaction switches from a slow, transition-state-limited association reaction in dilute and semidilute conditions to a fast, diffusion-limited reaction in crowded conditions (Zhou et al., 2008).

In vitro RNA editing at molecular crowding conditions

In order to analyze whether the described structural, thermodynamic and kinetic consequences at crowded solvent conditions directly affect the catalytic conversion of a pre-edited mRNA into an edited reaction product, we measured the RNA editing activity of the two gRNA/pre-mRNA substrate RNAs directly. As before, the measurement was performed at different cosolute concentrations covering dilute, semidilute and concentrated solvent properties. The two model RNAs represent synthetic versions of the first editing site of the subunit 6 of the mitochondrial ATPase (A6) from *Trypanosoma brucei* (Igo et al., 2000; Igo et al., 2002). Depending on the presence of cognate gRNAs, either the site-specific insertion of 3 U nucleotides into the pre-mRNA is monitored or alternatively the deletion of 4 U's from the pre-mRNA is analyzed (Fig. 5A). Fig. 5B shows representative examples of the two *in vitro* editing reactions in the absence/presence of PEG2000 as a cosolute. At dilute reaction conditions (Φ < Φ*) *in vitro* editing is not affected. When the PEG concentration increases to semidilute (Φ ≈ Φ*) and finally to crowded conditions (Φ > Φ*) the formation of the fully edited reaction products is completely stalled. At 20% (w/v) PEG2000 (Φ/Φ* = 3.3), insertion-type RNA editing is >50-fold reduced while deletional editing is decreased by a factor of >10. Identical results were gained with PEG4000 at Φ/Φ* = 4.9 (suppl. Fig. 3A): both, U-insertion and U-deletion editing are inhibited between 50- to 100-fold. The U-insertion reaction is stalled at the TUTase and the mRNA ligation step, while the U-deletion reaction is inhibited at the exoUase and ligation reaction. Importantly, while the ligation reaction (in both cases) is inhib-

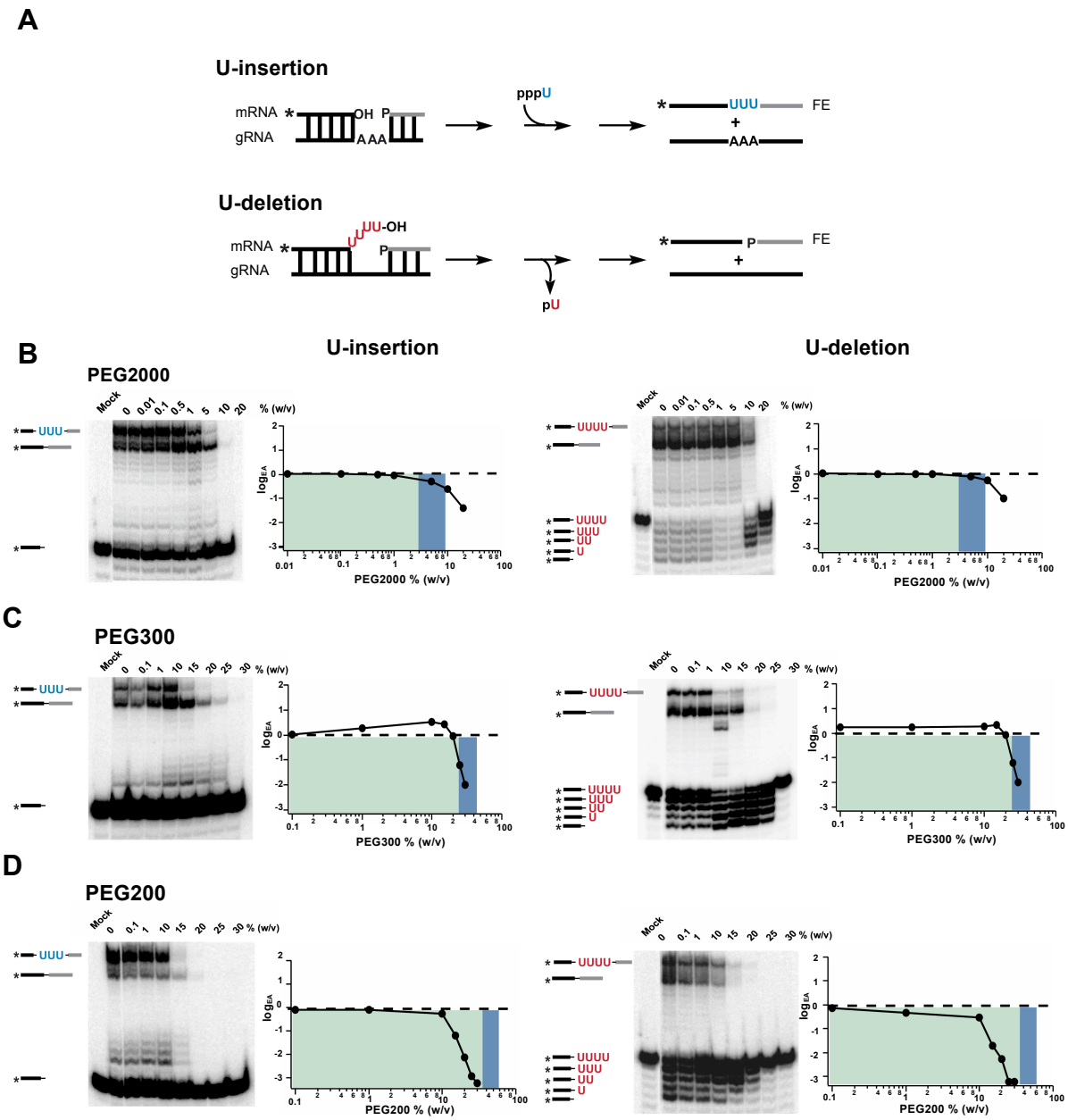

Figure 5. *In vitro* RNA editing at dilute, semidilute and crowded cosolute conditions. (A) Schematic representation of *in vitro* U-insertion and U-deletion editing reactions. Substrates in the assays are "precleaved" pre-mRNA/gRNA hybrid RNAs, which are converted to edited products either by the gRNA-dependent insertion of 3 U nucleotides (blue) or the deletion of 4 U's (red). Assays were performed at varying concentrations of PEG2000 (B), PEG300 (C) and PEG200 (D). RNA reactants, products and intermediates (sketched on the left of the gels) were resolved electrophoretically and densitometrically quantified. Editing activities (EA) were normalized to the EA in the absence of PEG (dashed line) and plotted as a function of the molecular crowder (MC) concentration: $\log_{EA}=f(\log c_{MC})$. Green background: dilute solvent conditions; blue background: semidilute conditions; white background: crowded conditions. Mock: minus 20S editosomes. (*) annotates the position of the radioactive label [^{32}P].

ited to ≥95% (at the highest PEG concentration) the exoUase is not fully inhibited. Given the precursor/product relationship of the two reactions in the editing cycle (Aphasizhev and Aphasizheva, 2011) this suggests that the exoUase and the mRNA ligation activity can be inhibited independently.

Next to the two high molecular PEG's we analyzed the influence of three low molecular mass polyethylene glycols: PEG200, PEG300 and PEG400. Fig. 5C/D and suppl. Fig. 3B show representative examples of the analysis. At dilute reaction conditions with cosolute concentrations ≤10% (w/v) the two types' of editing are not affected: The three crowding

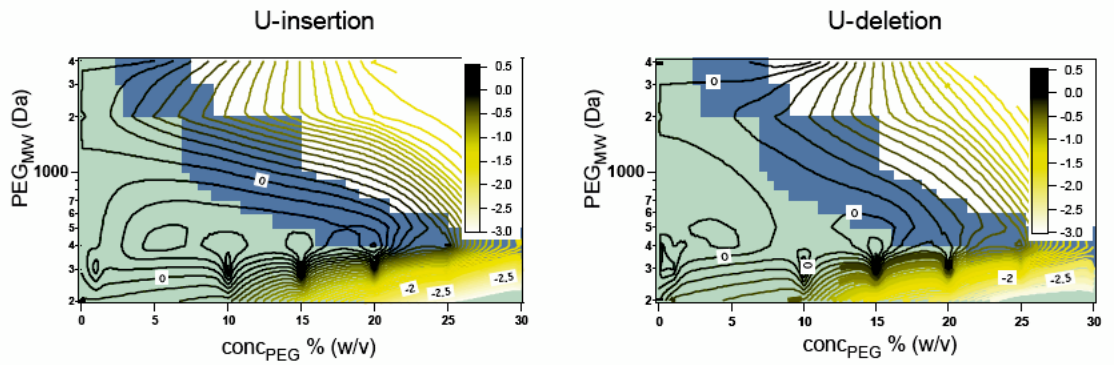

Figure 6. Contour plot correlating the U-insertion (left) and U-deletion (right) RNA editing activity to the polymer length and concentration of the different PEG molecules. Editing activities (EA) are normalized to the EA in the absence of PEG and are expressed as logEA on a scale of 0.5 to -3.0 (inserts). Green background: dilute solvent conditions; blue background: semidilute conditions; white background: crowded regimen.

reagents display editing activities identical to the situation in the absence of a cosolute ($\Phi/\Phi^* = 0$). However, at PEG concentrations >10% (w/v) both, insertion and deletion editing are inhibited ≥100-fold identical to the situation at crowded conditions ($\Phi > \Phi^*$) in the presence of high molecular mass PEG's. For PEG300 and PEG400 the inhibition takes place at or around the crossover concentration from a dilute to a semidilute regime, while for PEG200 the inhibition already occurs at dilute solvent conditions. Fig. 6 summarizes the concentration-dependence of the *in vitro* RNA editing activity for all PEG molecules tested.

A comparison of the inhibition profiles of the fully edited mRNA ligation products *versus* the non-edited ligation side-products showed for the U-insertion reaction that the fully edited mRNA is always inhibited at lower PEG concentrations when compared to the non-edited ligation product. By contrast, the U-deletion reaction showed an inverse behavior: the formation of non-edited side-product was always more sensitive to increased PEG concentrations in comparison to the fully edited mRNA (as an example see Fig. 5C). This supports a scenario in which the two RNAs are ligated by two different RNA ligase activities (McManus et al., 2001; Cruz-Reyes et al., 2002).

Lastly, we analyzed whether other crowding reagents show similar characteristics as PEG and performed *in vitro* U-insertion editing reactions in the presence of high molecular mass cosolutes of different chemical origins: the high molecular mass polysaccharides Dextran150 and Ficoll400 as well as bovine serum albumin (BSA) as a protein-type crowding reagent. All three compounds were analyzed at concentrations up to 10% (w/v). The results are shown in suppl. Fig. 4. At dilute and semidilute conditions none of the reagents showed any effect. However, at crowded cosolute conditions inhibition of editing was identified identical to the situation with PEG. This demonstrates that the described inhibitory effect is independent of the chemical signature of the crowding reagent.

Discussion

The U nucleotide-specific insertion/deletion-type RNA editing reaction in kinetoplastid organisms is a mitochondria-specific biochemical process and as such it must be tolerant to the highly crowded environment within the organelle (Dieteren et al., 2011). However, the processing reaction has so far only been analyzed at dilute, buffered solvent conditions, which fail to measure the contribution of other factors to RNA stability and functionality, especially the excluded volume and hydration effects triggered by chemically inert

cosolutes. Here, we investigated the structures of two synthetic model gRNA/pre-mRNA editing substrates, their interaction with 20S editosomes and their *in vitro* RNA editing activity at dilute, semidilute and crowded cosolute conditions. We identified that both, high and low molecular mass crowding reagents (PEG's) affect the structure of the two RNAs. Low molecular PEG's (PEG200, PEG300, PEG400) have a destabilizing effect at semidilute conditions in the range of 60 kJ/mol, while high molecular mass PEG's (PEG2000, PEG4000) at crowded conditions stabilize the two RNAs by about -30 kJ/mol. The stabilization correlates with the polymer size and concentration of the different PEG's with a value of about -1.0 kJ/mol/N/conc. In line with published data, the stabilization is most likely explained by the volume exclusion effect, while the destabilization is caused by a decrease in water activity (Nakano et al., 2004; Koumoto et al., 2008). Importantly, both phenomena are able to inhibit RNA editing *in vitro* (see below).

In order to initiate the processing reaction, pre-edited mRNAs and guide RNAs have to bind to the single substrate RNA binding site of the editing machinery (Böhm et al., 2012). RNA binding to editosomes has been analyzed before at dilute solvent conditions and was characterized as a high affinity interaction with K_d's in the nanomolar range (Golas et al., 2009; Böhm et al., 2012). Here we measured the RNA-binding capacity of editosomes in real time using semidilute and crowded solvent conditions. In both cases, the macroscopic K_d's decreased only by a factor ≤3. Thus, even at crowded cosolute conditions can editosomes and mRNA/gRNA hybrid RNAs interact with high affinity. However, a comparison of the rate constants for the association and dissociation of the editosome/RNA complexes identified a crucial difference between the two solvent settings: While the k_{ass}- and k_{diss}-values increased at semidilute conditions, the two constants decreased in crowded conditions. Similarly, while the half-lives of the complexes decreased at semidilute conditions, they increased at crowded conditions. This suggests that the processing reaction converts from a slow, transition-state-limited association reaction in dilute and semidilute conditions to a fast, diffusion-limited reaction in crowded conditions (Zhou et al., 2008). As a consequence, both subtypes of the editing reaction (U-insertion and U-deletion) are inhibited. For the two tested high molecular mass PEG's (PEG2000, PEG4000), the inhibition occurs exactly at the crossover concentration from a semidilute to crowded solvent regime suggesting volume exclusion as the dominant factor. The low molecular PEG's inhibit the reaction at lower concentrations (PEG400> PEG300 > PEG200) perhaps as a result of a combination of hydration and excluded volume effects.

The reaction is inhibited at every step of the enzymatic reaction cycle (TUTase, exoUase, RNA ligation). This classifies the cosolute-induced inhibition as a general phenomenon, which is further supported by the fact that other crowding reagents (Ficoll400, Dextran150, BSA) inhibit the reaction with similar characteristics. A comparison of the inhibition profiles of the fully edited reaction products *versus* the non-edited side products demonstrated that the two ligase reactions are inhibited at different cosolute concentrations. This suggests the presence of two different enzymes in line with the fact that 20S editosomes harbor two RNA ligases (TbMP48/REL2 and TbMP52/REL1) (reviewed in Aphasizhev and Aphasizheva, 2011). This is further supported by the structural observation that 20S editosomes consist of two prominent globular subdomains (Golas et al., 2009), likely representing

the individual subdomains of the U-insertion and U-deletion reactions (Göringer, 2012).

Whether the inhibition is a direct consequence of the structural stabilization of the RNA substrate molecules or a result of the decreased k_{ass}- and k_{diss}-values (or both) cannot be deduced from the data presented here. However, the sensitivity of the *in vitro* assay to crowded cosolute conditions demonstrates that the assay does not recapitulate a central aspect of the *in vivo* situation: editing must be conducted in the densely volume-occupied environment inside the mitochondria. Though the *in vitro* assay has been instrumental in elucidating the basic aspects of the editing reaction cycle, clearly, the *in vivo* reaction cannot rely on a diffusion-limited, collision-based mechanism (which might also explain other inconsistencies of the editing *in vitro* assay). Our data advocate a scenario in which editing *in vivo* is conducted by non-diffusional means perhaps through the coupling of substrate RNAs by physically interfacing the participating machineries downstream and upstream of the editing reaction. Precedence for such a situation can be found in the physical and functional tethering of the gene expression pathway in eukaryotes. The entire process (transcription, pre-mRNA processing, cytoplasmic export, translation) is conducted by several macromolecular, multi-component complexes, which act as an extensively coupled network that executes the individual biochemical reactions in a highly coordinated fashion (reviewed in Maniatis and Reed, 2002; Bentley, 2005). This involves a "handover" or "channeling" of substrate RNAs from one complex to the next instead of relying on free aqueous-phase diffusion. Evidence for a possible coupling of editing to down- and upstream processes can be found in the literature. For instance, Aphasizheva et al., 2011 have shown that mitochondrial mRNAs, gRNAs and editosomes interact with the mitochondrial translation machinery: pre-edited mRNAs, gRNAs and editosomes bind predominantly to the large subunit of the ribosome and fully edited, A/U-tailed mRNAs associate with the small ribosomal subunit. This suggests a functional tethering of editing, polyadenylation and protein biosynthesis. The interaction likely involves one or more pentatricopeptide repeat-type (PPR) proteins, which have been shown to bind to ribosomes and have been implicated in the stabilization of rRNAs (Aphasizheva et al., 2011; Pusnik et al., 2007). A potential coupling of transcription and editing can be deduced from the work of Read et al., 1992. They demonstrated polycistronic transcription of mitochondrial genes in trypanosomes and verified that RNA editing can precede processing and polyadenylation of the primary transcript.

Finally, another factor possibly contributes to the non-diffusional characteristics of the editing reaction *in vivo*. The physical interaction of editosomes with the mitochondrial translation machinery might position the processing machinery in close proximity to the inner mitochondrial membrane (IM). A membrane-association of mitochondrial ribosomes is presumably essential in order to couple the synthesis of hydrophobic membrane proteins to the membrane integration process (Marzuki and Hibbs, 1986). Mitochondrial ribosomes have been shown to associate with membranes either through electrostatic interactions (Liu and Spremulli, 2000) or *via* specific, membrane-associated protein(s) (reviewed in Ott and Herrmann, 2010). Since the majority of genes that require RNA editing are components of membrane-associated, respiratory complexes (NADH-ubiquinone oxidoreductase - complex I, cytochrome bc1 - complex III, cytochrome oxidase - complex

IV and ATP synthase - complex V), fixing the editosome (indirectly) to the inner mitochondrial membrane should increase the local concentration of all reaction partners and substrate molecules thereby generating a "diffusion-independent" scenario (Fig. 7). Although a membrane-association of editosomes has not been documented today, this is likely due to the fact that the standard enrichment protocol for 20S editosomes involves a detergent extraction step (Panigrahi et al., 2007). In conclusion, we propose that mitochondrial transcription, RNA editing, 3'-end processing and mitochondrial translation occur in close physical association in African trypanosomes. The individual machineries possibly interact in a coordinate, membrane-associated form thereby side-stepping diffusional processes, which is not mimicked in the current *in vitro* RNA editing assay.

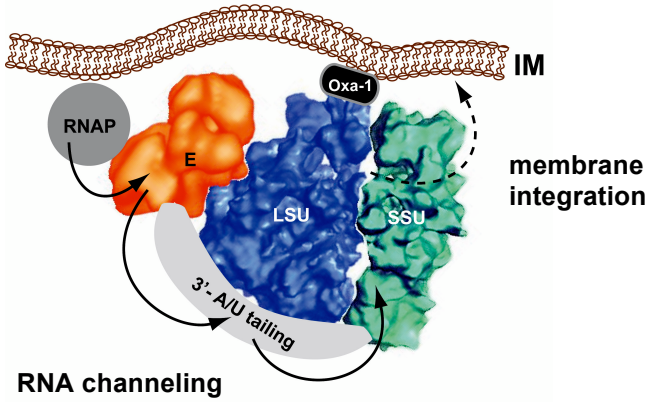

Figure 7. Tethering of mitochondrial transcription, RNA editing, 3'-end processing and translation. Schematic representation of a coupled, inner membrane-associated (IM) assembly of 20S editosomes (E) (Golas et al., 2009) with mitochondrial ribosomes (SSU/LSU) (Sharma et al., 2009) and the mitochondrial transcription machinery (RNAP) (Grams et al., 2002). The different macromolecular complexes interface physically in order to foster the channeling of substrate RNAs (arrows) from one machinery to the next thereby side-stepping free aqueous-phase diffusion. A coupling of polycistronic gRNA transcripts with RNA editing complexes has been demonstrated by Grams et al., 2000. Read et al., 1992 verified polycistronic transcription of mitochondrial genes and showed that RNA editing can precede processing and polyadenylation. Edited mRNAs are polyadenylated by the extension of A/U-heteropolymers, which is catalyzed by the poly(A) polymerase KPAP and the terminal uridyltransferase RET1. The reaction is coordinated by the pentatricopeptide-repeat (PPR) proteins KPAF1 and KPAF2 (Aphasizheva et al., 2011). Fully edited, A/U-tailed mRNAs have been shown to preferentially interact with the SSU, while pre-edited mRNAs, gRNAs and 20S editosomes have been shown to bind to the LSU (Aphasizheva et al., 2011). Mitochondrial ribosomes associate with membranes either through electrostatic interactions (Liu and Spremulli, 2000) or *via* specific membrane-associated protein(s) such as Oxa-1 (Ott and Herrmann, 2010). The dashed arrow annotates the membrane-integration of the translation products.

References

Aphasizhev R and Aphasizheva I. (2011) Uridine insertion/deletion editing in trypanosomes: a playground for RNA-guided information transfer. *Wiley Interdiscip. Rev. RNA* 2:669-685.

Aphasizheva I, Maslov D, Wang X, Huang L and Aphasizhev R. (2011) Pentatricopeptide repeat proteins stimulate mRNA adenylation/uridylation to activate mitochondrial translation in trypanosomes. *Mol. Cell* 42:106-117.

Batra J, Xu K, Qin S and Zhou HX. (2009) Effect of macromolecular crowding on protein binding stability: modest stabilization and significant biological consequences. *Biophys. J.* 97:906-911.

Bentley DL. (2005) Rules of engagement: co-transcriptional recruitment of pre-mRNA processing factors. *Curr. Opin. Cell. Biol.* 17:251-256.

Böhm C, Katari VS, Brecht M and Göringer HU. (2012) *Trypanosoma brucei* 20S editosomes have one RNA substrate-binding site and execute RNA unwinding activity. *J. Biol. Chem.* 287:26268-26277.

Breslauer KJ. (1994) Extracting thermodynamic data from equilibrium melting curves for oligonucleotide order-disorder transitions. *Methods Mol. Biol.* 26:347-372.

Brun R and Schönenberger M. (1979) Cultivation and in vitro cloning or procyclic culture forms of *Trypanosoma brucei* in a semi-defined medium. *Acta Tropica.* 36:289–292.

Chebotareva NA, Kurganov BI and Livanova NB. (2004) Biochemical effects of molecular crowding. *Biochem. (Moscow)* 69:1239-1251.

Cross GA. (1975) Identification, purification and properties of clone specific glycoprotein antigens constituting the surface coat of *Trypanosoma brucei*. *Parasitol*. 71:393–417.

Cruz-Reyes J, Zhelonkina AG, Huang CE and Sollner-Webb B. (2002) Distinct function of two RNA ligases in active *Trypanosoma brucei* RNA editing complexes. *Mol. Cell. Biol.* 22:4652-4660.

De Gennes,P. (1979) Scaling concepts in polymer physics. Cornell University Press, Ithaca, NY.

Denesyuk NA and Thirumalai D. (2011) Crowding promotes the switch from hairpin to pseudoknot conformation in human telomerase RNA. *J. Am. Chem. Soc.* 133:11858-11861.

Dieteren CJE, Gielen SCAM, Nijtmans LGJ, Smeitink JAM, Swarts HG, Roland B, Willems PHGM and Koopman WJH. (2011) Solute diffusion is hindered in the mitochondrial matrix. *Proc. Natl. Acad. Sci. USA,* 108:8657-8662.

Elcock AH. (2010) Models of macromolecular crowding effects and the need for quantitative comparisons with experiments. *Curr. Opinion Struc. Biol.* 20:196-206.

Ellis RJ. (2001) Macromolecular crowding: an important but neglected aspect of the intracellular environment. *Curr. Opinion Struc. Biol.* 11:114-119.

Fujimoto T, Nakano S, Miyoshi D and Sugimoto N. (2011) The effects of molecular crowding on the structure and stability of G-quadruplexes with an abasic site. *J. Nucl. Acids*, 2011:857149. doi: 10.4061/2011/857149.

Golas MM, Böhm C, Sander B, Effenberger K, Brecht M, Stark H and Göringer HU. (2009) Snapshots of the RNA editing machine in trypanosomes captured at different assembly stages *in vivo*. *EMBO J.* 28:766-778.

Göringer HU, Koslowsky DJ, Morales TH and Stuart K. (1994) The formation of mitochondrial ribonucleoprotein complexes involving guide RNA molecules in *Trypanosoma brucei*. *Proc. Natl. Acad. Sci. USA* 91:1776–1780.

Göringer HU. (2012) 'Gestalt,' composition and function of the *Trypanosoma brucei* editosome. *Annu. Rev. Microbiol.* 66:65-82.

Grams J, McManus MT and Hajduk SL. (2000) Processing of polycistronic guide RNAs is associated with RNA editing complexes in *Trypanosoma brucei*. *EMBO J.* 19:5525-5532.

Grams J, Morris JC, Drew ME, Wang Z, Englund PT and Hajduk SL. (2002) A trypanosome mitochondrial RNA polymerase is required for transcription and replication. *J. Biol. Chem.* 277:16952-16959.

Harve KS, Lareu R, Rajagopalan R and Raghunath M. (2010) Understanding how the crowded interior of cells stabilizes DNA/DNA and DNA/RNA hybrids-*in silico* predictions and *in vitro* evidence. *Nucl. Acids Res.* 38:172-181.

Hauser R, Pypaer M, Häusler T, Horn EK and Schneider A. (1996) *In vitro* import of proteins into mitochondria of *Trypanosoma brucei* and *Leishmania tarentolae*. *J. Cell Sci.* 109:517-523.

Igo RP Jr, Palazzo SS, Burgess ML, Panigrahi AK and Stuart K. (2000) Uridylate addition and RNA ligation contribute to the specificity of kinetoplastid insertion RNA editing. *Mol. Cell. Biol.* 20:8447–8457.

Igo RP Jr, Weston DS, Ernst NL, Panigrahi AK, Salavati R and Stuart K. (2002) Role of uridylate specific exoribonuclease activity in *Trypanosoma brucei* RNA editing. *Eukar. Cell* 1:112-118.

Karimata H, Nakano S and Sugimoto N. (2006) The roles of cosolutes on the hammerhead ribozyme activity. *Nucl. Acids Symp. Ser.* 50:81-82.

Karimata H, Nakano S, Ohmichi T, Kawakami J and Sugimoto N. (2004) Stabilization of a DNA duplex under molecular crowding conditions of PEG. *Nucl. Acids Symp. Ser.* 48:107-108.

Kilburn D, Roh JH, Guo L, Briber RM and Woodson SA. (2010) Molecular crowding stabilizes folded RNA structure by the excluded volume effect. *J. Am. Chem. Soc.* 132:8690-8696.

Koslowsky DJ, Reifur L, Yu LE and Chen W. (2004) Evidence for U-tail stabilization of gRNA/mRNA interactions in kinetoplastid RNA

editing. *RNA Biol.* 1:28-34.

Koumoto K, Ochiai H and Sugimoto N. (2008) Hydration is an important factor to regulate thermodynamic stability of DNA duplex under molecular crowding conditions. *Chem. Lett.* 37:864-865.

Kozer N and Schreiber G. (2004) Effect of crowding on protein-protein association rates: Fundamental differences between low and high mass crowding agents. *J. Mol. Biol.* 336:763-774.

Kozer N, Kuttner YY, Haran G and Schreiber G. (2007) Protein-Protein association in polymer solutions: from dilute to semidilute to concentrated. *Biophy. J.* 92:2139-2149.

Lambert D and Draper DE. (2007) Effects of osmolytes on RNA secondary and tertiary structure stabilities and RNA-Mg2+ interactions. *J. Mol. Biol.* 370:993-1005.

Lambert D, Leipply D and Draper DE. (2010) The osmolyte TMAO stabilizes native RNA tertiary structures in the absence of Mg2+: evidence for a large barrier to folding from phosphate dehydration. *J. Mol. Biol.* 404:138-157.

Liu M and Spremulli L. (2000) Interaction of mammalian mitochondrial ribosomes with the inner membrane. *J. Biol. Chem.* 275:29400-29406.

Maniatis T and Reed R. (2002) An extensive network of coupling among gene expression machines. *Nature* 416:499-506.

Marzuki S and Hibbs AR. (1986) Are all mitochondrial translation products synthesized on membrane-bound ribosomes? *Biochim. Biophys. Acta* 866:120-124.

McManus MT, Shimamura M, Grams J and Hajduk SL. (2001) Identification of candidate mitochondrial RNA editing ligases from *Trypanosoma brucei*. *RNA* 7:167–175.

Minton AP. (1998) Molecular crowding: analysis of effects of high concentrations of inert cosolutes on biochemical equilibria and rates in terms of volume exclusion. *Methods Enzymol.* 295:127-149.

Minton AP. (2001) The influence of macromolecular crowding and macromolecular confinement on biochemical reactions in physiological media. *J. Biol. Chem.* 276:10577-10580.

Miyoshi D, Muhuri S, Mimura K and Sugimoto N. (2009) DNA junction structure stabilized by molecular crowding. *Nucl. Acids Symp. Ser.* 53:59-60.

Miyoshi D, Nakao A and Sugimoto N. (2002) Molecular crowding regulates the structural switch of the DNA G-quadruplex. *Biochem.* 41:15017-15024.

Muhuri S, Mimura K, Miyoshi D and Sugimoto N. (2009) Stabilization of three-way junctions of DNA under molecular crowding conditions. *J. Amer. Chem. Soc.* 131:9268-9280.

Nakano S, Karimata H, Omichi T, Kawakami J and Sugimoto N. (2004) The effect of molecular crowding with nucleotide length and cosolute structure on DNA duplex stability. *J. Amer. Chem. Soc.* 126:14330-14331.

Nakano S, Karimata HT, Kitagawa Y and Sugimoto N. (2009) Facilitation of RNA enzyme activity in the molecular crowding media of cosolutes. *J. Amer. Chem. Soc.* 131:16881-16888.

Nashimoto M. (2000) Correct folding of a ribozyme induced by nonspecific macromolecules. *Eur. J. Biochem.* 267:2738-2745.

Odom OW, Robbins Jr DJ, Lynch J, Dottavio-Martin D, Kramer G and Hardesty B. (1980) Distances between 3' ends of ribosomal ribonucleic acids reassembled into *Escherichia coli* ribosomes. *Biochem*. 19:5947–5954.

Ott M and Herrmann JM. (2010) Co-translational membrane insertion of mitochondrially encoded proteins. *Biochim. Biophys. Acta* 1803:767-775.

Panigrahi AK, Schnaufer A and Stuart KD. (2007) Isolation and compositional analysis of trypanosomatid editosomes. *Methods Enzymol.* 424:3-24.

Pincus DL, Hyeon C and Thirumalai D. (2008) Effects of trimethylamine N-oxide (TMAO) and crowding agents on the stability of RNA hairpins. *J. Am. Chem. Soc.* 130:7364-7372.

Pramanik S, Nagatoishi S, Saxena S, Bhattacharyya J and Sugimoto N. (2011) Conformational flexibility influences degree of hydration of nucleic acid hybrids. *J. Phys. Chem. B.* 115:13862-13872.

Pusnik M, Small I, Read LK, Fabbro T and Schneider A. (2007) Pentatricopeptide repeat proteins in *Trypanosoma brucei* function in mitochondrial ribosomes. *Mol. Cell. Biol.* 27:6876-6888.

Read LK, Myler PJ and Stuart K. (1992) Extensive

editing of both processed and preprocessed maxicircle CR6 transcripts in *Trypanosoma brucei*. *J. Biol. Chem.* 267:1123-1128.

Reifur L and Koslowsky D. (2008) *Trypanosoma brucei* ATPase subunit 6 mRNA bound to gA6-14 forms a conserved three-helical structure. *RNA* 14:2195-2211.

Sharma MR, Booth TM, Simpson L, Maslov DA and Agrawal RK. (2009) Structure of a mitochondrial ribosome with minimal RNA. *Proc. Natl. Acad. Sci. USA.* 106:9637-9642.

Spink CH and Chaires JB. (1995) Selective stabilization of triplex DNA by poly(ethylene glycols). *J. Am. Chem. Soc.* 117:12887-12888.

Srere PA. (1980) The infrastructure of the mitochondrial matrix. *TIBS* 5:120-121.

Stuart K, Salavati R, Igo RP, Ernst NL, Palazzo SS and Wang B. (2004) *In vitro* assays for kinetoplastid U insertion-deletion editing and associated activities. *Methods Mol. Biol.* 265:251-272.

Wang YZ, Li BH, Xiong XM, Wang B and Zhang JX. (2010) Universal scaling description of the strain softening behavior in the semidilute uncross-linked polyacrylamide-water solution. *Soft Matter* 6:3318-3324.

Zhou HX and Qin S. (2013) Simulation and modeling of crowding effects on the thermodynamic and kinetic properties of proteins with atomic details. *Biophys. Rev.* 5:207-215.

Zhou HX, Rivas G and Minton AP. (2008) Macromolecular crowding and confinement: biochemical, biophysical, and potential physiological consequences. *Annu. Rev. Biophys.* 37:375-397.

Zhou HX. (2008) Protein folding in confined and crowded environments. *Arch. Biochem. Biophys*. 469:76-82.

Zimmerman SB and Trach SO. (1988) Effects of macromolecular crowding on the association of *E. coli* ribosomal particles. *Nucl. Acids Res.* 16:6309-6326.

Supplementary material

crowding reagent	mol. mass distribution (g/mol)	conc. range tested % (w/v)	*N*	Φ* % (w/w)	L/L_P	η distribution (cSt)
PEG200	180 – 220	0.1 – 30	3.2	39	1.3	21 – 25
PEG300	270 – 330	0.1 – 30	5	28	2	31 – 35
PEG400	370 – 430	0.1 – 30	7	23	3	40 – 45
PEG2000	1810 – 2200	0.01 – 20	32	6	13	150 – 210
PEG4000	3740 – 4480	0.01 – 20	65	4	26	260 – 360
Ficoll400	300 000 – 500 000	0.001 – 10	1170	0.35	-	-
Dextran150	125 000 – 175 000	0.001 – 10	833	0.46	-	-
BSA	65 000	0.001 – 10	609	0.6	-	-

Suppl. Table 1. Relevant physical parameters of the different molecular crowding reagents: molecular mass distribution, number of monomers/polymer (N), crossover polymer concentration (Φ*), polymer length/persistence length (L/Lp) and viscosity (η).

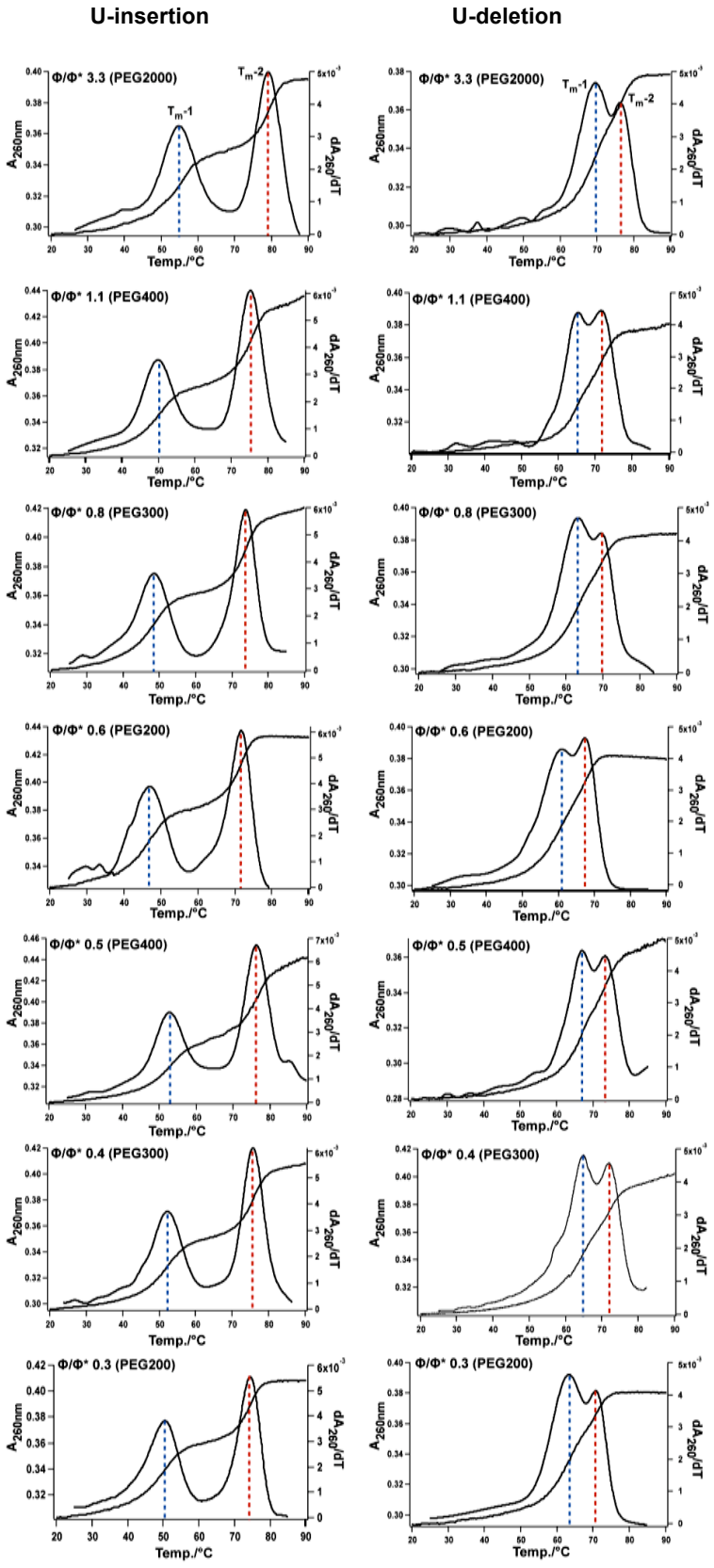

Suppl. Figure 1. UV melting profiles (A_{260}=f(T)) and 1st derivatives (dA_{260}/dT=f(T)) of U-insertion (left) and U-deletion (right) pre-mRNA/gRNA hybrid RNAs at Φ/Φ* ratios of 3.3, 1.1, 0.8, 0.6, 0.5, 0.4 and 0.3. Dotted lines indicate the half maximal melting transitions of the two helical elements (blue: T_m-1; red T_m-2).

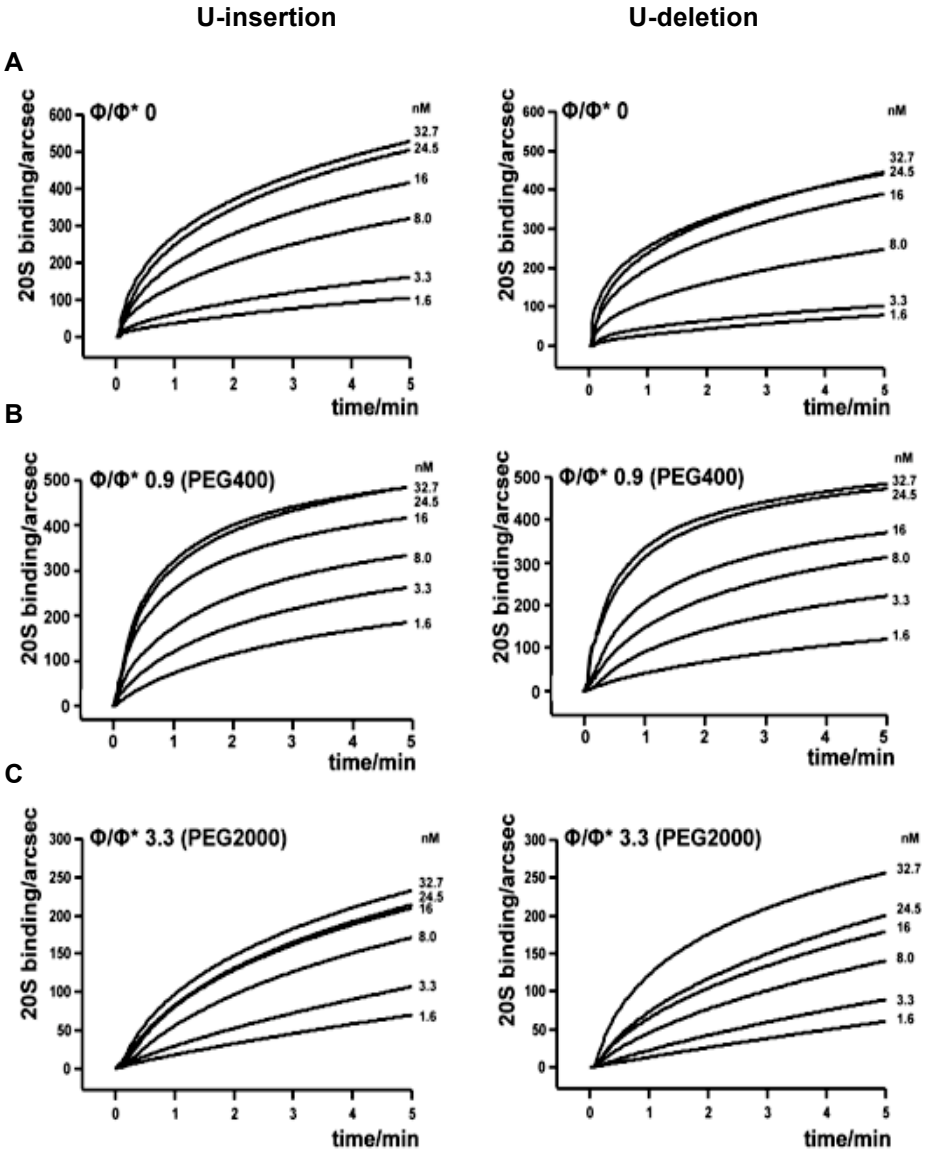

Suppl. Figure 2. Real time monitoring of the 20S editosome/pre-mRNA/gRNA interaction. Sensograms of the concentration-dependent binding of 20S editosomes (32.7nM, 24.5nM, 16nM, 8nM, 3.3nM, 1.6nM - top to bottom) to U-insertion and -deletion mRNA/gRNA hybrid RNAs. (A) Binding isotherms at dilute solvent conditions in the absence of PEG (Φ/Φ* = 0); (B) at semidilute conditions (Φ/Φ* = 0.9) and (C) at crowded conditions (Φ/Φ* = 3.3).

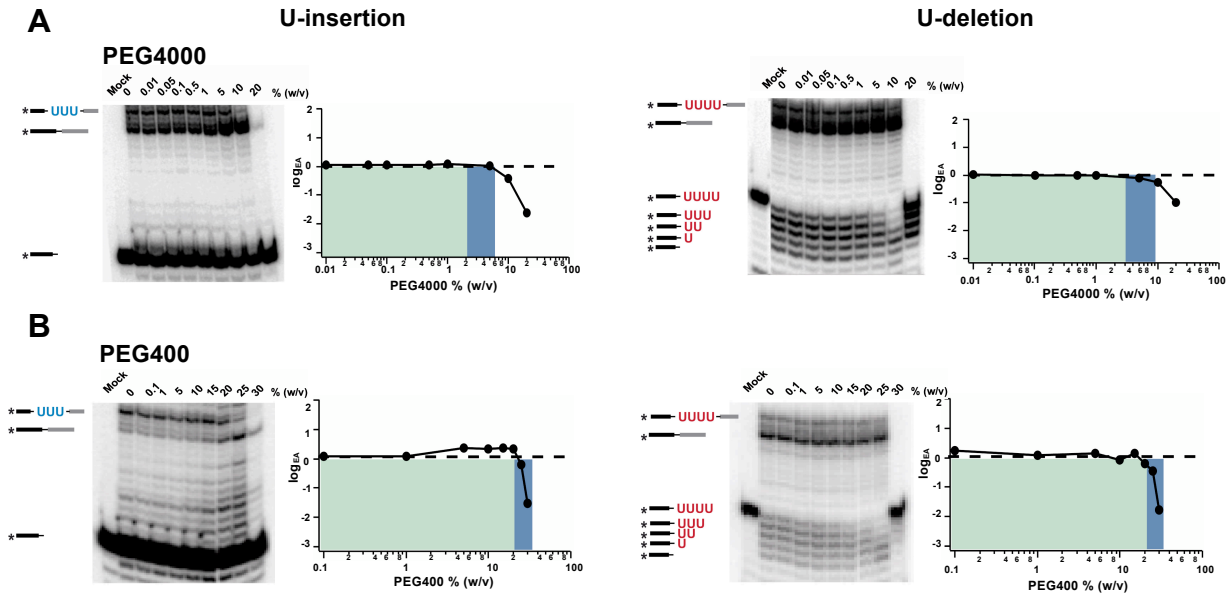

Suppl. Figure 3. *In vitro* RNA editing at dilute, semidilute and crowded cosolute conditions. Assays were performed at varying concentrations of PEG4000 (A) and PEG400 (B). RNA reactants, products and intermediates (sketched on the left of the gels) were resolved electrophoretically and quantified. Editing activities (EA) were normalized to the EA in the absence of cosolute (dashed line) and plotted as a function of the molecular crowder (MC) concentration: $\log_{EA} = f(\log c_{MC})$. Green background: dilute solvent conditions; blue background: semidilute conditions; white background: crowded cosolute conditions. Mock: minus 20S editosomes. (*) annotates the position of the radioactive label [^{32}P].

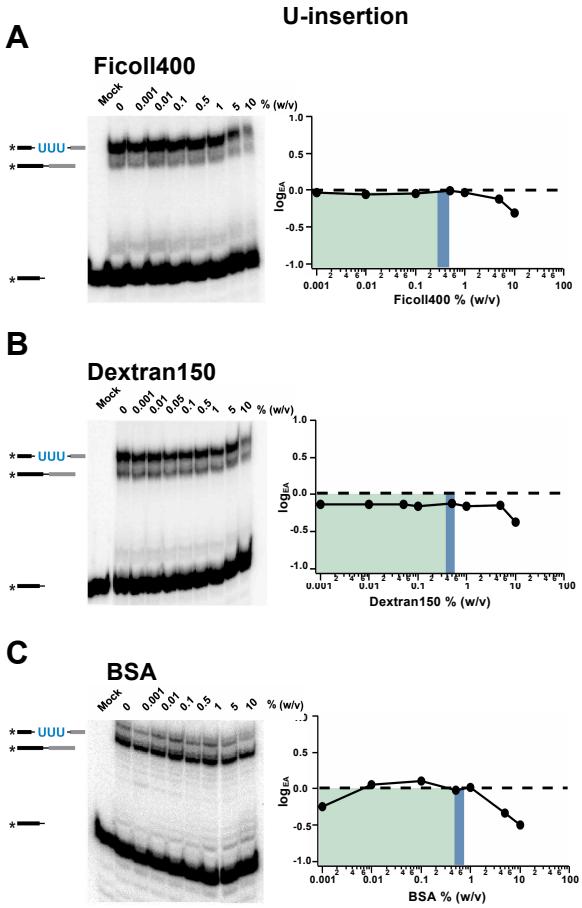

Suppl. Figure 4. *In vitro* U-insertion RNA editing at dilute, semidilute and crowded cosolute conditions in the presence of varying concentrations of (A) Ficoll400, (B) Dextran150 and (C) BSA. RNA reactants, products and intermediates were resolved electrophoretically and quantified. Editing activities (EA) were normalized to the EA in the absence of cosolute and plotted as a function of the concentration of molecular crowding (MC) reagent: $\log_{EA} = f(\log c_{MC})$. Green background: dilute solvent conditions; blue background: semidilute conditions; white background: crowded cosolute conditions. Mock: minus 20S editosomes. (*) annotates the position of the radioactive label [^{32}P].

Summary

Most mitochondrial transcripts in African trypanosomes are edited to generate translatable transcripts. The reaction is catalyzed by a macromolecular protein complex, the 20S editosome. Editing is characterized by the site-specific insertion and/or deletion of exclusively U nucleotides and in order to catalyze the reaction, editosomes must bind a panel of different substrate pre-mRNAs.

The experiments documented in **chapter one** verify that 20S editosomes bind different "*in vivo*-sized" transcripts with nanomolar affinities and association/dissociation rate constants typical for RNA/protein complexes. The editosome/RNA interaction is non-discriminative, thus enabling the interaction with different pre-edited mRNAs as well as with partially edited mRNAs and guide RNAs. Using immunogold-labeling in combination with transmission electron microscopy (TEM) I was able to demonstrate that editosomes have only one RNA substrate-binding site, which suggests that both subtypes of the RNA editing reaction (U-insertion and U-deletion) are catalyzed within a single, bifunctional reaction center.

In **chapter two** I present the first atomicforce microscopy (AFM)-based pictures of 20S editosomes and 20S editosome/RNA complexes. The data confirm that editosomes have a single RNA binding domain and further demonstrate that editosomes contain a so far unknown "chaperone-type" RNA unwinding activity. Upon RNA binding, transcripts become progressively unwound, ultimately enabling multiple 20S editosomes to interact with one substrate RNA.

RNA editing is a pre-requisite for the survival of *Trypanosoma brucei.* The life cycle of the parasite involves the cyclic transmission between a mammalian host and the Tsetse fly as the insect vector. Since RNA editing has been shown to be regulated between the two developmental stages, I analyzed in **chapter three** whether RNA editing is also regulated within the cell cycle of the parasite. Editosome isolates from the G1- and G2-phase of the trypanosome cell cycle were tested for their RNA editing activity. The experiments identified catalytic activity in both phases thus demonstrating that the processing reaction is not cell cycle-regulated.

The basic steps of the editing reaction cycle have been unraveled with the help of an *in vitro* assay that is performed at dilute solvent conditions. However, *in vivo* the reaction takes place inside the highly "crowded" mitochondrial environment. In **chapter four** I analyzed the effects of macromolecular crowding on RNA editing using defined conditions from dilute to semidilute to crowded solvent properties. I was able to demonstrate that the thermodynamic stabilities of the pre-mRNA/gRNA hybrid RNAs differ at these conditions. Crowded solvent properties stabilize the RNA molecules and alter the rate constants for the association and dissociation of the substrate RNAs to editosomes. Ultimately, the processing reaction is inhibited. These results imply that the *in vivo* reaction cannot rely on a diffusionally-controlled, collision-based mechanism. The data advocate a scenario in which RNA editing is conducted by a "hand-over" or "channeling" of substrate RNAs from one processing machinery to the next.

Zusammenfassung

Die Mehrheit der mitochondrialen Transkripte in afrikanischen Trypanosomen muss editiert werden, um translatierbare mRNA-Moleküle zu generieren. Die Reaktion wird von einem makromolekularen Proteinkomplex, dem sogenannten 20S Editosom, katalysiert. RNA-Editing zeichnet sich durch die Insertion und/oder Deletion von ausschliesslich U-Nukleotiden aus, und um die Reaktion zu initiieren müssen Editosomen mit den zu prozessierenden, präeditierten mRNAs im Mitochondrium wechselwirken.

Die in **Kapitel eins** dokumentierten Experimente zeigen, dass 20S Editosomen unterschiedliche mitochondriale Transkripte mit nano-molarer Affinität binden können. Die korrespondierenden Assoziations- und Dissoziationsraten-Konstanten entsprechen dabei typischen Werten für die Wechselwirkung von RNA-Molekülen mit Proteinen. Die Editosom/RNA-Interaktion ist nicht diskriminativ, wodurch Editosomen in der Lage sind mit unterschiedlichen prä-editierten mRNAs, mit partiell editierten mRNAs, als auch mit guide RNAs zu interagieren. Immunogold-Markierungsexperimente in Kombination mit einer Visualisierung durch Transmissions-Elektronen-Mikroskopie (TEM) zeigten, dass Editosomen eine einzige Substrat-RNA Bindestelle aufweisen. Dies legt nahe, dass beide Editing-Partialreaktionen (U-Insertion /U-Deletion) in einem bifunktionalen reaktiven Zentrum ablaufen.

In **Kapitel zwei** werden die ersten Rasterkraftmikroskop-basierten Bilder von 20S Editosomen und 20S Editosom/RNA-Komplexen präsen-tiert. Die Darstellungen bestätigen, dass Editosomen eine einzige RNA-Bindedomäne haben. Fortführend zeigen die Daten, dass Editosomen eine bisher unbekannte, “chaperone”-artige RNA-Entwindungsaktivität exekutieren. RNA-Trankripte werden nach Bindung an den Proteinkomplex strukturell entwunden, letztlich um mehreren Editingkomplexen die Bindung an ein Substrat RNA-Molekül zu ermöglichen.

RNA-Editing stellt eine Voraussetzung für das Überleben afrikanischer Trypanosomen dar. Der Lebenzyklus der Parasiten zeichnet sich durch die zyklische Übertragung zwischen einem Säugetierwirt und Tsetse-Fliegen als übertragendem Insekt aus. Da RNA-Editing zwischen diesen beiden Entwicklungsstadien (Fliege/Säugetierwirt) reguliert wird, wurde in **Kapitel drei** untersucht, ob die Editingreaktion ebenfalls innerhalb des Zellzyklus des Parasiten reguliert ist. Hierzu wurden Editosomen von Zellzyklus-sychronisierten Trypanosomenzellen der G1- und G2-Phase präpariert. Die Experimente zeigen, dass in beiden Zellzyklusphasen katalytische Aktivität nachweisbar ist. D.h. RNA-Editing ist innerhalb des Zellzyklus nicht reguliert.

Die basalen Reaktionsschritte der RNA-Editingreaktion wurden unter Verwendung eines biochemischen *in vitro* Systems identifiziert. Die Reaktion wird dabei in einem verdünnten, wässrigen Milieu durchgeführt, was ignoriert, dass die Editingreaktion *in vivo* innerhalb der Mitochondrien stattfindet. Mitochondrien zeichnen sich durch extreme makromolekulare “crowding”-Bedingungen aus. In **Kapitel vier** wird der Einfluss von verdünnten, “semiverdünnten” und “crowded” Reaktionsbedingungen systematisch untersucht. Die Experimente zeigen, dass sich die thermody-

namischen Stabilitäten der prä-mRNA/gRNA-Hybrid RNAs ändern. “Crowded” Bedingungen stabilisieren die RNA-Moleküle. Gleichzeitig ändern sich die Assoziations- und Dissoziationsratenkonstanten für die Bildung der RNA/Editosom-Komplexe, was letztlich zu einer Inhibition der Reaktion führt. Hieraus ergibt sich, dass die Reaktion *in vivo* nicht diffusionskontrolliert ablaufen kann. Die Ergebnisse legen einen Reaktionsweg nahe, bei dem die Substrat-RNAs der Editingreaktion von einer Prozessierungsmachinerie zur Nächsten weiter gereicht werden und nicht durch freie Diffusion migrieren.

Ehrenwörtliche Erklärung

Ich erkläre hiermit an ehrenwörtlich, dass ich die vorliegende Arbeit entsprechend den Regeln guter wissenschaftlicher Praxis selbstständig und ohne unzulässige Hilfe Dritter angefertigt habe.

Sämtliche aus fremden Quellen direkt order indirekt übernommenen Gedanken sowie sämtliche von Anderen direkt order indirekt übernommenen Daten, Techniken und Materialien sind als solche kenntlich gemacht. Die Arbeit wurde bisher bei keiner anderen Hochschule zu Prüfungszwecken eingericht.

Venkata Subbaraju Katari
Darmstadt, 05.09.2013

Curriculum vitae

Personal

Name:	Venkata Subbaraju Katari
Date of birth:	21. 04. 1976
Place of birth:	Siddhapuram, India

Education and Professional Experience

03/2008 – 08/2012	Dissertation, Fachbereich Biologie, Arbeitskreis Molekulare Genetik, Technische Universität Darmstadt, Darmstadt, Germany
10/2004 – 01/2007	Master of Science (M.Sc.) – Biotechnology, Technische Universität Hamburg-Harburg, Hamburg, Germany
04/2001 – 07/2003	Manufacturing Engineer, Process Control Maintenance, PalmTech India Ltd., Kakinada, India
09/1995 – 08/2000	Bachelor in Chemical Technology and Biotechnology, Mendeleev University of Chemical Technology, Moscow, Russia
09/1994 – 08/1995	Engineering Disciplines and Russian Language Prep. Course, Mendeleev University of Chemical Technology, Moscow, Russia
07/1992 – 05/1994	Intermediate Education, Board of Intermediate Education, Sri Vagdevi Junior College, Hyderabad, India
04/1980 – 05/1992	Primary and Secondary School Education, Central Board of Secondary Education Rex Higher Secondary School, Ooty, India

Acknowledgements

I am indebted to Prof. Dr. Göringer for giving me an opportunity to work in his esteemed lab. Without his critical and valuable inputs, I would not have able to come up to this step of my PhD. His support as a friend, guardian, teacher and philosopher has instilled me all the strength and confidence to face the difficult times that can't be explained in words. I salute! - To his endurance and patience. Thanks "Uli" ! It's because of you I am able to Ski.

I am grateful to Michael, who helped me as a colleague and supported me as friend. His help, in keeping my spirits up is highly appreciated. Thanks for being helpful in my personal and professional life. A special thanks to Dr. Böhm for her help during her stay in this lab.

I would like to thank Christin, Elisabeth, Matthias, Pedro, Andreas and Heike for all the fun and frolic throughout my stay, though the PhD was a serious "BeeZ WaX". I had a good time working with you all and I wish you all the very best in your future endeavors.

I would like to thank all my Indian friends Bineet, his wife Niyanta and their son Aarav; Dr. Thangaraj and his wife Sunaka; Lalith and his wife Ruchika and their daughter Pranati; Kishore and his wife Sirisha; Ram and his wife Priya; Keely; and Vasu for always being there for me. "Thanks" for making me feel we are a big family. I would like to thank all my Bulgarian friends: Denitza; Marin and Anisha. A whole hearted thanks to my so called brother Christoph Miks and his friend Anja and his family who have always been with me on my side. Last but not least, a special thanks to Florian. True friends are revealed when circumstances are difficult and you people have made the words come true to me **"Amicu certus in re incerta cernitur"**- *Quintus Ennius*.

"Matha Pitha Guru Deivam" – Mother, Father and Teacher precede God. I thank my parents for their encouragement and support and **I dedicate this work to them** by placing it at their feet. A sincere thanks to my sisters: Triveni akka and Padma akka and my nephews: Sumanth, Yashwant and Mitheesh for cheering me up and supporting me in all times.